Mode Coupling In A Non-Uniform Magnetised Plasma

David Ramsay B.Sc.

Thesis
submitted to the
University Of Glasgow
for the degree
of Ph.D.

Department of Physics and Astronomy,
Glasgow University,
Glasgow, G12 8QQ.

August 25, 1994

ProQuest LLC.
789 East Eisenhower Parkway
P.O. Box 1346
Ann Arbor, MI 48106 – 1346

To Mum and Dad

Abstract

This thesis presents an analysis of radial waves in a helically structured cold plasma. The problem is solved by numerically integrating a set of coupled differential equations for the electric field. Results showing the conversion of energy between different modes of propagation are presented. Relevance to plasma heating is discussed, and the merits and demerits of different solution methods are compared.

Chapter 1 surveys the ubiquity of the plasma state and focuses on two areas which motivate this work: coronal loops and tokamak heating.

In Chapter 2, the mathematics necessary for the description of the plasma state is introduced and the cold, multi-fluid equations used later in the thesis are derived. An overview of linear waves in a cold plasma is presented.

A general survey of the modelling of non-uniform plasma media is given in Chapter 3, where the WKB solutions and the notion of a local dispersion relation are introduced.

The specifics of our chosen system are introduced in Chapter 4. A consistent equilibrium field, of constant magnitude, but varying in direction is obtained and described. Linear wave solutions to the cold plasma equations for electrons are sought, and a set of coupled odes for the electric fields are derived, in the regime of negligible equilibrium flow. It is shown that asymptotic solutions may be obtained for these equations, and their form and range of validity is discussed. Wave equations for the electric field which include the full effects of equilibrium flow are then discussed.

Splicing the helical field onto a uniform one at a fixed radius gives a useful simple model of a number of relevant physical structures, whose solution is investigated in detail in Chapter 5. Expressions for amplitudes of converted and reflected waves are found in terms of the value of electric fields and their gradients at the boundary between the two regions. The values of these are found numerically for a variety of plasma parameters, and the implications of the results discussed. The results are compared with the asymptotic approximations found earlier, and the agreement found to be very good.

The possibility of deriving WKB solutions to the model equations and of applying one other commonly used technique is considered in Chapter 6.

Chapter 7 summarises the conclusions of this work, and gives suggestions for future research.

The original work of this thesis is contained in Chapters 4 to 6.

Acknowledgments

I would like to thank Professor R.P. Ferrier for the provision of facilities in the Department of Physics and Astronomy, Glasgow University, where I was a post-graduate student during the period in which this research was carried out. Thanks are also due to my supervisor, Professor Ernest Laing for his help during my time here, and to Dr. Declan Diver for many useful discussions. I would also like to acknowledge the financial assistance of the erstwhile Science and Engineering Research Council.

On a less formal level, my thoughts and attitudes over the last few years have been stimulated, shaped, and challenged by my association with a large number of other colleagues of various descriptions. The plasma people (Carolyn, Amarjit, Graeme, Saad, Jack, Liz, David K.) have been helpful office mates, sounding boards for new ideas, and companions on many a night out. Across the corridor, thanks are due to Gerry and Gary for always providing political debate, the Daily Record and a football fanzine or two, and to Brian and Luke for putting up with all my questions about LaTeX. The denizens of the coffee club have enlightened many a dreich morning for me with their comment, analysis, and plans to put the world to rights.

I should also mention many mountaineering friends, most notably Amanda, Paul, Bonnie, wee Pete, and Brian for bearing the brunt of my doubts and blues and enabling me to forget it all at weekends. More recently, friends from the world of conservation, including Jenny, Stewart and Catherine have also been much appreciated. Thanks also to Colette and Lesley who have generally prevented life from being too much of a drag.

David Ramsay

Contents

List of Figures

Chapter 1

The Occurrence And Importance Of Plasmas

> The word 'plasma'[1] will be used to designate that part of an arc-type discharge in which the densities of ions and electrons are high but substantially equal.
> *I. Langmuir, L. Tonks, 1929*

1.1 The Plasma Universe

Plasma Physics aims to describe the behaviour of highly ionised, quasi-neutral matter, and, in particular, its collective properties. Our immediate environment is too cold to be significantly ionised, and so the plasma state is considered an oddity. In the universe as a whole, it is the norm. Both direct measurements from space probes and inferred parameter values from remote observations combine to give a picture of a universe filled with magnetic and electric fields and currents, which can exchange momentum over large distances. The currents can become pinched to form lines or surfaces, dividing space up into cells, each with their own magnetic field values. In short, a plasma universe naturally becomes filamentary and inhomogeneous (Alfvén, 1990). The effects of such structure on physics on a cosmic scale have been neglected until recently. It is now being realised that an understanding of plasma physics is essential in many branches of astrophysics where it was previously considered a side-issue. Electromagnetic forces may have an important role to play

[1] The term was coined under the mistaken impression that it was Greek for jelly. Despite this inauspicious origin, the word has stuck.

in the dynamics of galaxies (Peratt, 1986). The realisation that interstellar and intergalactic space may be filled with tenuous plasma, has led to new interpretations of red-shifts in terms of Compton scattering by the interstellar, or intergalactic, medium which have far-reaching consequences both for cosmology (Reber, 1986), and for the interpretation of data from a wide variety of objects in our own galaxy (Marmet, 1990).

1.2 The Sun

The Sun is a gravitationally bound sphere of fusing plasma, composed of 90% hydrogen, 10% helium, and 0.1% other elements. It is now known to be a complex and highly structured object. Several aspects of its behaviour are still obscure: the well-known discrepancy between observed and predicted neutrino fluxes is one example. More pertinent is the problem of coronal heating.

1.2.1 Coronal Plasma Loops And Heating

The visible surface of the Sun (the *photosphere*) has a temperature of about 6000K. Moving radially outwards, the next layer, the *chromosphere*, has a temperature of between 6000K and $10^5 K$. This is followed by a rapid rise in temperature over a few hundred kilometres to about $10^6 K$ at two solar radii. The reason for this heating is still unclear. More specifically, it is now known that a large part of the energy emitted from the corona comes from well-defined curved paths, known as *loops*. These structures may be consistently identified across a wide range of wavelengths in many of the large number of observations which have become available in the last twenty years or so. Loops are anchored to the solar surface by *footpoints* (usually associated with sunspots) $\sim 10^7 m$ apart, and rise about the same distance above the surface, with a thickness estimated to be from $10^5 m$ to $10^6 m$. They usually have a lifetime of a few minutes, although they are often observed in systems which can persist for hours and have temperatures ranging from $10^1 K$ (cool loops) to $\sim 3 \times 10^6 K$ for hot loops. An exhaustive survey of this topic is given in Bray et al, 1991. These general data apart, there is little agreement about the exact physical processes occurring in coronal plasma loops.

It is generally assumed that the observed loop structures act as tracers of equally well defined structures in the solar magnetic field, and that this field provides some sort of mechanism which contains and supports the denser plasma found there. This is a fairly compelling viewpoint, since it is hard to see what other source the struc-

ture could derive from. However, it is worth remembering that there is no detailed information about magnetic field structure available, although there are more or less accurate estimates of the average values occurring in certain regimes. Even if we accept the general principle that the visible structures follow field lines, the limited definition of observations means that more complex topologies cannot be ruled out i.e. braided and tangled field lines may be present. These caveats aside, the notion that a coronal loop corresponds to a magnetic flux tube has become the accepted view. The lack of detailed observational data means that producing feasible magnetic field structures (usually within the MHD approximation) and finding their consequences has become a major industry. Most work centres on finding force-free, or potential magnetic equilibria which mimic the structures thought to occur, and studying their stability and possible heating mechanisms which they may support. Of particular interest for this thesis, are the large number of models which have as their basis helical magnetic fields.

Clearly, predicting how and where heating occurs in the corona and, in particular, the generation mechanism for solar flares is a major goal for solar physics. At the moment, a bewildering number of candidate schemes exist. Broadly speaking, these assume that some form of wave propagates up from the photosphere and is then damped, or steepens to form a shock, or undergoes mode conversion to form another mode which is then dissipated in some manner. However, if theories of coronal loop structure are uncertain, theories of coronal loop heating, relying, as they do, on the little known conditions in the photosphere, are even more speculative, and only the broad forms of any conclusions obtained thus far are likely to be useful. A complete account of coronal loop heating is likely to involve a number of these mechanisms, together with an understanding of the way in which photospheric conditions interact with coronal physics.

The possible occurrence of helical fields in coronal loops, together with the potentially important role which mode conversion may play in this context, motivates us to study waves in a helical field using a plasma model which is slightly more general than the MHD approximation, with particular emphasis on mode conversion.

1.3 Laboratory Fusion Plasmas

Since about 1950, a vast amount of research has been devoted to the peaceful harnessing of fusion energy. The most favoured reaction (that with the highest cross-section) occurs between deuterium and tritium, which results in the production of

a helium nucleus and a neutron. The energy released in such a reaction is greater per fusing nucleus than for fission involving a uranium isotope. This, and the easy availability of the fuel, makes fusion power an attractive proposition. For such a reaction to generate net power, however, the nuclear power produced must be enough to compensate for bremsstrahlung losses and heating the plasma. Assuming the ions and electrons have the same temperature, and that some mechanism is available for 'recycling' lost energy and heating the plasma with it, then one can show that for there to be a net production of energy, the plasma electron density n, confinement time τ and temperature T must satisfy

$$n\tau \geq \frac{T}{a - bT^{1/2}} , \tag{1.3.1}$$

where a, b are positive quantities which depend only on nuclear reaction rate and the efficiency of the 'recycling'. This is the *Lawson criterion* (Lawson, 1957). It is impossible to achieve breakeven for temperatures of less than 2keV, and the optimum temperature is around 30keV. To achieve ignition, that is to produce enough neutrons to sustain the reaction, one must satisfy a criterion of the same form, but with differing a, b. No ignition is possible below 2keV, and the optimum temperature is, again, about 30keV. Assuming we choose such favourable temperatures, the Lawson criterion becomes, roughly

$$n\tau \geq 10^{20} m^{-3} s . \tag{1.3.2}$$

Clearly, a number of regimes are possible which satisfy this criterion. For instance, if very high densities are used the confinement time need only be very small: this is the principle behind *inertial confinement fusion*. If everyday densities (densities which can be sustained by standard engineering structures) are used, then $n \leq 10^{20} m^{-3}$, so that $\tau \geq 1s$. A number of candidates for such a containment exist, the most favoured being magnetic confinement in a *tokamak*. This is a Russian acronym for toroidal magnetic containment vessel – the concept was invented and early trials carried out in the former Soviet Union. A purely toroidal magnetic field will not confine the plasma, as an electric field is set up which causes the particles involved to drift radially outwards. This field can be 'shorted out' by introducing a poloidal component, giving an overall magnetic field which twists around the toroidal flux surfaces. However, too large a twist can lead to instabilities, with consequent loss of confinement. Much theoretical and experimental effort has gone into studying and controlling these instabilities, and a good deal of progress has been made. Major experiments (JET Team, 1992) have now achieved the required temperature

and $n\tau$ value separately, although not in the same experimental run. The TFTR experiment recently produced an output power of about 20% of the power required to heat and maintain their D-T plasma.

1.3.1 Plasma Heating

The necessary heating is provided partly by the toroidal current which is used to produce the poloidal magnetic field. However, typical plasmas have a resistivity which is low and decreases with increasing temperature, so that this 'Ohmic' heating must be supplemented. Firing high velocity beams of neutral particles into the plasma is one alternative. Another is to launch electromagnetic waves of some form into the tokamak. The trick of this technique is to pick the wave so that it mode converts effectively into a mode which is heavily damped and thus deposits most of its energy in the plasma interior. This, and other strategies, is considered in some detail in Cairns, 1991.

The basic concept is that a mode, considered to be well approximated by a cold plasma mode, propagates inwards until it meets a layer in the device where the spatially varying plasma parameters produce a resonance. According to cold plasma theory this can result in either a reflection and/or absorption. The point is somewhat academic however, since, near a resonance, other effects dominate.

To obtain the cold plasma waves, particle collisions and thermal motion are neglected and both of these can give rise to damping. Assuming the plasma to be collisionless is, in fact, a good approximation, which becomes better with increasing temperature, though a little non-resonant absorption is always present. The finite temperature effects result in resonant interactions between the electron's Larmor orbit and the wave field which become stronger as the temperature rises. Firstly, if an electron travelling along a field line at velocity $v_{\|}$ sees a Doppler-shifted frequency, $\omega - k_{\|}v_{\|}$, which is close to an integer multiple of its cyclotron frequency, it is accelerated in its Larmor motion. This requires a circularly-polarised wave electric field at right angles to the magnetic field $\mathbf{B}_o$ and so could result from the presence of an X-mode. Acceleration along $\mathbf{B}_o$ can also happen because the finite size of the Larmor radius means the electron samples electric field, at gyrofrequency Ω_o, over a range of positions. The wave electric field oscillates at its own frequency ω. If these satisfy the resonance condition $\omega = \Omega_o + k_{\|}v_{\|}$, then E_z averages to a non-zero value and parallel acceleration results. This mechanism is associated with an O-mode.

To obtain qualitative predictions of damping decrement, the hot plasma disper-

sion relation must be solved. Exact solutions are usually not possible or necessary and treating temperature as a small correction via an expansion in $\frac{2kT}{m_e c^2}$ (to lowest order this gives cold plasma modes) is quite adequate.

Because of the interest in such heating techniques, this is clearly another area where the study of wave propagation in a helical field will be an informative exercise.

Chapter 2

The Mathematical Description Of A Plasma

2.1 Liouville's Equation And The Chain Of Kinetic Equations

In what follows, the main ideas used in the mathematical analysis of the plasma state are introduced and it is shown that numerous levels of description exist, from the comprehensive but unworkable, to the crude, but easily solved. In particular, the derivation of the plasma fluid equations, which are extensively used later, is given.

Consider a system composed of N interacting bodies in a volume V, where N is a very large number. The motion of such a system may be described by the coordinates $q_1, \ldots, q_k, p_1, \ldots, p_k$, where the qs are coordinates for each degree of freedom of the N bodies and the ps are the corresponding momenta. In our case, we wish to model the interaction of particles, so there are 3 degrees of freedom for each particle, and hence $6N$ coordinates in total. The totality of such points is referred to as the *phase space* for the system. As time advances, the system will trace out a trajectory in phase space which is determined by Newton's Laws. This can be taken as the first (and only exact) description of a plasma. It is clearly of no practical use: even if the necessary calculations could be carried out, we would never have precise enough knowledge of the initial conditions, and the detail of the description would be superfluous.

To obtain models of greater utility, much of the existing information must be

somehow 'averaged out'. To do this, the system is replaced by an ensemble of similar systems, each of which will evolve as discussed above. Rather than having definite values, physical quantities now have probable (or expectation) values, defined by the average over the ensemble. A *generic N particle distribution function* f_N can now be defined, such that $f_N(X_1,\ldots,X_N)\,dX_1\ldots dX_N$ is the probability that particle i, or any particle of the same type as i is within $dX_1\ldots dX_N$, at time t, where we have taken $X_i = (\mathbf{x}_i, \mathbf{v}_i)$ as shorthand for the coordinates for the ith particle. For a single species plasma, f_N is normalised such that,

$$\int f_N dX_1\ldots dX_N = N!\,, \tag{2.1.1}$$

since there are $N!$ permutations of the N particles. As a result, the expectation value of a physical quantity Q, is:

$$\langle Q(X_1,\ldots,X_N,t)\rangle = \int\ldots\int f_N(f_1,\ldots,X_N,t)\,Q(X_1,\ldots,X_N,t)\,dX_1\ldots dX_N\,. \tag{2.1.2}$$

By using Hamiltonian mechanics, f_N may be found to satisfy the Liouville equation, viz.:

$$\frac{\partial f_N}{\partial t} + \sum_{j=1}^{N} \mathbf{v}_j \cdot \frac{\partial f_N}{\partial \mathbf{x}_j} + \sum_{j=1}^{N} \mathbf{a}_j \cdot \frac{\partial f_N}{\partial \mathbf{v}_j} = 0\,, \tag{2.1.3}$$

where $\mathbf{a}_i$ is the acceleration of the ith particle due to the other $N-1$ particles. It will be, in general, a formidably complex function of $X_1,\ldots,X_{i-1},X_{i+1},\ldots,X_N$, and of fields applied externally to the plasma.

The averaging process outlined above has still not reduced the problem in complexity, in the general case. When the system is in thermodynamic equilibrium, however, it can be shown that:

$$f_N = C\exp\left[-W(X_1,\ldots,X_N)/kT\right]\,, \tag{2.1.4}$$

where W is the total energy for state $X_1,\ldots,X_N$, k is Boltzmann's constant, and T is the temperature of the system. The problem of macroscopic modelling of the plasma would then come down to evaluating integrals like Eq. 2.1.2, with f_N given by Eq. 2.1.4. To model non-equilibrium processes, we must try to construct 'equations of motion' for the physical quantities required. This procedure is now outlined in the case of one species of particle. The method can also be applied, with only a little modification, to multi-species plasmas, at the cost of rather greater complexity.

Firstly, we integrate over $N-s$ sets of phase space variables to produce reduced

distribution functions f_s, defined as

$$f_s(X_1, \ldots, X_s, t) = \frac{1}{(N-s)!} \int f_N \prod_{i=s+1}^{N} dX_i \,. \tag{2.1.5}$$

This represents the probability of finding a particle at X_1, a particle at X_2, ..., a particle at X_s, and assumes that particles do not occupy the same position. We now proceed to integrate the Liouville equation over the space of all but s particles, at the same time multiplying by $\frac{1}{(N-s)!}$, to obtain an evolution equation for f_s. The first term becomes $\partial f_s/\partial t$. In the other terms, all contributions for which $s+1 \leq j \leq N$ may be transformed into surface integrals which can be assumed to vanish, since f_s is non-zero over a bounded volume of phase space. The result is:

$$\frac{\partial f_s}{\partial t} + \sum_{j=1}^{s} \mathbf{v}_j \cdot \frac{\partial f_s}{\partial \mathbf{x}_j} + \frac{1}{(N-s)!} \sum_{j=1}^{s} \mathbf{a}_j \cdot \frac{\partial f_N}{\partial \mathbf{v}_j} \prod_{i=s+1}^{N} dX_i = 0 \,. \tag{2.1.6}$$

To complete the derivation, rewrite $\mathbf{a}_j$ as

$$\mathbf{a}_j = \sum_{i=0}^{N} \mathbf{a}_j^{(i)} \,, \tag{2.1.7}$$

where $\mathbf{a}_j^{(i)}$, is the acceleration of the particle j due to the presence of particle i, and $\mathbf{a}_j^{(o)}$ is the acceleration due to any external forces. This expression may be substituted into the third term in Eq. 2.1.6. On noting that the terms for $s+1 \leq i \leq N$ are identical (for given j) by the symmetry of f_N with respect to permutations of like particles, Eq. 2.1.6 becomes:

$$\frac{\partial f_s}{\partial t} + \sum_{j=1}^{s} \mathbf{v}_j \cdot \frac{\partial f_s}{\partial \mathbf{x}_j} + \sum_{j=1}^{s} \sum_{i=0}^{s} \mathbf{a}_j^{(i)} \cdot \frac{\partial f_s}{\partial \mathbf{v}_j} + \sum_{j=1}^{s} \int \mathbf{a}_j^{(s+1)} \cdot \frac{\partial f_{s+1}}{\partial \mathbf{v}_j} dX_{s+1} = 0 \,. \tag{2.1.8}$$

This set of N coupled equations is known as the BBGKY hierarchy (named after Bogoliubov, Born, Green, Kirkwood and Yvon). The first three terms describe the interaction of s particles, while the last includes the forces due to the other $N-s$. The sth member of the set gives an equation for f_s , but also involves f_{s+1}.

This description is equivalent to the Liouville equation, but our intention was to provide a simpler picture. Consider Eq. 2.1.8 for $s = 1$,

$$\frac{\partial f_1}{\partial t} + \mathbf{v}_1 \cdot \frac{\partial f_1}{\partial \mathbf{x}_1} + \mathbf{a}_1^{(o)} \cdot \frac{\partial f_1}{\partial \mathbf{v}_1} + \int \mathbf{a}_1^{(2)} \cdot \frac{\partial f_2}{\partial \mathbf{v}_1} d\mathbf{v}_2 d\mathbf{x}_2 = 0 \,. \tag{2.1.9}$$

This would provide a suitable equation for f_1 were it not for the presence of f_2 in the last term. The next section shows that this term may be approximately rewritten in terms of f_1, for most cases of physical interest.

2.2 Uncorrelated Particles: The Debye Length

If the particles in question are non-interacting and thus the only forces are external, then the last term in Eq. 2.1.9 can be neglected. In fact, in this case the Liouville equation can be solved by taking

$$f_N(X_1,\ldots,X_N,t) = \frac{N!}{N^N}\prod_{j=1}^{N} f_1(X_j,t)\ . \tag{2.2.1}$$

where f_1 is the solution of Eq. 2.1.9 with the integral term set to zero. In this approximation, the probability of finding a second particle in a particular position in phase space is independent of where the first was located. This method of solution can be justified as follows. Consider a species with charge q and mass m, then

$$\begin{aligned} \mathbf{a}_j^{(o)} &= \frac{q}{m}\left[\mathbf{E}^{(o)} + \mathbf{v}_j \times \mathbf{B}^{(o)}\right]\ , \\ \mathbf{a}_j^{(i)} &= \frac{q}{m}\left[\mathbf{E}_j^{(i)} + \mathbf{v}_j \times \mathbf{B}_j^{(i)}\right]\ , \end{aligned} \tag{2.2.2}$$

where $\mathbf{E}_0$, $\mathbf{B}_0$ are the externally applied fields. $\mathbf{E}_j^{(i)}$, $\mathbf{B}_j^{(i)}$ are the electric and magnetic fields felt by particle j through the presence of particle i, and are given by Coulomb's Law and the Biot-Savart Law respectively:

$$\begin{aligned} \mathbf{E}_j^{(i)} &= \frac{q}{4\pi\epsilon_0}\frac{\mathbf{x}_j - \mathbf{x}_i}{|\mathbf{x}_j - \mathbf{x}_i|^3} \\ \mathbf{B}_j^{(i)} &= \frac{\mu_0 q}{4\pi}\frac{\mathbf{v}_i \times \mathbf{x}_j}{|\mathbf{x}_j - \mathbf{x}_i|^3} \end{aligned} \tag{2.2.3}$$

It should be noted that *retarded potentials* have not been used here, since we have assumed that the effect of changes in the velocity or position of a source particle are felt instantaneously at the field point. The light travel time is thus assumed to be much less than the timescale over which physical quantities of interest vary.

We now consider the result of a process in which the particles in the volume V, are subdivided in such a way that $n = N/V \to \infty, q \to 0, m \to 0$, but the total mass and charge stay constant and, consequently, q/m is constant also. Now switch to dimensionless variables by using the plasma frequency as time scale, and the thermal velocity as a characteristic speed. This gives, for time, velocity and length scales,

$$\frac{1}{\omega_p} = \left[\frac{\epsilon_0 m}{nq^2}\right]^{1/2},\quad v_{th} = \left[\frac{kT}{m}\right]^{1/2},\quad h = \left[\frac{\epsilon_0 kT}{nq^2}\right]^{1/2} \tag{2.2.4}$$

where h is the Debye length. The new variables, denoted by a bar, are defined by:

$$\begin{gathered} \mathbf{v} = h\omega_p\overline{\mathbf{v}}\ , \qquad \mathbf{x} = h\overline{\mathbf{x}}\ , \qquad t = \overline{t}/\omega_p\ , \\ \mathbf{a}^{(o)} = h\omega_p^2\overline{\mathbf{a}}^{(o)}\ ,\quad n^s f_s = (h\omega_p)^{3s}\overline{f}_s,\quad dX = h^6\omega_p^3 d\overline{X}\ . \end{gathered} \tag{2.2.5}$$

And, since

$$\mathbf{a}_j^{(i)} = \frac{q^2}{4\pi\epsilon_o m}\left[\frac{\mathbf{x}_j - \mathbf{x}_i}{|\mathbf{x}_j - \mathbf{x}_i|^3}\right] = \frac{\omega_p^2}{4\pi n h^2}\left[\frac{\mathbf{x}_j - \mathbf{x}_i}{|\mathbf{x}_j - \mathbf{x}_i|^3}\right] = \frac{\omega_p^2}{nh^2}\overline{\mathbf{a}}_j^{(i)} , \qquad (2.2.6)$$

the BBGKY hierarchy becomes,

$$\frac{\partial \overline{f}_s}{\partial \overline{t}} + \sum_{j=1}^{s} \overline{\mathbf{v}}_j \cdot \frac{\partial \overline{f}_s}{\partial \overline{\mathbf{x}}_j} + \sum_{j=1}^{s} \overline{\mathbf{a}}_j^{(o)} \cdot \frac{\partial \overline{f}_s}{\partial \overline{\mathbf{v}}_j} + \frac{1}{nh^3}\sum_{j=1}^{s}\sum_{i=1}^{s} \overline{\mathbf{a}}_j^{(i)} \cdot \frac{\partial \overline{f}_s}{\partial \overline{\mathbf{v}}_j} \; + \; \sum_{j=1}^{s} \int \overline{\mathbf{a}}_j^{(s+1)} \cdot \frac{\partial \overline{f}_{s+1}}{\partial \overline{\mathbf{v}}_j} d\overline{X}_{s+1} \; = \; 0 \, . \qquad (2.2.7)$$

If the process mentioned above is taken to its limit we will have 'smoothed out' the charges, and can expect a corresponding change in the mathematical description. The number of particles in a cube of side h is nh^3, and as $n \rightarrow \infty$, this number tends to infinity also. The double summation term in Eq. 2.2.7 may then be neglected since it is $O(1/n^{5/2})$. Physically, the interactions of individual particles become less important than the self-consistent, bulk fields. This property, namely that the number of particles in a Debye sphere should be very large, is usually regarded as an essential prerequisite for the term 'plasma' to be used. Specifically, we require that,

$$nh^3 = N_D = \left[\frac{\epsilon_o kT}{n^{1/3}q^2}\right]^{3/2} \gg 1 \, . \qquad (2.2.8)$$

Dropping the double summation term, and putting

$$f_s = \prod_{j=1}^{s} f_1(X_j, t) \; , \qquad (2.2.9)$$

in accordance with the assumption of uncorrelated particles, it can be shown that all the equations in the set 2.1.8 can be satisfied, provided that

$$\frac{\partial f_1(X_1,t)}{\partial t} + \mathbf{v}_1 \cdot \frac{\partial f_1(X_1,t)}{\partial \mathbf{x}_1} + \left[\mathbf{a}_1^{(o)} + \int \mathbf{a}_1^{(2)} f_1(X_2.t) dX_2\right] \cdot \frac{\partial f_1(X_1,t)}{\partial \mathbf{v}_1} = 0 \, . \qquad (2.2.10)$$

On dropping the subscripts, this may be compactly written

$$\frac{\partial f}{\partial t} + \mathbf{v} \cdot \frac{\partial f}{\partial \mathbf{x}} + \mathbf{a} \cdot \frac{\partial f}{\partial \mathbf{v}} = 0 \, , \qquad (2.2.11)$$

where

$$\mathbf{a} = \frac{q}{m}\int [\mathbf{E} + \mathbf{v} \times \mathbf{B}] f(\mathbf{x}', \mathbf{v}', t) d\mathbf{x}' d\mathbf{v}' + \frac{q}{m}\left[\mathbf{E}^{(o)} + \mathbf{v} \times \mathbf{B}^{(o)}\right] \; , \qquad (2.2.12)$$

and $\mathbf{E}$ and $\mathbf{B}$ are the fields produced by particles at $(\mathbf{x}', \mathbf{v}')$.

Eq. 2.2.11 is the *Vlasov equation*, which describes the evolution of a plasma's distribution function under the influence of the fields given by Eq. 2.2.3.

2.3 Moments Of The Vlasov Equation: The Fluid Picture

The complexity of the Vlasov model is still considerable: a set of highly non-linear coupled pdes must be solved before the plasma motion may be extracted. Models of great utility may be found by reducing still further the information content of the description used. This is done by multiplying the kinetic equation by appropriate functions of velocity and then integrating over velocity space. Appropriate in this case means of a form such that we can easily relate the integrals thus found to physical quantities. Initially, the distribution function is renormalised so that

$$n(\mathbf{x},t) = \int f(\mathbf{x},\mathbf{v},t)d\mathbf{v}\ , \tag{2.3.1}$$

where n is the number density of particles at $(\mathbf{x},t)$. Hence the ensemble average of a physical quantity Q, becomes:

$$\langle Q(\mathbf{x},t)\rangle = \frac{1}{n}\int f(\mathbf{x},\mathbf{v},t)Q(\mathbf{x},\mathbf{v},t)d\mathbf{v}\ . \tag{2.3.2}$$

To find the zeroth moment equation, multiply Eq. 2.2.11 by 1, and integrate over velocity space, then:

$$\int \frac{\partial f}{\partial t}d\mathbf{v} + \int \mathbf{v}\cdot\frac{\partial f}{\partial \mathbf{x}}d\mathbf{v} + \int \mathbf{a}\cdot\frac{\partial f}{\partial \mathbf{v}}d\mathbf{v} = 0\ . \tag{2.3.3}$$

The first term becomes $\partial n/\partial t$, by definition. The second may be written

$$\int \mathbf{v}\cdot\frac{\partial f}{\partial \mathbf{x}}d\mathbf{v} = \frac{\partial}{\partial \mathbf{x}}\cdot\int \mathbf{v}f d\mathbf{v} = \frac{\partial}{\partial \mathbf{x}}\cdot\langle n\mathbf{v}\rangle\ . \tag{2.3.4}$$

In the third term, the part of $\mathbf{a}$ due to velocity independent forces, $\mathbf{a}_I$, say can be written

$$\int \mathbf{a}_I\cdot\frac{\partial f}{\partial \mathbf{v}}d\mathbf{v} = \mathbf{a}_I\cdot\int\frac{\partial f}{\partial \mathbf{v}}d\mathbf{v} = \mathbf{a}_I\cdot\int_s f dS = 0\ , \tag{2.3.5}$$

where we have used the divergence theorem and assumed that $f\rightarrow 0$ as $|\mathbf{v}|\rightarrow\infty$. The velocity dependent part, $\mathbf{v}_D$ becomes

$$\int \mathbf{a}_D\cdot\frac{\partial f}{\partial \mathbf{v}}d\mathbf{v} = \int\frac{\partial}{\partial \mathbf{v}}(\mathbf{a}_D f)d\mathbf{v} = \int_s f\mathbf{a}_D\cdot d\mathbf{S} = 0\ , \tag{2.3.6}$$

on noting that $(\mathbf{v}\times\mathbf{B})_i$ does not contain v_i and then repeating the argument above (this time, $|\mathbf{a}_D f|\rightarrow 0$). Thus the zeroth moment of the Vlasov equation may be written

$$\frac{\partial n}{\partial t} + \nabla\cdot\langle n\mathbf{v}\rangle = 0\ . \tag{2.3.7}$$

This is the *continuity equation*, which expresses the fact that the flux of particles into a volume must be balanced by change of density in that volume.

We now proceed to take the first moment of Eq. 2.2.11,

$$\int \mathbf{v}\frac{\partial f}{\partial t}d\mathbf{v} + \int \mathbf{vv}\cdot\frac{\partial f}{\partial \mathbf{x}}d\mathbf{v} + \int \mathbf{va}\cdot\frac{\partial f}{\partial \mathbf{v}}d\mathbf{v} = 0\ . \tag{2.3.8}$$

The first term gives $\frac{\partial}{\partial t}\langle n\mathbf{v}\rangle$. The second may be rewritten as

$$\int \mathbf{vv}\cdot\frac{\partial f}{\partial \mathbf{x}}d\mathbf{v} = \frac{\partial}{\partial \mathbf{x}}\cdot\int \mathbf{vv}f d\mathbf{v} = \nabla\cdot\langle n\mathbf{vv}\rangle\ . \tag{2.3.9}$$

The transformation of the third term can best be understood if we give it in full, viz.:

$$\int \mathbf{v}\left\{\frac{q}{m}\left[\mathbf{E}^{(o)} + \mathbf{v}\times\mathbf{B}^{(o)}\right] + \frac{q}{m}\int\left[\mathbf{E}+\mathbf{v}\times\mathbf{B}\right]f(\mathbf{x}',\mathbf{v}',t)\mathbf{dx}'d\mathbf{v}'\right\}\cdot\frac{\partial f}{\partial \mathbf{v}}d\mathbf{v}\ , \tag{2.3.10}$$

where $\mathbf{E}$ is the electric field felt by the particle at x due to the particle at $\mathbf{x}'$. $\mathbf{E}^{(o)}$ is dealt with in the same way as the velocity independent forces above, as is the term involving the integral. The $\mathbf{v}\times\mathbf{B}^{(o)}$ term is dealt with as above, and so Eq. 2.3.10 becomes

$$\frac{nq}{m}\left\{\mathbf{E}^{(o)} + \mathbf{v}\times\mathbf{B}^{(o)} + \int\left[\mathbf{E}+\mathbf{v}\times\mathbf{B}\right]f(\mathbf{x}',\mathbf{v}',t)d\mathbf{x}'d\mathbf{v}'\right\}\ . \tag{2.3.11}$$

To be consistent with the analysis above, and to avoid having to perform complex integrals in order to find the acceleration term, we do the integral over $\mathbf{v}'$ in Eq. 2.3.11 and obtain

$$\begin{aligned} & \frac{nq}{m}\left[\mathbf{E}+\mathbf{v}\times\mathbf{B}\right]\ , \\ \mathbf{E} &= \mathbf{E}^{(o)} + \int\frac{nq}{4\pi\epsilon_o}\frac{\mathbf{x}-\mathbf{x}'}{|\mathbf{x}-\mathbf{x}'|^3}\mathbf{dx}'\ , \\ \mathbf{B} &= \mathbf{B}^{(o)} + \int\frac{\mu_o q n}{4\pi}\frac{\mathbf{v}\times(\mathbf{x}-\mathbf{x}')}{|\mathbf{x}-\mathbf{x}'|^3}\mathbf{dx}'\ . \end{aligned} \tag{2.3.12}$$

The first moment of the Vlasov equation is thus:

$$\frac{\partial}{\partial t}\langle n\mathbf{v}\rangle + \nabla\cdot\langle n\mathbf{vv}\rangle = \frac{nq}{m}\left[\mathbf{E}+\mathbf{v}\times\mathbf{B}\right]\ . \tag{2.3.13}$$

This is the *momentum equation* and can be viewed as expressing Newton's second law for a differential element of a fluid. The time rate of change and flux of momentum across the surface of the element are balanced by the electromagnetic fields, which act as sources of momentum. Taken along with Eq. 2.3.7, we have a simplified picture of a plasma. Eq. 2.3.7 can be viewed as an equation for n (zeroth moment), given $\mathbf{v}$(first moment), while Eq. 2.3.13 determines $\mathbf{v}$ given $\mathbf{vv}$ (second moment). The process described above could be continued to third moments and beyond, but in no case would there arise a closed set of equations. The system of two equations derived above will, in fact, be sufficient for the study of plasma waves later in this thesis, once we have added some extra assumptions concerning the plasma structure.

2.4 The Cold Plasma Approximation

If thermal motion is neglected, then the plasma is said to be *cold*, which means that all particles move at the fluid velocity, so that the distribution function contains a delta function:

$$f(\mathbf{x},\mathbf{v},t) = n(\mathbf{x},t)\,\delta(\mathbf{v}-\mathbf{v}_s)\ . \tag{2.4.1}$$

Then the momentum equation becomes, on using the subscript s to denote the species of interest;

$$\frac{\partial}{\partial t}(n_s\mathbf{v}_s) + \nabla\cdot(n_s\mathbf{v}_s\mathbf{v}_s) = \frac{n_s q_s}{m_s}[\mathbf{E}+\mathbf{v}_s\times\mathbf{B}]\ . \tag{2.4.2}$$

Expanding the divergence term and using the continuity equation, gives Eq. 2.4.2 its more normal form, viz.

$$\frac{\partial \mathbf{v}_s}{\partial t} + (\mathbf{v}_s\cdot\nabla)\mathbf{v}_s = \frac{q_s}{m_s}[\mathbf{E}+\mathbf{v}_s\times\mathbf{B}]\ . \tag{2.4.3}$$

To complete this plasma model we need an easier description of the evolution of the electromagnetic field than that encapsulated in Eq. 2.2.3, which requires knowledge of the positions of all particles; precisely the level of detail which we were trying to avoid. This description is provided by Maxwell's equations:

$$\begin{aligned} \nabla\times\mathbf{E} = -\frac{\partial\mathbf{B}}{\partial t} \quad &, \quad \nabla\times\mathbf{B} = \mu_o\mathbf{J} + \mu_o\epsilon_o\frac{\partial\mathbf{E}}{\partial t}\ , \\ \nabla\cdot\mathbf{E} = \frac{\rho}{\epsilon_o} \quad &, \quad \nabla\cdot\mathbf{B} = 0\ , \end{aligned} \tag{2.4.4}$$

where ϵ_o and μ_o are, respectively, the permittivity and permeability of free space and the speed of light in vacuo, $c = (\epsilon_o\mu_o)^{-1/2}$. To employ these for a plasma containing M species, we must also note that the charge density and current are given by

$$\rho = \sum_{s=1}^{M} q_s n_s \quad , \quad \mathbf{J} = \sum_{s=1}^{M} n_s q_s \mathbf{v}_s\ . \tag{2.4.5}$$

The mathematical description of a cold plasma is now complete and comprises equations 2.3.7, 2.4.3, 2.4.4, 2.4.5. This description will be used extensively in what follows.

2.5 Waves: The Cold Plasma Dispersion Relation

Waves in a cold, uniformly magnetised plasma are a benchmark for analysing and understanding other, more complex wave modes, and provide in themselves a useful illustration of much pertinent physics.

To perform this derivation, we seek linear wave solutions to the cold plasma model. Assuming a spatially and temporally uniform magnetic field , $\mathbf{B}_o$, pointing in the z-direction at every point in space, and setting all solutions proportional to $\exp i\,(\mathbf{k}\cdot\mathbf{x}-\omega t)$, the two Maxwell curl equations may be combined to obtain

$$\mathbf{k}\times\mathbf{k}\times\mathbf{E} = i\omega\mu_o\mathbf{J} + \frac{\omega^2}{c^2}\mathbf{E}\,, \tag{2.5.1}$$

where $\mathbf{E}$ and $\mathbf{J}$ now denote small perturbations to the equilibrium situation. Eq. 2.5.1 could be written down for any medium; to solve for the situation in hand, the remaining model equations must be used to express the current in terms of electric field. The contribution to the velocity from species s is

$$\mathbf{v}_s = \frac{i\omega q_s}{m_s\left(\omega^2-\Omega_s^2\right)}\left\{\mathbf{E}+\frac{\Omega_s}{i\omega}\mathbf{E}\times\hat{\mathbf{z}}-\frac{\Omega_s^2}{\omega^2}\hat{\mathbf{z}}\mathbf{E}\cdot\hat{\mathbf{z}}\right\}\,, \tag{2.5.2}$$

where we have introduced the *algebraic gyrofrequency* for species s, defined as $\Omega_s = \frac{q_s|B|}{m_s}$, so that Ω_s has the same sign as q_s. It is conventional to introduce the refractive index, $\mathbf{n}$, such that $\mathbf{n} = \mathbf{k}c/\omega$, and to express its direction in terms of θ, the angle between the propagation vector and the z-axis. Then the wave equation may be expressed as

$$\begin{bmatrix} S-n^2\cos^2\theta & -iD & n^2\cos\theta\sin\theta \\ iD & S-n^2 & 0 \\ n^2\cos\theta\sin\theta & 0 & P-n^2\sin^2\theta \end{bmatrix}\begin{bmatrix} E_x \\ E_y \\ E_z \end{bmatrix} = 0\,, \tag{2.5.3}$$

where we have used the notation of Stix (1992), in which,

$$S = 1-\sum_j\frac{\omega_{pj}^2}{\omega^2-\Omega_j^2}\,, \qquad D = \sum_j\frac{\Omega_j\omega_{pj}^2}{\omega\left(\omega^2-\Omega_j^2\right)}\,,$$

$$P = 1-\sum_j\frac{\omega_{pj}^2}{\omega^2}\,,$$

$$R = S+D\,, \qquad L = S-D\,. \tag{2.5.4}$$

Here, the *plasma frequency* for the jth species has been defined as $\omega_p = \sqrt{\frac{n_{oj}q_j^2}{\epsilon_o m_j}}$. The symbols R, L, S, D, P are not arbitrary. R and L stand for right and left, since equating these terms to zero gives, respectively, right and left circularly polarised waves, S and D stand for sum and difference (of R and L), while P stands for plasma, since requiring this term to be zero gives the dispersion relation for plasma oscillations. For future convenience, note that the dielectric tensor is given by

$$\epsilon = \begin{bmatrix} S & -iD & 0 \\ iD & S & 0 \\ 0 & 0 & P \end{bmatrix}\,. \tag{2.5.5}$$

This tensor is Hermitian ($\epsilon^{\dagger} = \epsilon$), and does not depend on $\mathbf{k}$.

For a non-trivial solution of the cold plasma equations, we must set the determinant of the matrix on the right-hand side of Eq. 2.5.3 equal to zero. This condition leads to a quartic equation for the allowed values of n, given ω (the sixth degree terms cancel out). The equation is, in fact, biquadratic, so that roots occur in pairs of the same magnitude, corresponding to two otherwise identical waves travelling in opposite directions. There can be no surprise about this conclusion, since our model contained no dissipation mechanisms. The medium is anisotropic, however, with the equilibrium magnetic field giving a preferred direction. Because of this, two obvious special cases present themselves; propagation parallel to, and perpendicular to, $\mathbf{B}_o$. In the parallel case, the determinant condition becomes,

$$\begin{vmatrix} S-n^2 & -iD & 0 \\ iD & S-n^2 & 0 \\ 0 & 0 & P \end{vmatrix} = 0 \,. \tag{2.5.6}$$

Expanding by the last row gives $P = 0$ as one solution, while, after a little reduction, the other factor gives $n^2 = R, L$. For perpendicular propagation,

$$\begin{vmatrix} S & -iD & 0 \\ iD & S-n^2 & 0 \\ 0 & 0 & P-n^2 \end{vmatrix} = 0 \,. \tag{2.5.7}$$

Expanding as before, the solutions are $n^2 = P$, and $n^2 = RL/S$. It is easy to see from Eq. 2.5.3 that the first solution corresponds to E_x and E_y being zero. Therefore, this mode has only E_z non-zero, and from Eq. 2.5.2, the velocity of all species is also along the z axis, so that the plasma experiences no magnetic forces, and the dynamics are unaffected by the magnetic spine. This mode is called the *ordinary* mode (or O-mode). The other solution has $E_z = 0$, and the other two components non-zero. This is the *extraordinary* mode.[1]

2.6 Waves: The CMA Diagram

The possible forms of wave motion in a uniformly magnetised cold plasma can be conveniently summarised using the CMA (Clemmow, Mullaly, Allis) diagram. This is a map of parameter space for the plasma model we have just discussed. For an electron plasma, the space is two-dimensional, and the two independent parameters

[1] Compared to more elementary forms of wave motion, this mode is indeed extraordinary, since it is both transverse and longitudinal!

Figure 2.1: The CMA diagram for an electron plasma

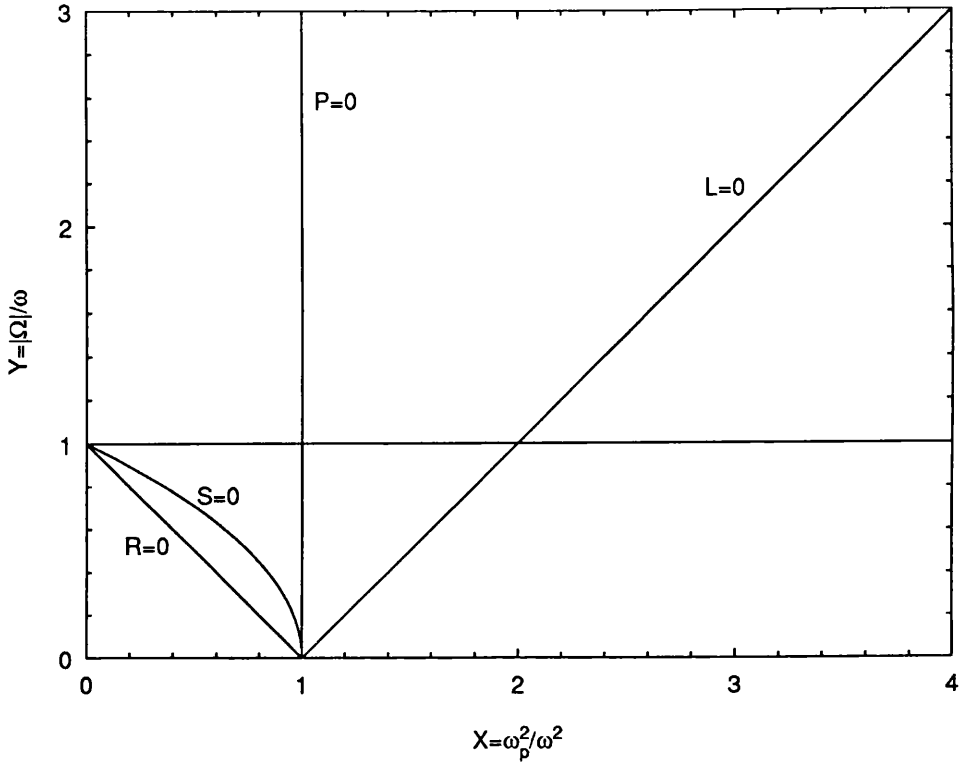

(density and magnetic field strength) can be neatly plotted in dimensionless form as ω_p^2/ω^2 and Ω/ω (other choices are sometimes used). The solutions described in section 2.5 may be expected to occur only in certain regions of this parameter space, each type of solution having conditions which must be satisfied if it is to propagate. Regions of propagation and evanescence are separated by boundaries on which some of the quantities in Eq. 2.5.3 change sign. [2] The CMA diagram for an electron plasma is given in Figure 2.1.

[2]More pedantically, the boundaries enclose regions in which the wave normal surface is topologically invariant.

Chapter 3

Analyses Of Non-Uniform Plasmas

3.1 Overview

The analysis of waves in non-uniform media is hard. Familiar procedures no longer apply and methods to replace them are rare and applicable only to special cases. In this chapter, existing methods are critically examined and the work of the rest of this thesis is placed in context.

In the first chapter, a number of situations were examined where plasmas were far from uniform. We wish to know the behaviour of waves in such media, and in particular, the manner in which a wave may convert into a physically distinct mode. *Mode conversion* is the process by which one type of wave, in passing through a non-uniform medium, may change its characteristics until, at some point it closely resembles another mode in wavelength (at that point). This may result in an admixture of the second mode, even though there was none in the original wave. It should be emphasised that the mode conversion studied in this thesis is based on purely linear processes. Owing to coupling between field components, normal modes of the plasma are position dependent. Any effects caused by nonlinearities of the dependent variables in the governing equations will appear in addition to those studied here.

We may identify as a recurring theme the problem of obtaining appropriate ordinary differential equations [1] to model the propagation of non-uniform waves.

[1] Hereinafter referred to as odes.

3.2 The Dispersion Relation

This is the result of Fourier transforming the governing equations for waves in a medium, (equivalently, it may be assumed that quantities vary as $\exp i\,(\mathbf{k}\cdot\mathbf{x}-\omega t)$) so that differential equations are transformed into algebraic ones which are, in general, easier to solve. From a more practical point of view, a dispersion relation gives either the allowed wavenumbers of waves of a given frequency, or shows whether perturbations of a certain wavelength will be damped or grow (depending on the sign of the imaginary part of ω). The underlying mathematical fact which makes this technique work is that Fourier transforming a derivative gives a term proportional to the variable transformed to. Linearity then tells us that we may transform any linear differential operator with constant coefficients, and obtain a polynomial in the new variable. It is fortunate that so many physical situations may be described by linear differential equations with constant coefficients. It is unfortunate that when more complex or detailed situations are modelled, we frequently encounter non-constant coefficients in the equations.

In principle, other properties of Fourier transforms can be brought into play so that the integrals involved may be re-written in a way which leads once more to an equation more easily solved than the original. This approach has been used by Brownell(1973), who uses the fact that the Fourier transform changes polynomials in configuration space into derivatives in wavenumber space, of order equal to the degree of the polynomial. This technique can be applied to a number of problems, but is clearly limited in scope. It is likely to be successful in cases where the original equation has coefficients which contain only low powers, since the resulting equation will be of low order and more likely to be easily solved. However, this is precisely the case where the original equation is most likely to be soluble directly (by a hypergeometric function, for instance). In many cases the exact coefficients are complex and a polynomial fit is chosen in order to use this method, but being limited to a low-degree obviously makes the approximation poor. In particular, polynomials are not good at approximating the singularities which may occur in the exact coefficients and which may be essential to physical understanding.

3.3 The Local Dispersion Relation

This is an approach introduced by Stix (1965), who used it to analyse the conversion of a cold plasma wave into a hot mode at a cold plasma resonance, and which has

been greatly used in much recent work. It starts from the plausible assumption that, if the plasma parameters vary sufficiently slowly then, locally, the governing differential equation has approximately constant coefficients, the gradient terms being small. In this case, a *local dispersion relation* can be introduced.

The technique normally used is to obtain a relevant dispersion relation, by judicious approximation of the appropriate version of the dielectric tensor. This often involves using the full Maxwell-Vlasov dielectric tensor and expanding in the Larmor radius ${\rho_L}^2$, or in ratios of characteristic frequencies which are assumed to be small. This leads to a dispersion relation which is a polynomial in the components of the wavenumber and is valid in a certain region of space and range of parameters, and, strictly, is limited to cases where an exact Fourier transform of the differential equation can be found. This is then transformed into an ode using the mapping

$$k_j \rightarrow -id/dx_j \ , \tag{3.3.1}$$

where x_j is the propagation direction of interest. This assignment is known as the *inverse Fourier transform* and it enables a simple set of odes to be derived, representing the coupling of a chosen set of modes.

This is clearly a powerful and straightforward method, but the basic argument, though compelling, is flawed. A mode conversion process owes its existence to gradients of plasma parameters, precisely the feature omitted in this model. The re-introduction of variable parameters later in the analysis does not allow gradient terms to be taken account of. A term $\frac{d}{dx}[a(x)y]$ in the model becomes iak in the local dispersion relation, and then $a(x)\frac{dy}{dx}$ when the inverse Fourier transform is applied, rather than the correct form $a(x)\frac{dy}{dx} + y\left(\frac{da}{dx}\right)$.

In the light of objections to the simplistic application of Eq. 3.3.1, two approaches of rather more complexity have evolved, which are usually named after their progenitors.

3.3.1 Fuchs, Ko, Bers

This approach takes the local dispersion relation as its starting point. This can be written as $D(k, z) = 0$, where the dispersion relation in the physical variable x has been analytically continued to produce an n-valued function, mapping z onto k (physically, there are several distinct modes at each position). Mode conversion here is the redistribution of energy between the different branches of k. Usually,

[2] Actually in ρ_L/λ and ρ_L/L, where λ is the wavelength of the perturbed fields and L is the inhomogeneity scale length

attention is restricted to a pair of modes, with the coupling of other waves to these two being taken as negligible, and an *embedded dispersion relation* is extracted, which we denote by $\hat{D}(k,z)$. The authors show that a mode conversion point occurs when we have a saddle point of $\hat{D}(k,z)$, which satisfies

$$\hat{D}(k(z),z)=0\ ,\quad \frac{\partial \hat{D}(k(z),z)}{\partial k}=0\ ,\quad \frac{\partial^2 \hat{D}(k(z),z)}{\partial k^2}\neq 0\ . \tag{3.3.2}$$

Within this picture, the ode obtained by the transform Eq. 3.3.1 is

$$y''+\mathcal{Q}(z)y=0\ ,\quad \mathcal{Q}(z)=-2\hat{D}(k(z),z)\,/\frac{\partial^2 \hat{D}}{\partial k^2}\ . \tag{3.3.3}$$

The mathematical detail is considerable because of the involved complex analysis used, (see Fuchs, Ko, Bers, (1981)), however the starting point is still the local dispersion relation and so an inconsistency enters at the very outset of the argument.

3.3.2 Cairns, Lashmore-Davies

This technique assumes that there are differential equations governing the propagation of any two modes, which are independent, except in a region of space where a mode conversion event is likely to occur (i.e. where local wavenumbers are nearly equal). Again, the starting point is the local dispersion relation, which is written, in the vicinity of the conversion region as,

$$[\omega-\omega_1(k,x)]\,[\omega-\omega_2(k,x)]=\eta(k,x)\ , \tag{3.3.4}$$

where we have taken one dimensional motion for clarity, and η is a quantity arising from the approximate factorisation: it contains information about the other modes and is only significant in the conversion region. Suppose that, for frequency ω_0, at x_0, there is a mode conversion point, where the value of k is k_0. Then, Taylor expanding about this point, with

$$k=k_0+\delta\ ,\quad x=x_0+\xi\ , \tag{3.3.5}$$

we obtain

$$\begin{aligned}\omega_1 &\simeq \omega_o+\frac{\partial\omega_1}{\partial k}\,|_{x_o,k_o}\,\delta\ +\ \frac{\partial\omega_1}{\partial x}\,|_{x_o,k_o}\,\xi \stackrel{\partial}{=} \omega_o+a\delta+b\xi\ ,\\ \omega_2 &\simeq \omega_o+\frac{\partial\omega_2}{\partial k}\,|_{x_o,k_o}\,\delta\ +\ \frac{\partial\omega_2}{\partial x}\,|_{x_o,k_o}\,\xi \stackrel{\partial}{=} \omega_o+f\delta+g\xi\ .\end{aligned} \tag{3.3.6}$$

Substituting this into Eq. 3.3.4 and using Eq. 3.3.1, gives the operator equation

$$\left[i\frac{d}{dx}-k_o+\frac{b}{a}\xi\right]\left[i\frac{d}{dx}-k_o+\frac{g}{f}\xi\right]=\frac{\eta_o}{af}\ . \tag{3.3.7}$$

It is now possible to assign wave amplitudes and to distribute the coupling symmetrically between the two equations so obtained:

$$\begin{aligned} \frac{d\phi_1}{d\xi} - i\left(k_o - \frac{b}{a}\xi\right)\phi_1 &= i\lambda\phi_2 \,, \\ \frac{d\phi_2}{d\xi} - i\left(k_o - \frac{g}{f}\xi\right)\phi_2 &= i\lambda\phi_1 \,, \end{aligned} \tag{3.3.8}$$

where $\phi_{1,2}$ are the wave amplitudes and $\lambda = \sqrt{\eta_o/af}$. η_o is the value of the coupling function at the mode conversion point. The coupled set of equations 3.3.8 can be combined into a second order equation, which can be transformed into the Weber equation (for details see Cairns, Lashmore-Davies (1983)). Asymptotic solutions of the Weber equation are then used to show how energy has been redistributed among the available channels.

A number of objections may be raised to this procedure. The manner of assigning the dependent variables is rather arbitrary, and is different from the approach of Fuchs, Ko and Bers. The structure of Eq. 3.3.8 is intuitively appealing, expressing as it does the idea of two interacting waves. However, the coupling term is taken as constant in the coupling region, whereas we know that such coupling arises from non-uniform plasma parameters in that region, which are, of course, absent from the local dispersion relation, so that there would seem to be a basic inconsistency in this approach. One might also question the validity of using an asymptotic expansion to solve an equation which applies close to one particular point.

3.4 Later Developments

Driven by the progress in experimental programs over the last decade and fueled by the need for a non-Ohmic heating source, the local dispersion relation has been extensively used. Recent papers by Swanson and Hu (1993), for example, perpetuate this method without comment, and use it in the study of propagation near cyclotron harmonics. An alternative strategy is seen in the recent work of Cairns and Lashmore-Davies, who, with a number of co-workers, have produced a different analysis of this situation, using kinetic theory. (See Cairns et al, 1991, McDonald, Cairns, Lashmore-Davies, 1994.) This promising line of enquiry derives an integral equation for the Fourier transform of the vector potential. Using the approximation $k\rho_L \ll 1$, one may derive a second order ode governing the electric field behaviour in this region, together with a conservation law, with no reference to any local dispersion relation. Higher order odes may be obtained by including more terms in the

$k\rho_L$ expansion. Unfortunately, the analysis at present only deals with equilibrium magnetic fields of the form $B_o\hat{\mathbf{z}}(1 + x/L)$.

Another noteworthy paper is Choudhury (1988), in which waves in a cylindrical plasma are analysed in the lower hybrid range of frequencies and with assumptions appropriate for tokamaks. Equilibrium flows are retained, and the model made manageable by expanding in $B_{o\theta}/|\mathbf{B}_o|$ (the toroidal field is small) and assuming $E_z = 0$ (high conductivity along magnetic field lines shorts out the electric field). Two coupled first order odes for field amplitudes are obtained. Again, the local dispersion relation concept is not used.

If progress is to be made in complex non-uniform wave propagation problems, the mindset involved in trying to reduce all cases to embroidered versions of the uniform case will have to be abandoned. In the light of the above experience, we adopt the following principle: that mode conversion processes should be tackled by deriving full and consistent equations within our chosen model framework, and that these equations should be solved numerically or analytically with, as far as is possible, no further approximations.

3.5 The WKB Method

This is a technique which is frequently used in the study of non-uniform wave propagation. It is named after Wentzel, Kramers and Brillouin, who used it in connection with problems in quantum mechanics, although it is, in fact, much older. Heading (1962) gives a detailed account, here the main points of the method are reviewed.

Briefly, the WKB method states that if $y(z)$ satisfies

$$y'' + \Theta(z)\, y = 0\,, \tag{3.5.1}$$

where Θ is a continuous function which tends to a finite constant as $z \to \infty$, and which satisfies $|\Theta'/\Theta| \ll 1$ and $|\Theta''/\Theta| \ll 1$, for all $|z| > z_c$ for some z_c, then the solutions of Eq. 3.5.1 are

$$y_{1,2} = \left\{\Theta^{-1/4} \exp\left[\pm i \int^z \Theta^{1/2} ds\right]\right\}\left\{1 + \mathcal{O}\left(\Theta'/\Theta, \Theta''/\Theta\right)\right\}\,. \tag{3.5.2}$$

In fact, a WKB solution is the first term in an asymptotic expansion of the solution of the ode in question, so that the WKB solutions can be made arbitrarily accurate by choosing z sufficiently large. This is an enormously useful fact; it means that we can start with an accurate analytic form for a solution for $z \gg 0$, analytically continue this solution and trace it round to $z \ll 0$, thus obtaining important

information about the relationship between the modes entering a region where non-uniformity exists, and the modes leaving. In particular, a *connection formula* may be derived, explicitly showing what mixture of asymptotic solutions for $z \ll 0$ an asymptotic solution for $z \gg 0$ will turn into. The changes which a solution undergoes on tracing it through the complex plane, arise from the *Stokes phenomenon.* The equation which we are attempting to solve, has a unique Taylor series expansion (in general, a Laurent series). This will have a different set of powers from the asymptotic expansion, and so, to remain close in value to the exact solution, the coefficients in the asymptotic expansion suffer a number of discontinuous jumps in value (*Stokes discontinuities*). This is permissible in a solution which is supposedly continuous because there is an error involved in using the WKB solutions in the first place, which is larger than the jump in value.

When the real part of the argument of the exponential in Eq. 3.5.2 is positive, then the solution contains a factor of the form *exp*(positive number) and is said to be *dominant*, if it is negative, the factor is *exp*(negative number) and the solution is *subdominant.* Clearly, the solution Eq. 3.5.2 changes from dominant to subdominant when

$$\Im\left\{\int_{z_0}^{z} \Theta^{1/2} ds\right\} = 0 \,. \tag{3.5.3}$$

The curves in the complex plane which satisfy this condition are called *Anti-Stokes lines* and, along them, neither solution is dominant. Also significant are *Stokes lines*, which are found where

$$\Re\left\{\int_{z_0}^{z} \Theta^{1/2} ds\right\} = 0 \,. \tag{3.5.4}$$

On these lines, the dominancy or subdominancy of a solution is very pronounced, and it is conventional to introduce the Stokes discontinuities in the subdominant solution on these lines, in order to minimise the error involved. Therefore, crossing a Stokes line 'switches on' an admixture of the (currently) subdominant solution.

3.5.1 Labelling of Modes In Higher Order Systems

There is some difficulty in labelling which mode is which in a complex propagation problem. When non-uniform media are involved, there is some ambiguity about what constitutes a 'mode', since the Fourier transform, by which this is usually defined, is not meaningful. The method set out below shows how this difficulty can be circumvented, and deeper physical understanding introduced at the same time.

Suppose a wave propagation problem is governed by an nth order differential equation. We can express this as a system of n first order equations, which may be

written

$$\mathbf{y}' = \mathsf{M}\mathbf{y} \,, \tag{3.5.5}$$

where $'$ denotes differentiation with respect to z, the independent variable in the problem. If the vector of dependent variables is now transformed by setting $\mathbf{y} = \mathsf{A}\mathbf{u}$ and the equation pre-multiplied by A^{-1}, then the system becomes

$$\mathbf{u}' = \mathsf{A}^{-1}\mathsf{M}\mathsf{A}\mathbf{u} - \mathsf{A}^{-1}\mathsf{A}'\mathbf{u} \,. \tag{3.5.6}$$

If the transformation A is chosen so that $\mathsf{A}^{-1}\mathsf{M}\mathsf{A}$ is diagonal, then the first term in Eq. 3.5.6 is particularly simple. For this to happen, A must be a matrix of eigenvectors of M. The associated position-dependent eigenvalues, $\lambda_i(z)$, which occur along the diagonal of $\mathsf{A}^{-1}\mathsf{M}\mathsf{A}$, then have a special significance. If the final term in Eq. 3.5.6 is negligible, then the system of equations may be easily solved to give

$$u_i(z) = C_i \exp\left[\int^z \lambda_i(s)ds\right] \,, \tag{3.5.7}$$

where C_i is an arbitrary constant, so that the eigenvalues are effectively wavenumbers in this limit. The λ_i are very useful for understanding non-uniform wave propagation because of this property of being 'generalised wavenumbers'. The last term in 3.5.6 is not diagonal, and can be viewed as modelling the coupling of the n different modes together, with the (i,j) element of $\mathsf{A}^{-1}\mathsf{A}'$ giving the coupling of mode i with mode j. This can be made more precise by examining the form of these elements in terms of the eigenvalues. In fact, these can be shown to be,

$$A_{ii} = \lambda_i' \sum_{k=1,k\neq i}^{n} \frac{1}{\lambda_i - \lambda_k} \,, \quad A_{ij} = \lambda_j' \frac{\prod_{k=1,k\neq i,j}^{n}(\lambda_j - \lambda_k)}{\prod_{k=1,k\neq i}^{n}(\lambda_i - \lambda_k)} \,, \tag{3.5.8}$$

for the diagonal and off-diagonal terms respectively. From these expressions, it can be seen that mode coupling is large either when the gradient in the eigenvalues is large, or when two modes have nearly equal eigenvalues. The latter case is physically reasonable if we remember that two waves which are close in 'local wavenumber' are likely to couple strongly. Note, however that the concept of local wavenumber introduced here has been consistently arrived at by manipulation of the governing equations, whereas that in the previous section was introduced through the *ad hoc* assumption of an inverse Fourier transform. It is intriguing to note also, that writing out the coupled system for $n = 2$, gives

$$\begin{aligned} u_1' + \left[\frac{\lambda_1'}{\lambda_1 - \lambda_2} - \lambda_1\right] u_1 &= -\frac{\lambda_2'}{\lambda_1 - \lambda_2} u_2 \,, \\ u_2' - \left[\frac{\lambda_2'}{\lambda_1 - \lambda_2} + \lambda_2\right] u_2 &= -\frac{\lambda_2'}{\lambda_1 - \lambda 2} u_1 \,, \end{aligned} \tag{3.5.9}$$

which is of a similar form to the coupled equations derived by the method of Cairns and Lashmore-Davies. However, once again, our prescription is to be preferred, since it derives couplings from the original equation and retains all the physical information found there.

Later, we will use an equivalent description to Eq. 3.5.8, though one derived a little more directly from the governing equations.

The description given in terms of eigenvalues does not solve the problem: that is done by applying the WKB method. But the foregoing is more than just re-labelling, since it enables an intuition for the problem to be formed, and the consideration of expressions like Eq. 3.5.8 shows which couplings are important in a particular parameter range, and which may be neglected. Of course, these are only general indicators of the behaviour to be expected. Diver (1986) gives one example where eigenvalues cross but negligible mode conversion occurs and another where the eigenvalues approach but do not cross, where a lot of mode conversion occurs.

In summary, the WKB method, when used with care and understanding, is a valuable and consistent tool in the analysis of wave motion in mildly non-uniform media.

Chapter 4

Waves In Helical Equilibria

In this chapter some preliminaries to the analysis of mode conversion are discussed. Linear waves in a cold, multi-fluid plasma are investigated by the usual technique of assuming a small perturbation from equilibrium and discarding any non-linear terms. To commence the analysis it is necessary to find out what the equilibrium electric fields and currents are. In the more familiar analysis of waves in a uniformly magnetised plasma, this stage is trivial: since $\nabla \times \mathbf{B}_o$ is zero, there is no current, no equilibrium velocity, and hence no electric field. In the non-uniform case, equilibrium flows always exist, and can be expected to modify the wave modes possible in the plasma.

4.1 A Consistent Equilibrium

Consider equilibria with a helical magnetic field, viz.

$$\mathbf{B}_o = B_o\,(0, f(r), g(r)) \ . \tag{4.1.1}$$

(From this point onwards cylindrical polar coordinates are used.) Any field of this form will give a helical structure, barring where f or g are zero or singular. Using the cold plasma model of Chapter 2, with two species, ions and electrons, gives

$$\begin{aligned}
\frac{\partial n_{os}}{\partial t} \ &+ \ \nabla \cdot (n_{os}\mathbf{v}_{os}) = 0 \ , \\
\frac{\partial \mathbf{v}_{os}}{\partial t} + (\mathbf{v}_{os} \cdot \nabla)\,\mathbf{v}_{os} \ &= \ \frac{q_s}{m_s}\,(\mathbf{E}_o + \mathbf{v}_{os} \times \mathbf{B}_o) \ , \\
\nabla \times \mathbf{E}_o = -\frac{\partial \mathbf{B}_o}{\partial t} \ , \qquad & \nabla \times \mathbf{B}_o = \frac{1}{c^2}\frac{\partial \mathbf{E}_o}{\partial t} - \mu_o \mathbf{J}_o \ , \\
\mathbf{J}_o \ &= \ \sum_s q_s n_{os} \mathbf{v}_{os} \ .
\end{aligned} \tag{4.1.2}$$

where s takes the values i, and e. For simplicity, assume that $\mathbf{E}_o = 0$, $n_{os} =$ constant, and that $\frac{\partial}{\partial t} \equiv 0$, then the equations above reduce to:

$$\nabla \cdot \mathbf{v}_{os} = 0 \,, \qquad (\mathbf{v}_{os} \cdot \nabla)\,\mathbf{v}_{os} = \frac{q_s}{m_s}\mathbf{v}_{os} \times \mathbf{B}_o \,,$$
$$\nabla \times \mathbf{B}_o = \mu_o \mathbf{J}_o \,, \qquad \mathbf{J}_o = \sum_s q_s n_{os} \mathbf{v}_{os} \,. \tag{4.1.3}$$

A completely general solution of these equations would be rather complex. The first implies that $v_{osr} =$ constant$/r$, but we are interested in finding a particular solution which fits our needs, rather than a catalogue of every possible solution, so the constant is chosen to be zero. After a little reduction, this leaves four equations to determine the electron and ion equilibrium velocities. Assuming the electrons and ions to have charges $-e$ and $\mathcal{Z}e$ respectively, where $\mathcal{Z}$ is the atomic number of the ion species, gives

$$-\frac{s_\theta^2}{r} = -\frac{eB_o}{m_e}(s_\theta g - s_z f) \,, \qquad -\frac{t_\theta^2}{r} = \frac{\mathcal{Z}eB_o}{m_i}(t_\theta g - t_z f) \,,$$
$$s_\theta = \mathcal{Z}t_\theta - x_\theta \,, \qquad s_z = \mathcal{Z}t_z - x_z \,, \tag{4.1.4}$$

where,

$$\mathbf{s} = \mathbf{v}_{oe} \,, \quad \mathbf{t} = \mathbf{v}_{oi} \,, \quad \mathbf{x} = \frac{1}{\mu_o n_o e}\nabla \times \mathbf{B}_o \,. \tag{4.1.5}$$

From these a quadratic equation for t_θ may be found, with discriminant

$$\Delta = -\frac{4m_i c^4 \Omega_e^2}{m_e \omega_p^4}\left\{g'^2 - \frac{\omega_p^2}{c^2}\left(1 + \frac{m_e}{m_i}\mathcal{Z}^2\right)\left[rgg' + f\,(rf)'\right]\right\} \,, \tag{4.1.6}$$

where $'$ denotes $\frac{d}{dr}$. Again, what is required is a fairly simple solution, rather than a comprehensive one, therefore we assume that $\Delta = 0$, so that the two solutions of the quadratic merge and we obtain the relatively simple condition on the equilibrium magnetic field:

$$g'^2 - \frac{1}{L^2}\left[rgg' + f\,(rf)'\right] = 0 \,. \tag{4.1.7}$$

Where the scale length L has been defined as

$$L = \frac{c}{\omega_p}\left(1 + \frac{m_e}{m_i}\mathcal{Z}^2\right)^{-\frac{1}{2}} \,, \tag{4.1.8}$$

and the plasma frequency, $\omega_p = \left[\frac{n_o e^2}{\epsilon_o m_e}\right]^{\frac{1}{2}}$ has been introduced. The quantity L will become all too familiar in later pages, so it is appropriate to give its value for a number of familiar plasma situations, where the quantity $\frac{m_e}{m_i}\mathcal{Z}^2$ has been regarded

as negligible:

Type of plasma	$n\ (m^{-3})$	$\omega_p\ (rad\ s^{-1})$	$L = \frac{c}{\omega_p}\ (m)$
Fusion	$10^{19} - 10^{22}$	$2 \times 10^{11} - 6 \times 10^{12}$	$5 \times 10^{-5} - 1.5 \times 10^{-3}$
Solar Corona	$10^{10} - 10^{14}$	$5 \times 10^{6} - 6 \times 10^{8}$	$0.5 - 60$
Solar Atmosphere	$10^{19} - 10^{21}$	$2 \times 10^{11} - 2 \times 10^{12}$	$1.5 \times 10^{-4} - 1.5 \times 10^{-3}$
Interstellar	$10^{4} - 10^{6}$	$6 \times 10^{3} - 6 \times 10^{4}$	$5 \times 10^{3} - 5 \times 10^{4}$

Solving for the electron and ion velocities is now easy, and gives,

$$m_i \mathbf{v}_{oi} + \mathcal{Z} m_e \mathbf{v}_{oe} = \mathbf{0} \,. \tag{4.1.9}$$

Physically, we have assumed that the momenta of the electron and ion fluids balance at every point, so that there is zero net equilibrium momentum in the plasma. If this assumption is made, and Eq. 4.1.7 holds then a consistent equilibrium situation has been achieved which takes into account both the electron and ion species. Equation 4.1.7 constrains, but does not determine, the magnetic field. The more common *force-free field* assumption, in which $\nabla \times \mathbf{B}$ is parallel to $\mathbf{B}$, is equivalent to the term in square brackets in Eq. 4.1.7 being zero.

To further particularise the problem, it is assumed that:

$$f = -\kappa g' \,. \tag{4.1.10}$$

On substitution, this gives a pair of odes for f and g:

$$\begin{aligned} g'' \; + \; \left[1 - \frac{L^2}{\kappa^2}\right] \frac{g'}{\rho} + g = 0 \,, \\ f \; = \; -g' \,, \end{aligned} \tag{4.1.11}$$

where $\rho = \frac{r}{\kappa}$, and $'$ now denotes $\frac{d}{d\rho}$. The first equation may be solved in terms of special functions (Abromowitz & Stegun, 1964), and substituted into the second to obtain

$$\begin{aligned} g \; &= \; A r^{\nu} J_{\nu}\left(\frac{r}{\kappa}\right) + B r^{\nu} Y_{\nu}\left(\frac{r}{\kappa}\right) \,, \\ f \; &= \; -A r^{\nu} J_{\nu-1}\left(\frac{r}{\kappa}\right) - B r^{\nu} Y_{\nu-1}\left(\frac{r}{\kappa}\right) \,, \end{aligned} \tag{4.1.12}$$

where A and B are arbitrary constants, J_{ν} and Y_{ν} are Bessel functions of the first and second kinds of order ν, and $\nu = \frac{L^2}{2\kappa^2}$. This analytic solution includes as special cases,

$$f = -\mathcal{A} \sin\left(\frac{r}{\kappa}\right) \,, \quad g = -\mathcal{A} \cos\left(\frac{r}{\kappa}\right) \tag{4.1.13}$$

for $\nu = \frac{1}{2}$ (i.e. $\kappa = L$),

$$f = 0 \,, \quad g = \text{constant} \,, \tag{4.1.14}$$

for $\kappa \rightarrow \infty$, with L remaining arbitrary, and

$$f = AJ_1\left(\frac{r}{\kappa}\right) \ , \ g = AJ_0\left(\frac{r}{\kappa}\right) \ , \tag{4.1.15}$$

for $L \rightarrow 0$, with κ remaining arbitrary. Since $\nu = 0$ corresponds to the force-free field situation, this last field is also that which occurs in a reversed-field pinch, relaxing to its state of minimum energy (Taylor, 1974). It is clear, then that a well-known equilibrium situation has been generalised. Later, attention will be focussed on Eq. 4.1.13.

4.1.1 Magnetic Field Lines

We know that the magnetic field solutions found are helical, but to find out more information, we need to explicitly find the equations of the field lines. This involves solving the system of equations

$$\dot{\mathbf{x}} = \mathbf{B}_o \ , \tag{4.1.16}$$

where $\dot{}$ denotes differentiation with respect to s, a parameter which varies along the field line, and $\mathbf{x}$ is a position vector. This implies that

$$\frac{rd\theta}{B_{o\theta}} = \frac{dz}{B_{oz}} \ , \tag{4.1.17}$$

or, using Eq. 4.1.1,

$$\frac{rd\theta}{f(r)} = \frac{dz}{g(r)} \ . \tag{4.1.18}$$

Integrating this gives

$$z = \frac{rg(r)}{f(r)}\theta + C \ , \tag{4.1.19}$$

for the equation of a typical field line, where C depends on the line chosen. This is the equation of a helix whose pitch varies with radius. There are two degenerate cases: when $g(r) = 0$, the field is purely azimuthal, while when $f(r) = 0$, it is a uniform field in the z-direction. A graph showing the field vector as a function of x and y is given in Figure 4.1, while Figure 4.2 shows the change in pitch of the helix with radius.

4.2 Linear Wave Solutions

Wave solutions to Eq. 4.1.2 may now be sought. Fourier transforming in time replaces $\frac{\partial}{\partial t}$ with $-i\omega$. A spatial Fourier transform in the coordinates along which quantities do not vary is also possible, but since the primary interest here is in

Figure 4.1: Variation of **B** field with x and y

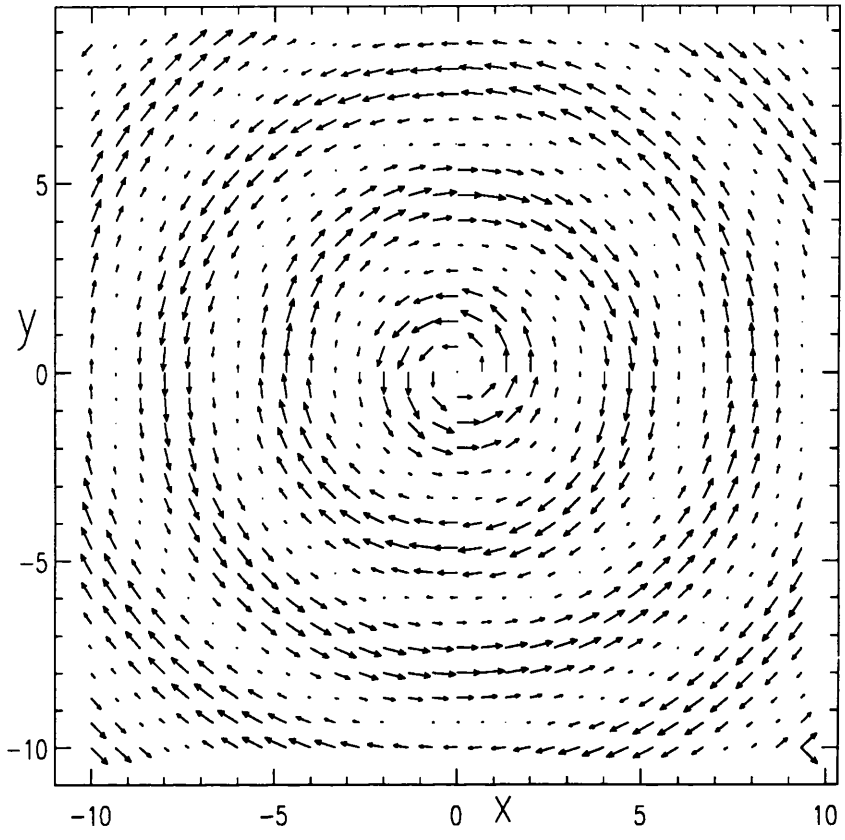

radially travelling waves, for instance in the context of heating tokamak plasmas, we simply assume the azimuthal and z wave numbers to be zero. A radial Fourier transform may in principle be carried out, but its utility is likely to be very limited: transforming a linear ode with constant coefficients in this way gives an algebraic equation, but if the ode has coefficients which are functions of the independent variable there may be no way of proceeding further.

The equations for linear waves, assuming the ion motion to be negligible, are

$$\begin{aligned} -i\omega n + n_o \nabla \cdot \mathbf{v} + \nabla n \cdot \mathbf{v}_o &= 0 \,, \\ m_e \left[-i\omega \mathbf{v} + (\mathbf{v}_o \cdot \nabla)\mathbf{v} + (\mathbf{v} \cdot \nabla)\mathbf{v}_o \right] &= -e \left[\mathbf{E} + \mathbf{v}_o \times \mathbf{B} + \mathbf{v} \times \mathbf{B}_o \right] \,, \\ \nabla \times \nabla \times \mathbf{E} &= i\omega\mu_o \mathbf{J} + \frac{\omega^2}{c^2}\mathbf{E} \,, \\ \mathbf{J} &= -e\left(n_o \mathbf{v} + n \mathbf{v}_o\right) \,, \end{aligned} \tag{4.2.1}$$

where the subscript o denotes an equilibrium quantity, and perturbations are de-

Figure 4.2: Variation of field line pitch with radius

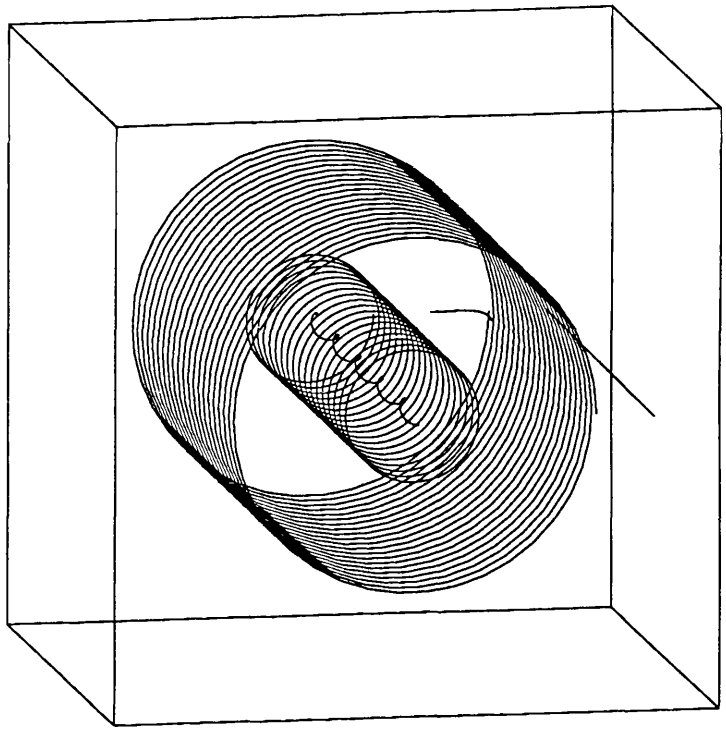

noted by unsubscripted quantities. Notice the complexity of the terms involving $\mathbf{v}_o$, which are absent in the uniform field case. The two Maxwell curl equations have been combined into a wave equation for $\mathbf{E}$. To complete the derivation, we clearly require values for n and $\mathbf{v}$, expressed in terms of $\mathbf{E}$, from the first two equations. One complication which arises is that the cyclotron frequency $e\,|\mathbf{B}|\,/m_e$ is now a function of position. It is convenient to define $\Omega_o = eB_o/m_e$ and $\mathbf{b} = (0, f, g)$. If consistency is sacrificed for the moment and the equilibrium flows are assumed negligible, then by using the momentum equation, together with its dot and cross products with $\mathbf{B}_o$, it is straightforward to show that,

$$\mathbf{v} = \frac{-i\omega e}{m\,(\omega^2 - \Omega^2)} \left[\mathbf{E} + \frac{\Omega_o}{i\omega} \mathbf{E} \times \mathbf{b} - \frac{\Omega_o^2}{\omega^2} \mathbf{b}\,(\mathbf{E} \cdot \mathbf{b}) \right] , \qquad (4.2.2)$$

where $\Omega^2 = \Omega_o^2(f^2 + g^2)$ which is just what would be expected from the simple-minded generalisation of Eq. 2.5.2. Using the variable $\rho = \frac{r}{\kappa}$, and eliminating E_r

from the resulting equation gives

$$\left[\frac{1}{\rho}(\rho E_\theta)'\right]' + \frac{\kappa^2}{L^2}\left\{\left[\frac{\omega^2-\omega_p^2}{\omega_p^2}+\beta g^2\right]E_\theta - \beta f g E_z\right\} = 0\,,$$

$$\frac{1}{\rho}[\rho E_z']' + \frac{\kappa^2}{L^2}\left\{\left[\frac{\omega^2-\omega_p^2}{\omega_p^2}+\beta f^2\right]E_z - \beta f g E_\theta\right\} = 0\,, \qquad (4.2.3)$$

where $'$ denotes $\frac{d}{d\rho}$, and

$$\beta = \frac{-\Omega_o^2}{(\omega^2-\Omega^2-\omega_p^2)}\,. \qquad (4.2.4)$$

Notice that Eqs. 4.2.3 do not have any singularity caused by the electron cyclotron resonance, in contrast to Eq. 4.2.2. Only the upper hybrid resonance occurs here. However, because of the variation of cyclotron frequency with radius, Eq. 4.2.3 will usually be singular at one or more values of radius, although perfectly well behaved outwith this set of points. In the analysis of waves in a uniformly magnetised plasma resonances occur at every point, or nowhere, so that at certain frequency values, the model may break down. In this case, resonant surfaces will have to be dealt with in any general attempt to solve Eq. 4.2.3. It is possible to avoid this difficulty entirely, by choosing the magnetic field given by Eq. 4.1.13, which gives $\mathbf{B}_0$ a constant magnitude and corresponds to choosing $\kappa = L$. The coupled equations for electric field then take the form,

$$\left[\frac{1}{\rho}(\rho E_\theta)'\right]' + \left[a+\frac{b}{2}+\frac{b}{2}\cos(2\rho)\right]E_\theta - \frac{b}{2}\sin(2\rho)\,E_z = 0\,,$$

$$\frac{1}{\rho}[\rho E_z']' + \left[a+\frac{b}{2}-\frac{b}{2}\cos(2\rho)\right]E_z - \frac{b}{2}\sin(2\rho)\,E_\theta = 0\,, \qquad (4.2.5)$$

where $a = \left(\omega^2-\omega_p^2\right)/\omega_p^2$ and $b = \beta$.

Simplified as they are, Eq. 4.2.5 are not trivial to solve. From their general form solutions in terms of any of the familiar special functions of analysis cannot be expected: the presence of sin and cos in the coefficients means that solutions in terms of hypergeometric functions are not possible. If the coupling terms are ignored, both of Eq. 4.2.5 have the form of Mathieu equations, but this similarity is not enough to produce a solution in terms of Mathieu functions.

The next section explains one analytic method which may be applied.

4.3 Asymptotic Solutions

The technique used here is similar to that explained in Diver, Laing, Sellar (1989), where an exact dispersion relation is obtained for waves in a spatially sheared magnetic field. This is no coincidence as, far from the origin, the field lines may be approximated as simply sheared.

If the dependent variables are changed to,

$$X = \sqrt{\rho} E_\theta \ , \ \ Y = \sqrt{\rho} E_z \ , \tag{4.3.1}$$

then the equations 4.2.5 are put into standard form and become,

$$\begin{aligned} X'' + \left[a + \frac{b}{2} + \frac{b}{2}\cos(2\rho) - \frac{3}{4\rho^2} \right] X &= \frac{b}{2}\sin(2\rho)\, Y \ , \\ Y'' + \left[a + \frac{b}{2} - \frac{b}{2}\cos(2\rho) + \frac{1}{4\rho^2} \right] Y &= \frac{b}{2}\sin(2\rho)\, X \ . \end{aligned} \tag{4.3.2}$$

Ignoring terms of order $1/\rho^2$, and changing to variables R and S, defined by,

$$R = e^{i\rho}(X + iY) \ , \ \ S = e^{-i\rho}(X - iY) \ , \tag{4.3.3}$$

Eq. 4.3.2 becomes

$$\begin{aligned} R'' - 2iR' + R\left[a + \frac{b}{2} - 1 \right] + \frac{b}{2} S &= 0 \ , \\ S'' + 2iS' + S\left[a + \frac{b}{2} - 1 \right] + \frac{b}{2} R &= 0 \ . \end{aligned} \tag{4.3.4}$$

The equations now have constant coefficients, and so may be Fourier transformed by setting $R = me^{i\sigma\rho}$ and $S = ne^{i\sigma\rho}$ to produce a dispersion relation. In addition the quantity m/n may be determined in terms of σ, giving

$$\sigma^2 = a + \frac{b}{2} + 1 \pm \sqrt{4a + \frac{b^2}{4} + 2b} \ , \tag{4.3.5}$$

$$\frac{m}{n} = \frac{b}{2\sigma^2 - 4\sigma - 2a - b + 2} \ . \tag{4.3.6}$$

The number of travelling wave solutions for each set of values of a and b can now easily be found by requiring that σ is real, and that $\sigma^2 > 0$. Figure 4.3 shows this information about spatial behaviour of harmonic waves graphically. One solution here corresponds to two physical solutions, travelling in opposite directions.

Although it is convenient to use the parameters a and b, it is important to relate these quantities to the physical parameters ω and Ω_o. Not all choices of a and b give harmonic time dependances. The condition for ω to be real, is

$$a = \frac{\omega^2}{\omega_p^2} - 1 \geq -1 \ . \tag{4.3.7}$$

All other a values give imaginary frequencies, corresponding to waves which are exponentially damped or amplified. In addition, for physical results, the cyclotron frequency must be positive, and if we use the easily provable fact that

$$\frac{\Omega_o^2}{\omega_p^2} = \frac{ab}{b-1} \ , \tag{4.3.8}$$

Figure 4.3: Number of travelling wave solutions in regions of parameter space

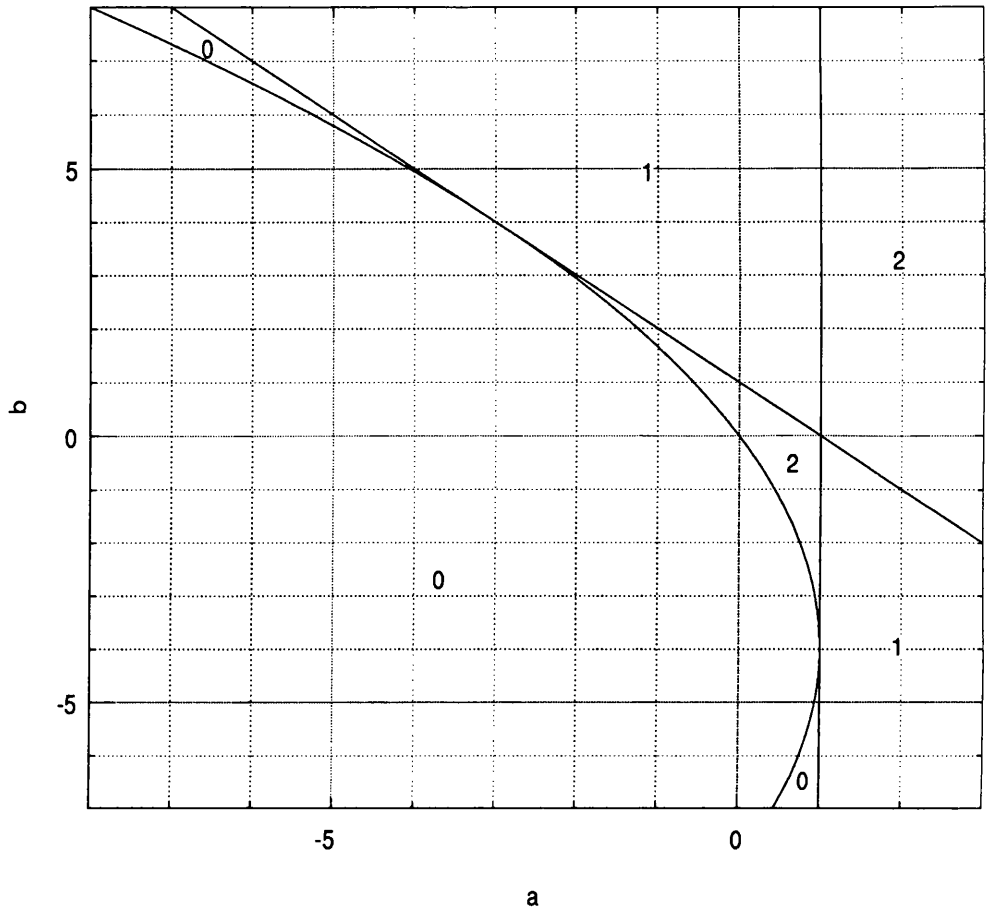

then, for $a > 0$, all b values in the range $[0, 1]$ are unphysical, while for $a < 0$, all b values outwith this interval are unphysical. The position of these exceptional ranges of frequency are shown in Figure 4.4.

Retracing our steps, the form found for the asymptotic behaviour of E_θ and E_z is

$$\begin{aligned} E_\theta &= \frac{1}{2\sqrt{\rho}} \sum_{j=1}^{4} c_j e^{i\sigma_j \rho} \left[(1 + d_j) \cos\rho + i\,(1 - d_j) \sin\rho \right] , \\ E_z &= \frac{i}{2\sqrt{\rho}} \sum_{j=1}^{4} c_j e^{i\sigma_j \rho} \left[(1 - d_j) \cos\rho + i\,(1 + d_j) \sin\rho \right] . \end{aligned} \tag{4.3.9}$$

where the quantities σ_j are the four solutions to Eq. 4.3.5, and $d_j = m_j/n_j$ (which is a function of σ_j). These formulae have a rich structure, and we can expect them to display a wide range of behaviour as the parameters are varied.

Some care is needed when interpreting these results. They were derived under

Figure 4.4: Unphysical regions in terms of a and b

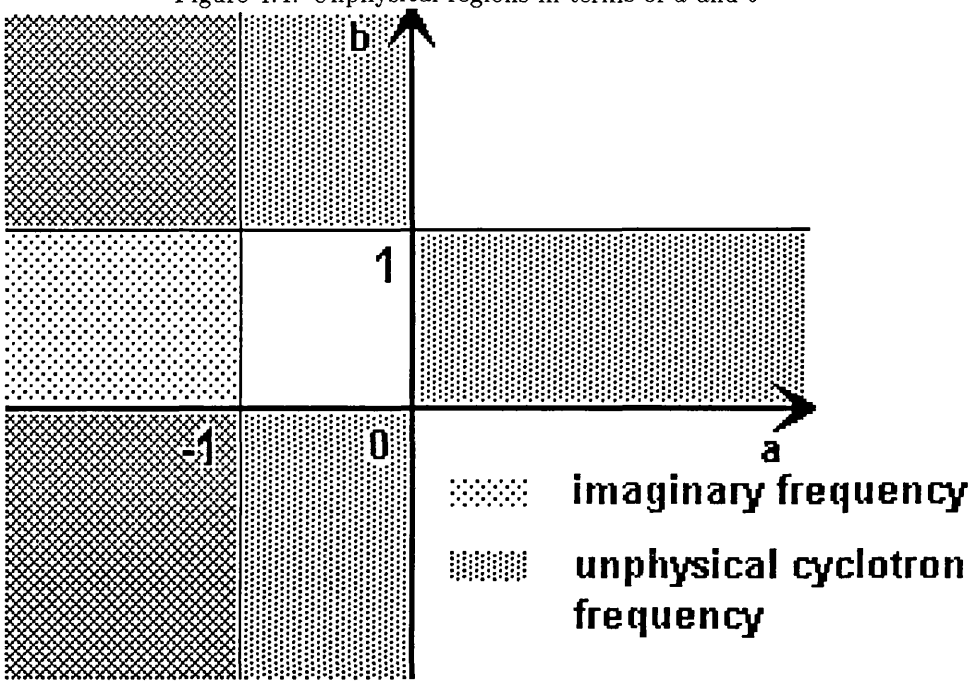

the assumption that

$$|a + b\cos^2\rho| \gg \left|\frac{3}{4\rho^2}\right| , \quad |a + b\sin^2\rho| \gg \left|\frac{1}{4\rho^2}\right| . \tag{4.3.10}$$

Applying the triangle inequality to these, and noting that $|\cos z|$, $|\sin z| \leq 1$, for all z, we obtain

$$|a| + |b| \gg \frac{3}{4\rho^2} , \quad |a| + |b| \gg \frac{1}{4\rho^2} , \tag{4.3.11}$$

since $\rho > 0$. Adopting the stronger of the two constraints and deleting the unnecessarily precise numerical factor gives the handy condition

$$\rho^2 \left[|a| + |b|\right] \gg 1 , \tag{4.3.12}$$

for the validity of the asymptotic solutions given here. The accuracy of these approximations, compared with more direct ways of solving the equations, is assesed in the next chapter.

4.4 Consistent Wave Equations

One of the objectives of this work was to examine consistently derived wave equations, so that the full effects of plasma non-uniformity could be included in analyses of waves. The derivation of a fully consistent set of wave equations for $\mathbf{E}$ is now considered.

The objective is to obtain a corresponding equation to Eq.4.2.3, but with equilibrium flows included. Examination of Eq.4.2.1, with $\mathbf{v}_o \neq 0$, reveals an extra term on the RHS of the momentum equation, which will succumb to the same analysis as given in the inconsistent case, a term in the equation for current density, which means the number density, n, must be calculated and the convective terms on the LHS of the momentum equation, which are probably the most awkward to deal with. Taking dot and cross products of the momentum equation with $\mathbf{B}_o$, $\hat{\mathbf{r}}$, and $\hat{\mathbf{z}}$, and once more ignoring azimuthal and z wavenumber, one can show that the solution for the velocity is

$$\mathbf{v} = \frac{1}{\Delta}\left\{ -\frac{\Omega_o}{B_o}\boldsymbol{\epsilon} - \frac{\lambda\Omega_o}{\Delta B_o}\hat{\mathbf{z}}\times\mathbf{x}_3 + \frac{\Omega_o^2}{i\omega B_o}\mathbf{x}_1 + \frac{\left[\mathbf{x}_2 + \frac{\Omega_o\lambda}{\Delta B_o}\hat{\mathbf{z}}\times\mathbf{x}_2\,\hat{\mathbf{r}}\cdot\mathbf{x}_3\right]}{\left(\Delta - \frac{\Omega_o}{i\omega}\hat{\mathbf{r}}\cdot\mathbf{b}\times\boldsymbol{\mu}\right)} \right\} , \quad (4.4.1)$$

where,

$$\begin{aligned}
\Delta &= -i\omega - \frac{\Omega_o}{i\omega}(\Omega_o - \lambda g) , \\
\mathbf{x}_1 &= \mathbf{b}\times\boldsymbol{\epsilon} + \frac{1}{i\omega}(\lambda\hat{\mathbf{z}} - \Omega_o\mathbf{b})\,\mathbf{b}\cdot\boldsymbol{\epsilon} , \\
\mathbf{x}_2 &= -\boldsymbol{\mu} + \frac{\Omega_o}{i\omega}\left[\mathbf{b}\times\boldsymbol{\mu} - \frac{\mathbf{b}\cdot\boldsymbol{\mu} - \lambda f}{i\omega}(\lambda\hat{\mathbf{z}} - \Omega_o\mathbf{b})\right] , \\
\mathbf{x}_3 &= -\boldsymbol{\epsilon} + \frac{\Omega_o}{i\omega}\mathbf{b}\times\boldsymbol{\epsilon} - \frac{\Omega_o}{\omega^2}(\lambda\hat{\mathbf{z}} - \Omega_o\mathbf{b})\,\mathbf{b}\cdot\boldsymbol{\epsilon} , \\
\boldsymbol{\epsilon} &= \mathbf{E} + \mathbf{v}_o\times\mathbf{B} , \quad \lambda = \frac{2v_{o\theta}}{r} , \quad \boldsymbol{\mu} = \left(0, v'_{o\theta} - \frac{v_{o\theta}}{r}, v'_{oz}\right) . \qquad (4.4.2)
\end{aligned}$$

This is a generalisation of Eq. 4.2.2, which may be recovered by putting $\lambda = 0$ and $\boldsymbol{\mu} = 0$. Note that $\mathbf{v}_o$ here is the electron velocity: the ion contribution would be of order $\frac{m_e}{m_i}$ smaller and has been ignored. These equations can be used to define $\mathbf{v}$ in terms of $\mathbf{E}$, albeit with some labour. The number density is then given by

$$n = -\frac{in_o}{\omega r}(r\mathbf{v}_r)' . \qquad (4.4.3)$$

Clearly, the derivative involved here will give an expression of great complexity. To complete the derivation, substitute the expressions obtained into

$$\nabla\times\nabla\times\mathbf{E} - \frac{\omega^2}{c^2}\mathbf{E} = -i\omega\mu_o e\,(n_o\mathbf{v} + n\mathbf{v}_o) , \qquad (4.4.4)$$

in order to find the final ode for $\mathbf{E}$. We do not pursue the fully consistent equations further, because of the complexity of this procedure, and because the flows are often negligible. Returning to Eq. 4.1.3, it is found that

$$\mathbf{J}_o = \frac{1}{\mu_o}\nabla\times\mathbf{B}_o , \quad \mathbf{J}_o = -n_o e\left(1 + \mathcal{Z}^2\frac{m_e}{m_i}\right)\mathbf{v}_{oe} . \qquad (4.4.5)$$

Using the expression for $\nabla\times$, and the definition of L, gives

$$\begin{aligned}\mathbf{v}_{oe} &= \frac{\mathbf{B}_o}{\mu_o n_o e(1+\frac{m_e}{m_i})}\left(0, \frac{dg}{dr}, -\frac{1}{r}\frac{d(rf)}{dr}\right) \\ &= \Omega_o L^2 \left(0, \frac{dg}{dr}, -\frac{1}{r}\frac{d(rf)}{dr}\right) . \end{aligned} \tag{4.4.6}$$

Referring back to the table of L values shows that, for a fusion plasma, or in the solar atmosphere, this is a very small quantity. In these cases at least, we are justified in ignoring equilibrium flows.

In the following chapter, we examine in detail the solutions of Eqs. 4.2.5, in the belief that this will shed light on the mode conversion occurring in our model plasma.

Chapter 5

The Solution Of Non-uniform Wave Equations

We now wish to solve a specific problem. In the physical examples of interest discussed in Chapter 1 (the postulated structure of coronal loops, for instance), there is a confined structure, surrounded by a region where the field is uniform, or nearly so. In view of this, in the rest of this thesis, a magnetic field structure will be studied in which a central helical region is surrounded by a uniform region. This may give insight into what happens when a wave propagates from a region of uniform field where its wavenumber is well-defined, into a structured region where it is a function of position. The external part being uniform makes it easy to identify modes in this region with the familiar motions examined in Section 2.5. In the external region, then, we will have an analytic form for the normal modes. In the internal region we must solve the governing odes to obtain them.

5.1 The Fröbenius Method

In order to solve the field equations in a complete and orderly manner it is important to know what type of singularities occur, and where. Ince (1926) describes the classification of singularities and shows in particular that a singularity will be *regular* if, at $\rho = \rho_o$, the differential equation may be expressed in the form

$$u^{(n)} + \frac{P_1(\rho)}{\rho} u^{(n-1)} + \cdots + \frac{P_{n-1}(\rho)}{\rho^{n-1}} u' + \frac{P_n(\rho)}{\rho^n} u = 0 \,, \qquad (5.1.1)$$

where n is the order of the equation, and $P_1, \cdots, P_n$ are all analytic functions of ρ at ρ_o. The significance of a regular singularity at ρ_o is that it does not prevent well-behaved solutions being found in a neighbourhood of ρ_o. It is a straightforward matter to eliminate one of the variables from Eq.4.2.5, and to show that the resulting fourth order equation is of the form Eq.5.1.1. Having verified this, solutions may be found using the *Fröbenius method*, which involves assuming a power series solution to the equation in question, and then substituting this in to obtain a set of coupled equations involving the unknown coefficients and the power of the leading term. The first member of this set is known as the *indicial equation* and is used to determine the power of ρ with which the series starts. The indicial equation is a polynomial of the same order as the ode being solved, so that in this case it is of fourth order and has four solutions. If these solutions do not differ by an integer, then constructing the series solutions is simple, however, in this case, the indicial equation produced by considering a fourth-order equation for u is,

$$(m+1)(m-1)(m-3)^2 = 0\,. \tag{5.1.2}$$

Ince (ibid. p396) shows that this need be no obstacle. Introducing new terms which are powers of $\log(\rho)$ multiplied by new power series which can be found from the existing ones can alleviate the problem. In the present case, if the computer algebra package REDUCE (Hearn, 1991) is used to minimise error, we find that the following can be taken as linearly independent solutions to the original equation.

$$\begin{aligned} u_A &= \rho - \frac{a}{8}\rho^3 + \frac{1}{24}\left[\frac{b}{3} + \frac{a}{8}(a-b)\right]\rho^5 + \mathcal{O}(\rho^7)\,, \\ v_A &= 1 - \frac{a}{4}\rho^2 + \frac{a^2}{64}\rho^4 + \mathcal{O}(\rho^6)\,, \end{aligned} \tag{5.1.3}$$

$$\begin{aligned} u_B &= \frac{b}{8}\rho^3 - \frac{b}{192}\left[3a + b\frac{16}{3}\right]\rho^5 + \mathcal{O}(\rho^7)\,, \\ v_B &= 1 - \frac{a}{4}\rho^2 + \frac{1}{16}\left[\frac{a^2}{4} - b\right]\rho^4 + \mathcal{O}(\rho^6)\,, \end{aligned} \tag{5.1.4}$$

$$\begin{aligned} u_C &= u_B \log(\rho) + \frac{b}{4(a+b)}\left\{\rho + \frac{1}{4}\left[\frac{5a^2}{48} + \frac{5ab}{36} - \frac{7a}{27} - \frac{5b}{54} + \frac{5b^2}{144}\right]\rho^5 + \mathcal{O}(\rho^7)\right\}\,, \\ v_C &= v_B \log(\rho) + 1 - \frac{1}{32(a+b)}\left[\frac{a^2}{4}(a+b) + b(a+\frac{b}{2})\right]\rho^4 + \mathcal{O}(\rho^6)\,, \end{aligned} \tag{5.1.5}$$

$$u_D = (a+b)\left\{-\frac{1}{2}\rho + \frac{(a+b)}{16}\rho^3 - \left[\frac{1}{8}(a+b)^2 + b\right]\rho^5 + \mathcal{O}(\rho^7)\right\}\log(\rho) + \frac{1}{\rho} +$$

$$\frac{1}{8}\left[b-\frac{3}{8}(a+b)^2\right]\rho^3+\frac{1}{288}\left[\frac{7}{8}(a+b)^3+b(a+4b-4)\right]\rho^5+\mathcal{O}(\rho^7)\,,$$

$$v_D \;=\; \left\{-\frac{b}{32}(a+b)\rho^4+\mathcal{O}(\rho^6)\right\}\log(\rho)+\frac{b}{4}\left\{1+\frac{3b-8}{48}\rho^4+\mathcal{O}(\rho^6)\right\}\,, \tag{5.1.6}$$

where we have written u for E_θ, v for E_z, and a and b are as defined in Eq. 4.2.5. These solutions satisfy the differential equation, but not necessarily the boundary conditions. Clearly, by the nature of cylindrical vector fields, E_θ must be zero at $\rho = 0$, in order that the electric field vector is uniquely defined there, and we put $E_z|_{\rho=0} = E_{zo}$, $E'_z|_{\rho=0} = E'_{zo}$, $E'_\theta|_{\rho=0} = E'_{\theta o}$. Assuming that any solution may be written

$$Au_A+Bu_B+Cu_C+Du_D\,,\;\; Av_A+Bv_B+Cv_C+Dv_D\,, \tag{5.1.7}$$

then the four conditions give, respectively,

$$\begin{aligned}
A\cdot 0+B\cdot 0+C\cdot 0+D\cdot\infty &= 0\,,\\
A+B-C\cdot\infty+D\cdot\frac{b}{4} &= E_{zo}\,,\\
A\cdot 0+B\cdot 0+C\cdot\infty+D\cdot 0 &= E'_{zo}\,,\\
A+B\cdot 0+C\cdot\frac{b}{4(a+b)}-D\cdot\infty &= E'_{\theta o}\,.
\end{aligned} \tag{5.1.8}$$

To maintain consistency, we require $D = 0$, $C = 0$. The third equation shows that $E'_{zo} = 0$, which is a result of the assumption of variation with ρ alone. The second and fourth then yield $A = E'_{\theta o}$, $B = E_{zo} - E'_{\theta o}$. An arbitrary solution which satisfies the boundary conditions can then be written as

$$E_{\theta o}u_A+[E_{zo}-E'_{\theta o}]\,u_B\,,\;\; E_{\theta o}v_A+[E_{zo}-E'_{\theta o}]\,v_B\,. \tag{5.1.9}$$

This expression was used to avoid the singularity at the origin when numerical solutions were sought to Eq. 4.2.5. By specifying E_{zo} and $E_{\theta o}$, the correct admixture of u_A and u_B could be found. The power series were then used to provide an approximation to the required solution up to $\rho = \epsilon$, where ϵ was a suitably chosen small number. Numerical solution of the odes was then attempted using field values at this point as new internal boundary values.

5.2 The Equilibrium

We obtain this by using the form of magnetic field Eq. 4.1.13, for the interior field, and splicing this onto a uniform field at $\rho = R$. Thus, we have

$$\mathbf{B}_o = \begin{cases} B_o(0, \sin\rho, \cos\rho)\,, & \rho < R \\ B_o(0,0,1)\,, & \rho \geq R \end{cases} \quad . \tag{5.2.1}$$

Both of these expressions satisfy the conditions for an equilibrium, as derived in Chapter 4. However, on the boundary the field, will, in general, suffer a discontinuous jump. This means that a sheet current must flow along the boundary. Integrating the Maxwell 'curl B' equation over a surface spanning the boundary gives,

$$\int_S \nabla \times \mathbf{B}_o \cdot \mathbf{dS} = \mu_o \int_S \mathbf{J}_o \cdot \mathbf{dS}\,. \tag{5.2.2}$$

Using Stokes' theorem, this is equal to $\oint_C \mathbf{B}_o \cdot \mathbf{dl}$. If the surface extends between $R - \Delta\rho$ and $R + \Delta\rho$, and subtends an angle θ, then

$$\theta R\,[B_{o\theta}(R+\Delta\rho) - B_{o\theta}(R-\Delta\rho)] = \mu_o \int_S \mathbf{J}_o \cdot \mathbf{dS}\,. \tag{5.2.3}$$

Letting $\Delta\rho \rightarrow 0$, and performing the θ integral on the RHS of Eq. 5.2.3, we find

$$[B_{o\theta}] = \frac{\mu_o}{R} \lim_{\Delta\rho \rightarrow 0} \left\{ \int_{R-\Delta\rho}^{R+\Delta\rho} \rho J_{zo} d\rho \right\}\,. \tag{5.2.4}$$

Where $[\cdots]$ denotes the jump in value of a quantity at the boundary. If the jump is non-zero, then the integrand on the RHS of Eq. 5.2.4, must contain a delta function at $\rho = R$. This is the sheet current referred to above. It is straightforward to show that the extra term required in the expression for J_{zo} is

$$-\frac{\sin R}{\mu_o}\delta(\rho - R). \tag{5.2.5}$$

Clearly, if R is a multiple of 2π, then there will be no such surface current, corresponding to the two forms of magnetic field joining smoothly on to one another. We wish to study effects arising from a structured, but continuous magnetic field, and a current sheet is an unnecessary complication which we accordingly avoid by setting $R = 2\pi$ from now on.

5.3 Conversion And Reflection Coefficients

Since our model of plasma waves is linear, we can Fourier analyse any incoming disturbance into harmonic waves, and need only solve the problem for such cases.

Given the possible channels available in the model, we expect this incoming wave to be partially reflected to give an outgoing wave of the same type, and partially converted and reflected to give an outgoing wave of the other type.

The normal modes in the uniform field case are easily obtained by mapping $\sin \mapsto 0$ and $\cos \mapsto 1$ in Eqs. 4.2.5. This gives the equations

$$\begin{aligned} E_\theta'' + \frac{E_\theta'}{\rho} + \left[a + b - \frac{1}{\rho^2}\right] E_\theta &= 0 , \\ E_z'' + \frac{E_z}{\rho} + a E_z &= 0 , \end{aligned} \tag{5.3.1}$$

which have solution

$$E_\theta \propto J_1(p\rho) , Y_1(p\rho) , \quad E_z \propto J_o(q\rho) , Y_o(q\rho) , \tag{5.3.2}$$

where $p = \sqrt{a+b}$ and $q = \sqrt{a}$. Note that, since $v = E_z$, a solution for v with $u = 0$ corresponds to an O-mode, while a solution for u with $v = 0$ corresponds to an X-mode. An X-mode solution means a non-zero value for E_r also, but we have eliminated this variable in favour of E_θ and E_z. The Ys must be included, because we are not applying this solution at the origin. If we suppose that we can somehow find a set of linearly independent normal modes for the interior region, then we can assume that the following interior and exterior solutions correspond,

interior	*exterior*
u_1	$A_1 J_1(p\rho) + B_1 Y_1(p\rho)$
v_1	$C_1 J_o(q\rho) + D_1 Y_o(q\rho)$
u_2	$A_2 J_1(p\rho) + B_2 Y_1(p\rho)$
v_2	$C_2 J_o(q\rho) + D_2 Y_o(q\rho)$

where the subscripts $1,2$ distinguish between the two internal modes present. [1] It is the coefficients of the Bessel functions here which contain information about the conversion and reflection coefficients. To satisfy continuity of electric field and its gradient, the following conditions must hold at $\rho = R$,

$$\begin{aligned} u_1 &= A_1 J_1(pR) + B_1 Y_1(pR) \quad , \quad u_1' = A_1 J_1'(pR) + B_1 Y_1'(pR) , \\ v_1 &= C_1 J_o(qR) + D_1 Y_o(qR) \quad , \quad v_1' = C_1 J_o'(qR) + D_1 Y_o'(qR) , \\ u_2 &= A_2 J_1(pR) + B_2 Y_1(pR) \quad , \quad u_2' = A_2 J_1'(pR) + B_2 Y_1'(pR) , \\ v_2 &= C_2 J_o(qR) + D_2 Y_o(qR) \quad , \quad v_2' = C_2 J_o'(qR) + D_2 Y_o'(qR) , \end{aligned} \tag{5.3.3}$$

where $'$ denotes $\frac{d}{d\rho}$. Equations 5.3.3 may be straightforwardly solved for $A_1, B_1, \cdots, C_2, D_2$,

[1] Only two of the potential four solutions are admissible, as described in Eq. 5.1.

to obtain

$$A_1 = \frac{\pi R}{2}\mathcal{W}\left[u_1, Y_1(pR)\right] \quad , \quad A_2 = \frac{\pi R}{2}\mathcal{W}\left[u_2, Y_1(pR)\right] \ ,$$
$$B_1 = -\frac{\pi R}{2}\mathcal{W}\left[u_1, J_1(pR)\right] \quad , \quad B_2 = -\frac{\pi R}{2}\mathcal{W}\left[u_2, J_1(pR)\right] \ ,$$
$$C_1 = \frac{\pi R}{2}\mathcal{W}\left[v_1, Y_o(qR)\right] \quad , \quad C_2 = \frac{\pi R}{2}\mathcal{W}\left[v_2, Y_o(qR)\right] \ ,$$
$$D_1 = -\frac{\pi R}{2}\mathcal{W}\left[v_1, J_o(qR)\right] \quad , \quad D_2 = -\frac{\pi R}{2}\mathcal{W}\left[v_2, J_o(qR)\right] \ , \qquad (5.3.4)$$

where $\mathcal{W}[\cdots]$ is the *Wronskian* , defined as $\mathcal{W}[\phi, \psi] = \phi\psi' - \psi\phi'$, and we have used the fact that $\mathcal{W}\left[J_\nu(z), Y_\nu(z)\right] = \frac{2}{\pi z}$ for all complex z (Watson, 1944). A general internal solution for u and v may be written using the arbitrary quantities α and β as

$$\alpha u_1 \ + \ \beta u_2 \ , \qquad (5.3.5)$$

$$\alpha v_1 \ + \ \beta v_2 \ , \qquad (5.3.6)$$

and, using the table above, this will correspond to an external solution of the form

$$\begin{aligned} (\alpha A_1 + \beta A_2)J_1(p\rho) \ &+ \ (\alpha B_1 + \beta B_2)Y_1(p\rho) \ , \\ (\alpha C_1 + \beta C_2)J_o(q\rho) \ &+ \ (\alpha D_1 + \beta D_2)Y_o(q\rho) \ . \end{aligned} \qquad (5.3.7)$$

It is of interest to distinguish between incoming and outgoing waves in the uniform field region, so it is more appropriate to use the *Hankel* functions (Watson, 1944) and therefore the external solution may also be considered as follows. The Hankel functions bear the same relation to Bessel functions as complex exponentials do to sin and cos, and are defined as $H_\nu^{(1)} = J_\nu + iY_\nu$, $H_\nu^{(2)} = J_\nu - iY_\nu$. With our choice of $e^{-i\omega t}$ for the time dependence, $H_\nu^{(1)}$ is an outgoing and $H_\nu^{(2)}$ an incoming wave. An arbitrary combination of outgoing and incoming waves then gives, for u and v respectively,

$$\begin{aligned} \mu H_1^{(1)} + \nu H_1^{(2)} \ &= \ (\mu + \nu)J_1 + i(\mu - \nu)Y_1 \ , \\ \sigma H_o^{(1)} + \tau H_o^{(2)} \ &= \ (\sigma + \tau)J_o + i(\sigma - \tau)Y_o \ . \end{aligned} \qquad (5.3.8)$$

Here, μ, ν, σ and τ are quantities which we can associate with the admixtures of outgoing X-mode, incoming X-mode, outgoing O-mode and incoming O-mode respectively. The two forms for the external electric field (Eqs. 5.3.7 and 5.3.8) must hold simultaneously for all points $\rho > R$, and so we may equate the coefficients of the Bessel functions and obtain:

$$\mu + \nu = \alpha A_1 + \beta A_2 \quad , \quad i(\mu - \nu) = \alpha B_1 + \beta B_2 \ ,$$
$$\sigma + \tau = \alpha C_1 + \beta C_2 \quad , \quad i(\sigma - \tau) = \alpha D_1 + \beta D_2 \ . \qquad (5.3.9)$$

If we regard the incoming amplitudes as given quantities, then it is possible to eliminate α and β and solve for the amplitudes of outgoing O-modes (τ) and X-modes (ν), viz.

$$\tau = \frac{2i\mu(C_1D_2 - C_2D_1) + \sigma\,[B_2D_1 - B_1D_2 + A_2C_1 - A_1C_2 + i(B_1C_2 - B_2C_1 + A_2D_1 - A_1D_2)]}{A_2C_1 - A_1C_2 + B_1D_2 - B_2D_1 + i(B_1C_2 - B_2C_1 + A_1D_2 - A_2D_1)},$$

$$\nu = \frac{\mu\,[B_2D_1 - B_1D_2 + A_2C_1 - A_1C_2 - i(B_1C_2 - B_2C_1 - A_2D_1 - A_1D_2)] + 2i\sigma(B_1A_2 - B_2A_1)}{A_2C_1 - A_1C_2 + B_1D_2 - B_2D_1 + i(B_1C_2 - B_2C_1 + A_1D_2 - A_2D_1)}. \tag{5.3.10}$$

The above derivation does not depend on the choice of u and v, as long as linearly independent modes are used. This fact is reflected in the absence of α and β from Eqs. 5.3.10. To put things another way: if the admixtures of modes 1 and 2 were scaled by constants $\mathcal{C}_1$ and $\mathcal{C}_2$ respectively, then, since each term in 5.3.10 carries subscripts 1 and 2, the factor $\mathcal{C}_1\mathcal{C}_2$ would cancel off throughout.

5.3.1 Some Special Cases

Conversion between modes will be particularly well defined if only one type of incoming wave is present. If the incoming wave is purely an O-mode, then the coefficient of the incoming X-mode, ν is zero. Using Eqns. 5.3.10, we can show that the ratio of reflected to incident O-mode is given by

$$\frac{\sigma}{\tau} = \frac{B_2D_1 - B_1D_2 + A_2C_1 - A_1C_2 + i(B_1C_2 - B_2C_1 + A_2D_1 - A_1D_2)}{A_2C_1 - A_1C_2 + B_1D_2 - B_2D_1 + i(B_1C_2 - B_2C_1 + A_1D_2 - A_2D_1)}, \tag{5.3.11}$$

and the ratio of converted X-mode to incident O-mode is

$$\frac{\mu}{\tau} = \frac{2i(B_1A_2 - B_2A_1)}{A_2C_1 - A_1C_2 + B_1D_2 - B_2D_1 + i(B_1C_2 - B_2C_1 + A_1D_2 - A_2D_1)}. \tag{5.3.12}$$

While, if there is only an incoming X-mode ($\sigma = 0$), then the coefficient of the incoming O-mode is zero, giving $\tau = 0$, and we can show that the ratio of reflected

to incident wave is

$$\frac{\mu}{\nu} = \frac{2i(C_1D_2 - C_2D_1)}{A_2C_1 - A_1C_2 + B_1D_2 - B_2D_1 + i(B_1C_2 - B_2C_1 + A_1D_2 - A_2D_1)}, \tag{5.3.13}$$

and the ratio of converted to incident wave is

$$\frac{\sigma}{\nu} = \frac{B_2D_1 - B_1D_2 + A_2C_1 - A_1C_2 + i(B_2C_1 - B_1C_2 + A_1D_2 - A_2D_1)}{A_2C_1 - A_1C_2 + B_1D_2 - B_2D_1 + i(B_1C_2 - B_2C_1 + A_1D_2 - A_2D_1)}. \tag{5.3.14}$$

5.4 Computational Issues

A number of FORTRAN-77 programs were written to tackle this problem. A listing of the most important can be found in Appendix A. The program **odeadam.for** was written to calculate the boundary values of $u_{1,2}$ and $v_{1,2}$ needed to use the formulae for reflection and conversion coefficients above. It uses an Adams method from the Nag fortran library (Numerical Algorithms Group, 1988), to numerically integrate the differential equations over the range $[0, 2\pi]$. The separate modes are distinguished by the values of E_z and E'_θ at the origin, viz.

mode no.	$E'_{\theta o}$	E_{zo}
1	0.0	1.0
2	1.0	0.0

The program finds boundary values for these starting values for a range of frequency values. The Fröbenius expansions discussed in Section 5.1 are used in the vicinity of the singular point at the origin. The expansions are used up to a matching point, and the values found for the fields at this point used to provide starting data for the numerical integration. The position of the matching point should be chosen so that the power series still converges well, but the ordinate is far enough past the singularity for the numbers involved in the integrating routine to be manageable. This position was found by choosing parameter values which reproduced the uncoupled equations, with solutions in terms of Bessel functions. The matching point was varied until the values found were as close as possible to Bessel function values found from tables. The value finally chosen was $\rho = 0.01$.

Frequencies are all measured in units of ω_p. This is both natural, in view of the length scale $L = \frac{c}{\omega_p}$ introduced in Chapter 4, and physically more sensible (one

expects significant things to happen when $\omega = \Omega_o$, irrespective of the numerical values of these quantities). This choice of units leaves the two parameters ω and Ω_o to define conditions in the plasma. Notice that fixing the cyclotron frequency fixes B_o, the magnitude of the equilibrium magnetic field.

To check on the accuracy of these calculations, a program using a Runge-Kutta method from the Nag library, and otherwise identical, was written. The results from both programs were stored in unformatted files to minimise the propagation of any errors which had occurred. Results from the two simulations were compared by examining the fractional differences of the two sets of electric field values (i.e. the quantities $|(E^{(i)}_{RK} - E^{(i)}_{AD})/E^{(i)}_{RK}|$, in an obvious notation). By choosing a suitably high tolerance in the input to the Nag routines, these deviations could be made consistently small and less than about 1×10^{-8}, so that these two differing numerical routines give answers which agree to at least single precision accuracy. [2]

The programs **concoefo.for** and **concoefx.for** implement the formulae 5.3.11, 5.3.12 and 5.3.13, 5.3.14 respectively. They take boundary values from **odeadams.for** and evaluate the reflection and conversion coefficients. The admixture of modes 5.3.8 holds for the entire external region, so that these quantities are not peculiar to the boundary, but hold for all $\rho > R$.

The invariance with respect to the normal modes chosen was also investigated. The field values for each mode were multiplied by arbitrarily chosen real numbers after being read in to the programs **concoefo.for** and **concoefx.for**. The conversion and reflection coefficients were found to be invariant, except very close to the upper hybrid resonance, where, of course, the model used does not apply.

One obvious test on the calculations is to check that the divergence of the magnetic field is zero. However, further thought reveals that this is not useful, since we have assumed that $\frac{\partial}{\partial z} = 0$ and $\frac{\partial}{\partial \theta} = 0$. Therefore, for the perturbed magnetic field,

$$\nabla \cdot \mathbf{B} = \frac{(rB_r)'}{r}\,, \tag{5.4.1}$$

and since $B_r = \frac{1}{i\omega}\left[\frac{1}{r}\frac{\partial E_z}{\partial \theta} - \frac{\partial E_\theta}{\partial z}\right] = 0$, the divergence of $\mathbf{B}$ within this model is, *a priori*, zero.

[2] This was the 'worst case' value. Typical values were a few orders of magnitude less

5.4.1 Comparison With Asymptotic Approximations

In section 4.3, it was shown that asymptotic solutions to our equations could be found, of the form

$$\text{field value} = \frac{1}{\sqrt{\rho}}[\text{combination of travelling waves}] \ . \tag{5.4.2}$$

To see how accurate this was, a selection of numerical solutions produced by the program `odeadams.for` were Fourier transformed and the result examined by a standard graphics package. [3] The results were multiplied by $\sqrt{\rho}$ beforehand, so that the travelling wave terms above would give a discrete set of spikes in Fourier space whose position could be compared with the values predicted by Eq. 4.3.5. A 2048-point discrete transform was used, and the solutions plotted over a range of 0 to 64π (much longer than the interval used previously, in order to pick out slowly varying 'beat' phenomena). Spectra were produced, consisting of well- defined peaks and a low level of background 'noise' of other components. In particular, there was no evidence of *aliasing* in the highest bins (Figure 5.2 shows only the first 200 of 1024 bins), so that the fields are very unlikely to contain frequencies higher than those found. A sample output and the relevant part of its Fourier spectrum are shown in Figures 5.1 and 5.2, while a table comparing the wavenumbers from numerical simulations and the asymptotic form, for a variety of values of a and b, is given below. The quantity plotted in Figure 5.2 is in fact the modulus of the discrete

[3] Easyplot Version 2.21

Fourier transform, which is a complex quantity.

a	b	Wavenumber from numerics	Wavenumber from asymptotic solution Eq. 4.3.5
−0.8	0.2	unstable oscillations	4 complex
−0.2	0.8	0.469 0.531 1.469 2.469	0.476 0.531 1.469 2.476
0.0	0.5	0.531 1.469 2.500	0.510 0.532 1.469 2.510
1.0	−2.0	0.406 1.000 2.406	0.414 1.000 2.414
1.0	−1.0	0.750 1.000 2.750	0.732 1.000 2.732
1.0	0.0	1.000	1.000 3.000
1.0	1.0	1.000 1.250 3.340	1.000 1.236 3.236
1.0	2.0	1.000 1.469 3.469	1.000 1.449 3.449
1.0	5.0	1.000 2.000	1.000 2.000 4.000
2.0	−2.0	unstable oscillations	2 real, 2 complex
2.0	−1.0	1.000 1.250 3.531	1.000 1.236 3.236
2.0	0.0	1.406	0.586 1.414 3.414
2.0	1.0	0.469 1.594 3.594	0.454 1.546 1.589 3.589
2.0	2.0	0.375 1.625 1.750 3.750	0.372 1.628 1.758 3.758

Note that the asymptotic wavenumber in the table is $\sigma \pm 1$, in the notation of Section 4.3. The values from the numerical Fourier spectra are of fairly modest accuracy. More precise calculations would require a lot more time and effort than this section deserves. Despite this the agreement is very good, both in terms of the values in the table, and in the absence of significant amounts of other frequencies in the Fourier spectrum. Not all the 'spectral lines' listed in this table occur with equal, or even vaguely equal amplitude, and some of those listed had only a tiny amplitude. This corresponds to the real-space solution having only a very small admixture of certain of the allowed frequencies. Presumably, the 'missing' values in the numerical column of the table corresponds to admixture so small as to be undetectable. Significantly, although some values are predicted but not observed, no values are observed which are not very close to solutions predicted by Eq. 4.3.5. The unstable behaviour in the first and tenth examples here is to be expected from a consultation of Figure 4.3, which shows that in these situations, there are no travelling solutions and one travelling solution respectively.

In the next section, we consider the possibility of finding a conservation law, which would act as a useful check on the numerical results obtained.

Figure 5.1: $\sqrt{\rho}E_z$ for $a = b = 2$

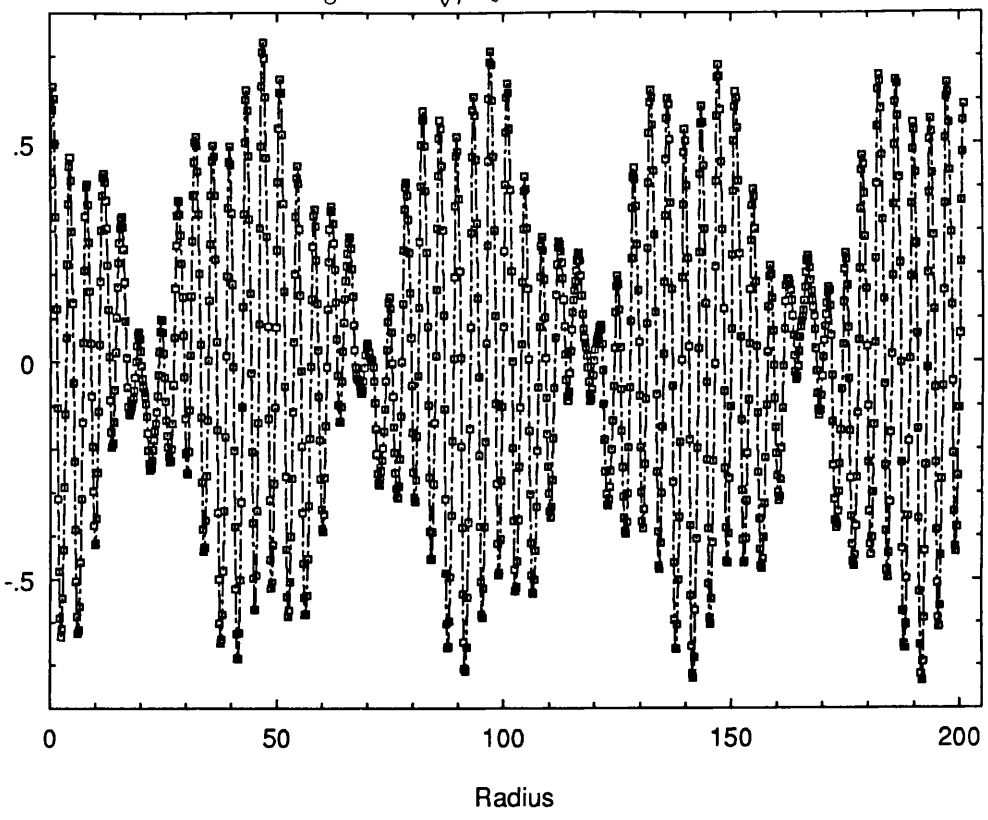

5.5 Conservation Laws

Naturally, we expect energy to be conserved in this non-dissipative system, and for this to be reflected in the expressions for reflection and conversion coefficients, representing as they do the amplitude of plasma waves.

5.5.1 Dielectric Materials And Nonlocal Behaviour

Defining the energy density of an inhomogeneous plasma is far more complex than one might suppose. In fact, there is no general procedure for doing this. Since plasmas may exchange momentum over large distances, we expect that, in general, only the overall system has a well defined energy (see Auerbach, 1979). However, if we can 'summarise' the influence of far-off points of the plasma on a particular element using electric and magnetic field vectors, then a local energy density involving these quantities may be consistently defined.

In order to produce a representation of the total energy in a plasma the plasma's response to an applied field must be included. This is done by introducing the

Figure 5.2: Detail of the Fourier transform of the last graph

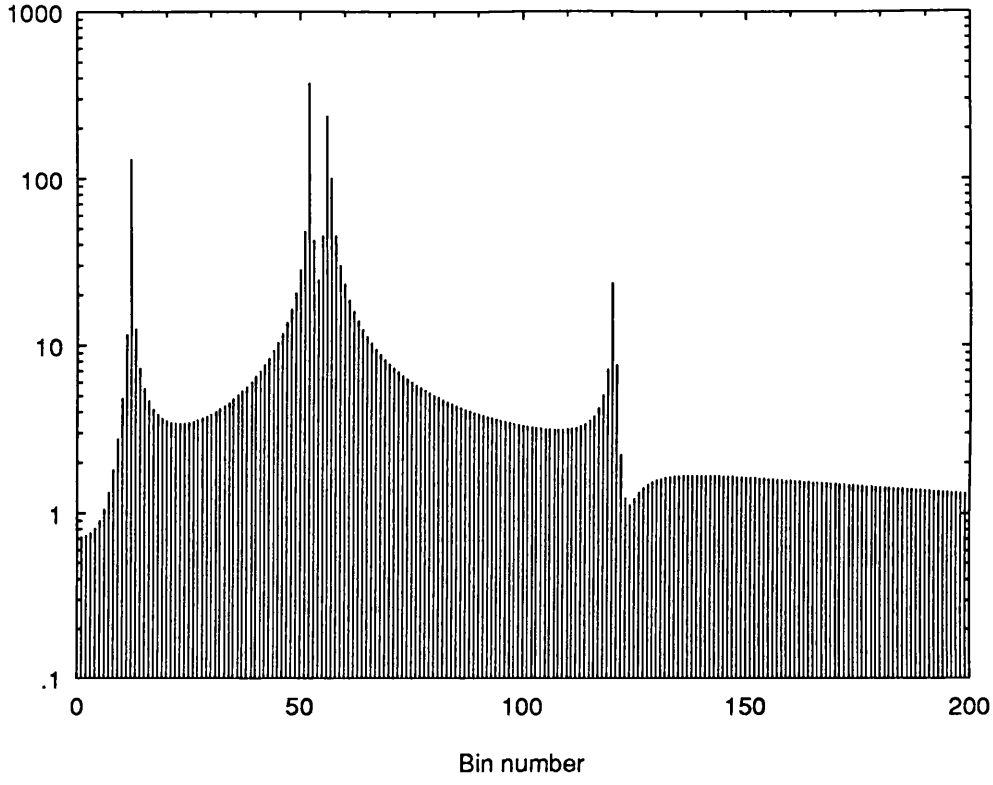

electric displacement vector, which can be defined as

$$\mathbf{D}(\mathbf{x},t) = \frac{1}{2\pi}\int\int \epsilon\,(\mathbf{x},t,\mathbf{x}',t')\cdot\mathbf{E}(\mathbf{x}',t')d\mathbf{x}'dt'\,, \tag{5.5.1}$$

where the *dielectric tensor* ϵ , describes the contribution to the plasma response from electric fields at each point of space and time. This expression requires only linearity of response for its validity, and is consequently very general. If a homogeneous plasma is specified, then the response will depend only on *differences* in position and time, and not on absolute values. Clearly, a homogeneous plasma may also be solved by Fourier transforming all variables of interest. This gives the rather more familiar expression

$$\mathbf{D}(\omega,\mathbf{k}) = \epsilon\,(\omega,\mathbf{k})\cdot\mathbf{E}(\omega,\mathbf{k})\,, \tag{5.5.2}$$

for the displacement vector. These two approaches are equivalent, as demonstrated in Stix (1992). It should be noted that the Fourier transformed version still includes nonlocal responses. Of course, all real plasmas are, to some extent, inhomogeneous, so that the more general form shown in Eq. 5.5.1 should be used. However, if the time and space variations are slow compared with the rates of change of the wave's electric and magnetic fields, i.e. on Fourier transforming the plasma structure, one

would obtain a distribution spanning values in Fourier space which were less than ω and $\mathbf{k}$, then the variation may be looked upon as *adiabatic*, and we may continue to use Eq. 5.5.2, with the dielectric tensor written as $\epsilon\,(\mathbf{x}, t, \omega, \mathbf{k})$ with reasonable accuracy. In the present case, the plasma has no inhomogeneity in time, so that we may Fourier transform in time with a clear conscience. The spatial variation of magnetic field, however, means that the use of Eq.5.5.2 may be restricted to cases where the 'wavelength' is small compared with the characteristic scale of magnetic field variation. Since we are using the cold plasma model, the dielectric tensor has no dependance on $\mathbf{k}$, so that, inasmuch as the medium is uniform, the response can be modelled as being local.

5.5.2 Conserved Quantities From Differential Equations

One approach which can be used to find conserved quantities in wave propagation problems is to examine the equations which govern the oscillatory motion. In simple, second order systems of equations where the dependent variable is y, the invariant quantities are y^*y and $\mathcal{W}(y^*, y)$. This result has been extended to fourth order systems (Diver, Laing (1990)), and has important implications for their behaviour, the main point being that the invariant quantities produced depend on the physical parameters appearing in the coefficients of the fourth order equation. However, the simple algebraic method given there applies only when the equations have constant coefficients and gives no information when the coefficients are functions of position, although it seems probable that the explicit dependence on physical parameters may also occur in the more general case.

5.5.3 Poynting's Theorem

We use the following version of Maxwell's equations:

$$\nabla \times \mathbf{E} = -\frac{\partial \mathbf{B}}{\partial t}\ ,\quad \nabla \times \mathbf{H} = \frac{\partial \mathbf{D}}{\partial t}\ , \tag{5.5.3}$$

where $\mathbf{H} = \mu\mathbf{B}$ and $\mathbf{D} = \epsilon\,\mathbf{E}$. Note that the effects of current are included in $\mathbf{D}$, in this formulation. The *Poynting vector* is defined as

$$\mathbf{P} = \mathbf{E} \times \mathbf{H}\ . \tag{5.5.4}$$

Taking the divergence of $\mathbf{P}$ and using the vector identity for the divergence of a cross product, gives

$$\begin{aligned} \nabla \cdot \mathbf{P} &= \mathbf{H} \cdot (\nabla \times \mathbf{E}) - \mathbf{E} \cdot (\nabla \times \mathbf{H})\ , \\ &= -\mathbf{H} \cdot \frac{\partial \mathbf{B}}{\partial t} - \mathbf{E} \cdot \frac{\partial \mathbf{D}}{\partial t}\ . \end{aligned} \tag{5.5.5}$$

The last equality gives a general version of *Poynting's Theorem*. Using the definitions of **H** and **D**, and Fourier transforming in time, we obtain

$$\nabla \cdot \mathbf{P} = i\omega\mu_o \mathbf{B}^2 + i\omega\epsilon_o \mathbf{E} \cdot \boldsymbol{\epsilon} \cdot \mathbf{E} \,. \tag{5.5.6}$$

Using the cold plasma dielectric tensor gives

$$\mathbf{E} \cdot \boldsymbol{\epsilon} \cdot \mathbf{E} = \epsilon_o \left[S(E_x^2 + E_y^2) + P E_z^2 \right] \,, \tag{5.5.7}$$

where the Hermitian property of the dielectric tensor has resulted in a purely real result for this term. Therefore, we have

$$\mu_o \nabla \cdot (\mathbf{E} \times \mathbf{B}) = \epsilon_o \left[S E_r^2 + P E_z^2 \right] \,, \tag{5.5.8}$$

where,

$$\begin{aligned} \mathbf{B} &= \mathbf{B}_o + \frac{1}{i\omega} \nabla \times \mathbf{E} \\ E_r &= \frac{i\Omega_o}{\omega(\omega^2 - 1 - \Omega_o^2)} \left[E_\theta \cos\rho - E_z \sin\rho \right] \,. \end{aligned} \tag{5.5.9}$$

Since all these quantities are available, this potential conservation law can be checked by numerical integration. We must remember, however, that the use of the uniform cold plasma approximation means this expression is valid only for situations close to uniform, i.e. where the contribution of the current to the dielectric tensor can be neglected. The code `odeadams.for`, described in Section 5.6 was modified to test Eq. 5.5.8, by evaluating the supposed invariant at a succession of points through the plasma. The results obtained were somewhat inconclusive, although for parameter ranges close to the uniform plasma regime, the quantity on the LHS of Eq. 5.5.8, when evaluated, was an order of magnitude or so less than its constituent parts. The poor results here suggest that the equilibrium currents may be more important than we predicted in Section 4.4.

5.6 Results

Results from the simulations described above are now given for a range of parameter values. First, results for an incoming O-mode are shown in figures 5.3 to 5.10, then results for an incoming X-mode are shown in figures 5.11 to 5.18. The results are given in terms of the amplitude and phase shift of each coefficient, and the scales are normalised by dividing by the amplitude of the incident wave: τ in the case of an incoming O-mode, and ν for an incoming X-mode. e.g., for $\frac{\sigma}{\tau}$, we plot $\left|\frac{\sigma}{\tau}\right|$ and $\arctan\left[\Im(\frac{\sigma}{\tau})/\Re(\frac{\sigma}{\tau})\right]$. Frequencies are expressed in units of ω_p. Each curve

Figure 5.3: Phase changes for incoming O-mode, $\Omega_o = 0.1\,\omega_p$.

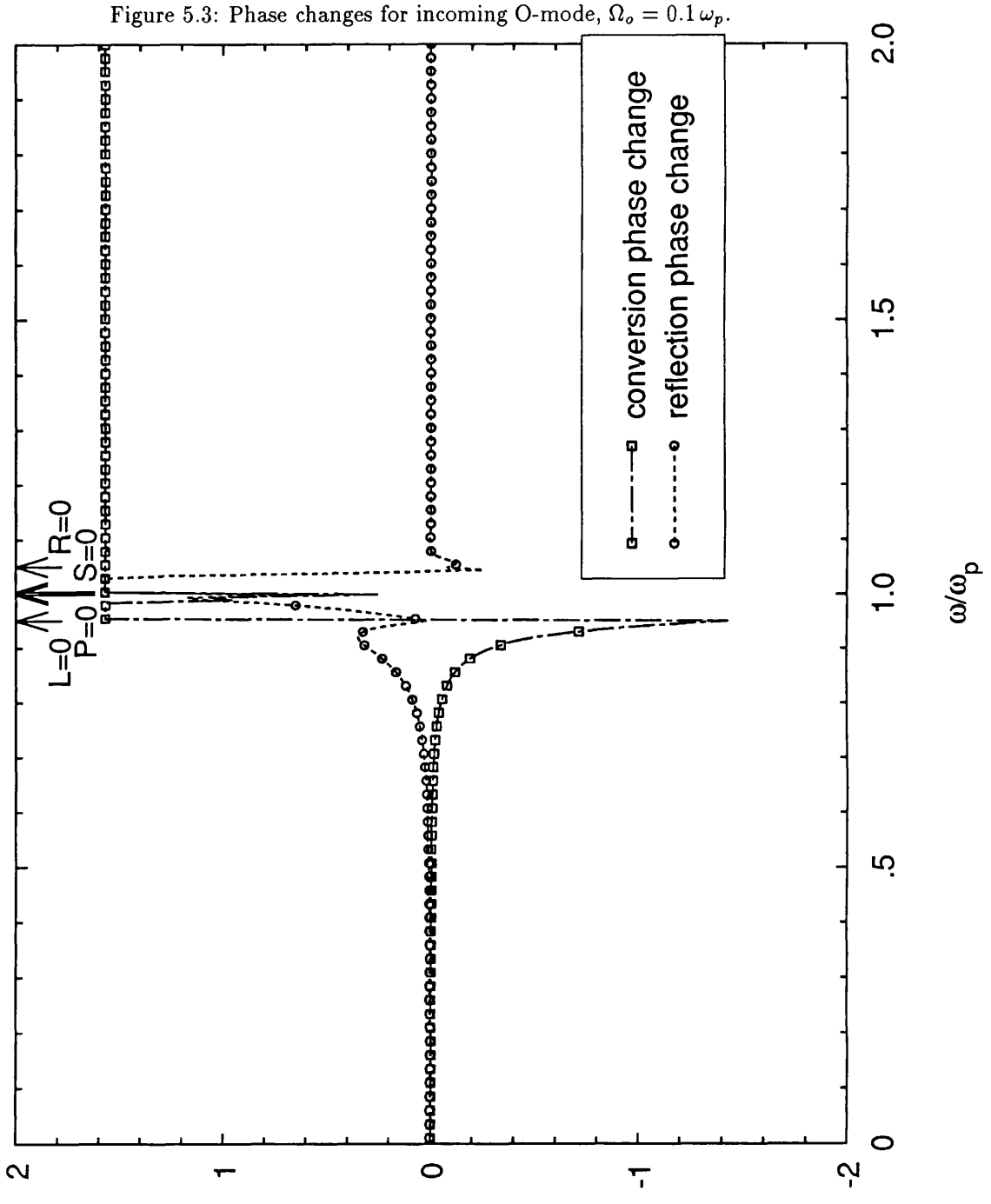

Figure 5.4: Amplitudes for incoming O-mode, $\Omega_o = 0.1\,\omega_p$.

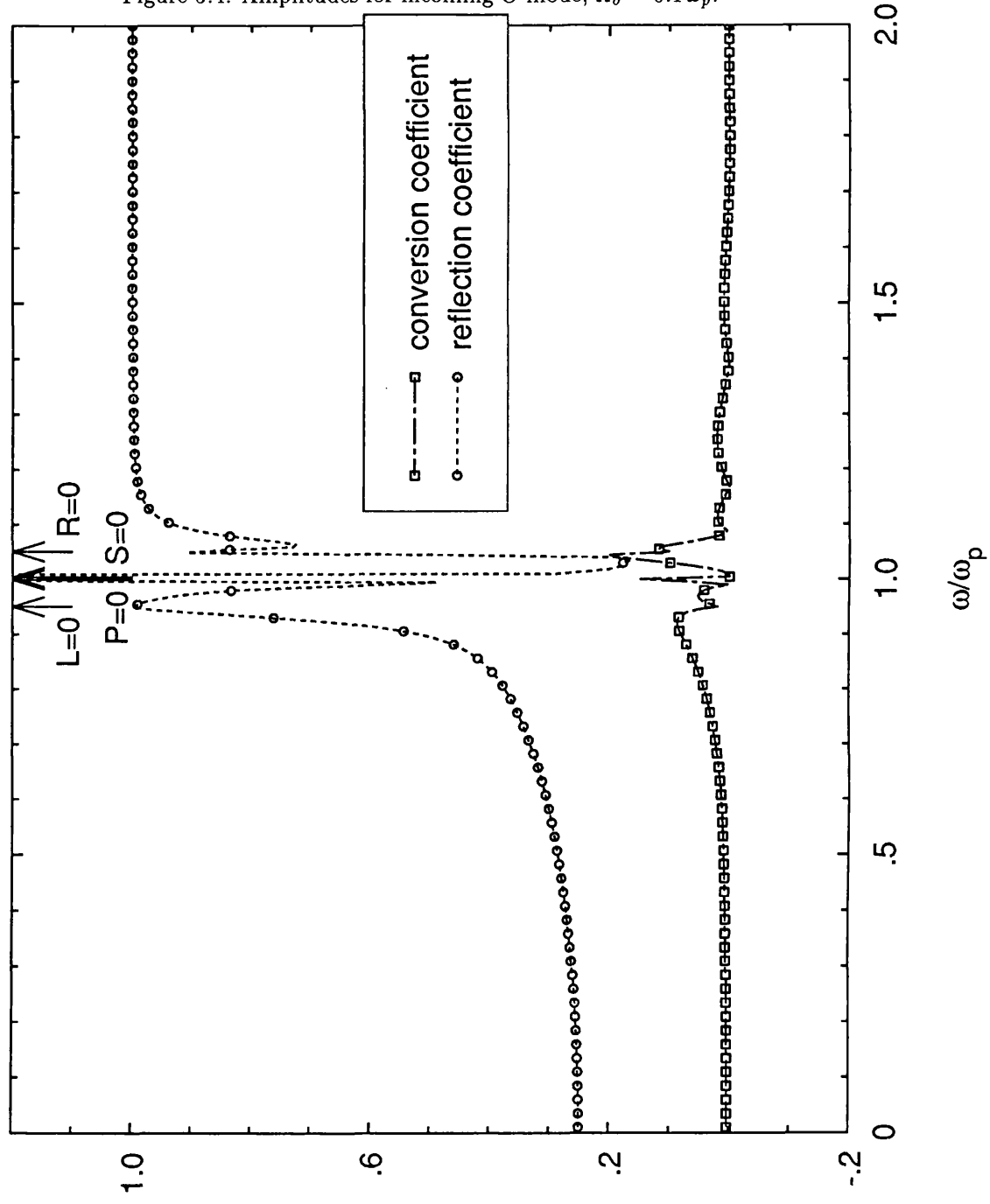

Figure 5.5: Phase changes for incoming O-mode, $\Omega_o = 0.5\,\omega_p$.

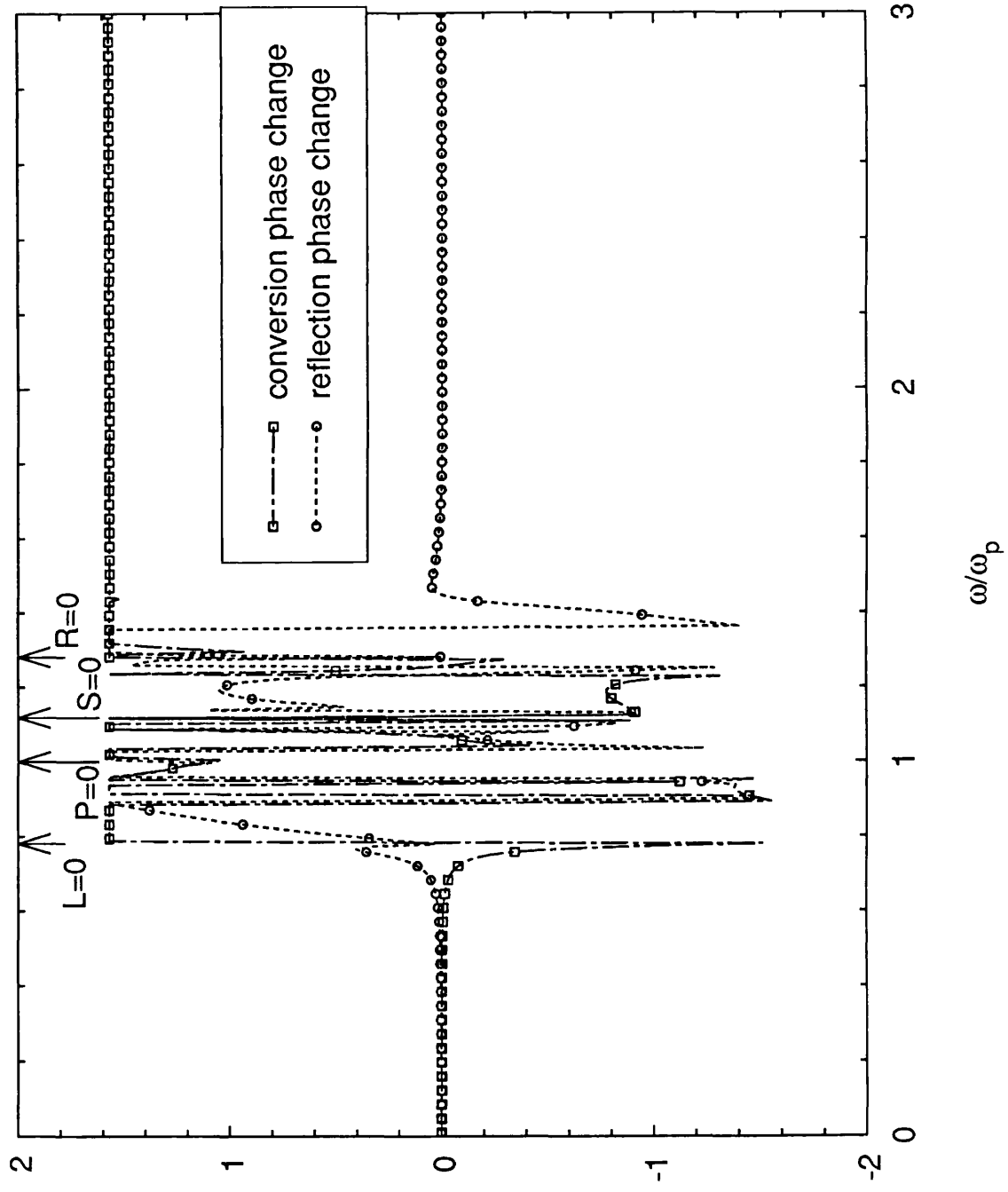

Figure 5.6: Amplitudes for incoming O-mode, $\Omega_o = 0.5\,\omega_p$.

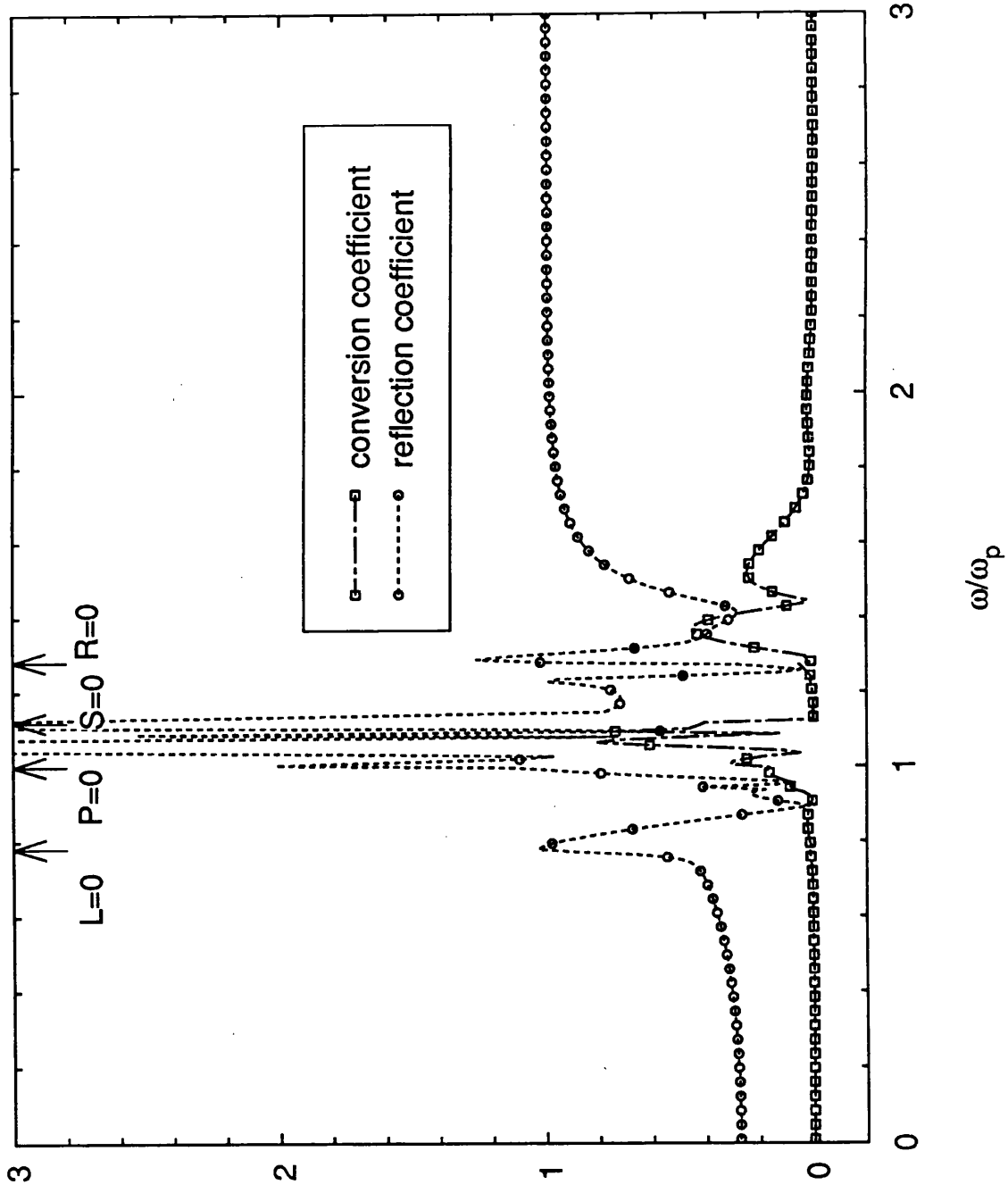

Figure 5.7: Phase changes for incoming O-mode, $\Omega_o = \omega_p$.

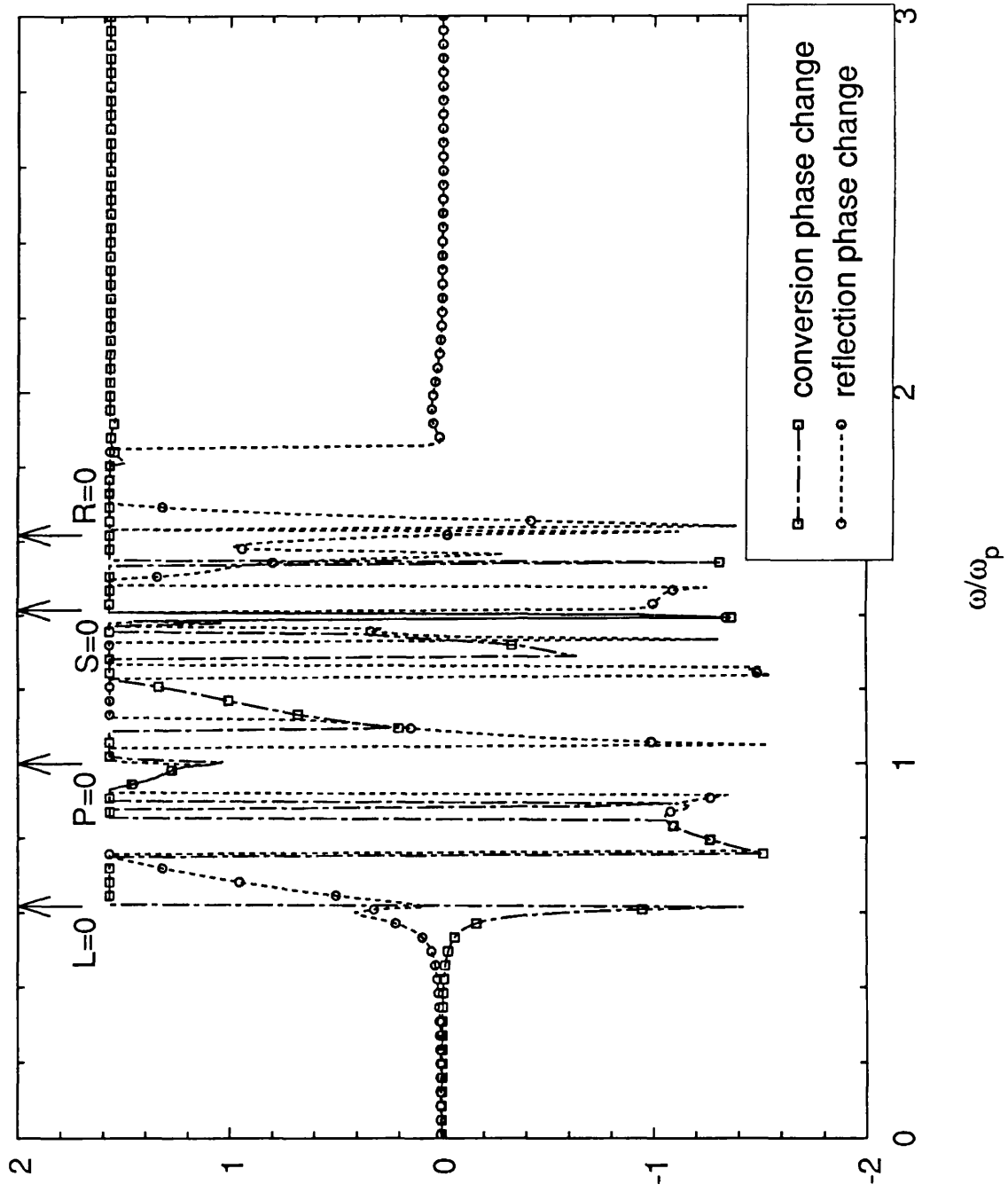

Figure 5.8: Amplitudes for incoming O-mode, $\Omega_o = \omega_p$.

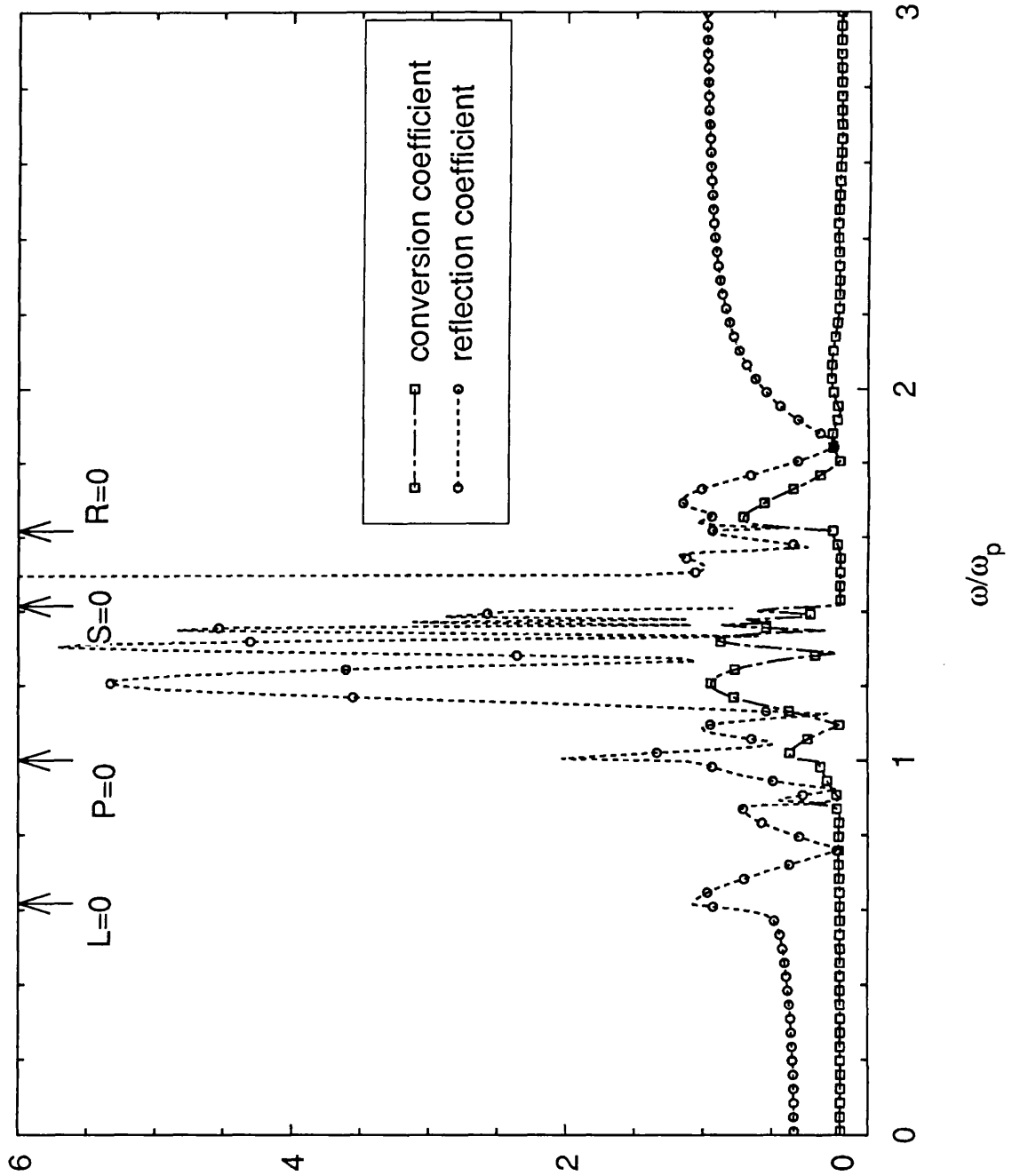

Figure 5.9: Phase changes for incoming O-mode, $\Omega_o = 3\,\omega_p$.

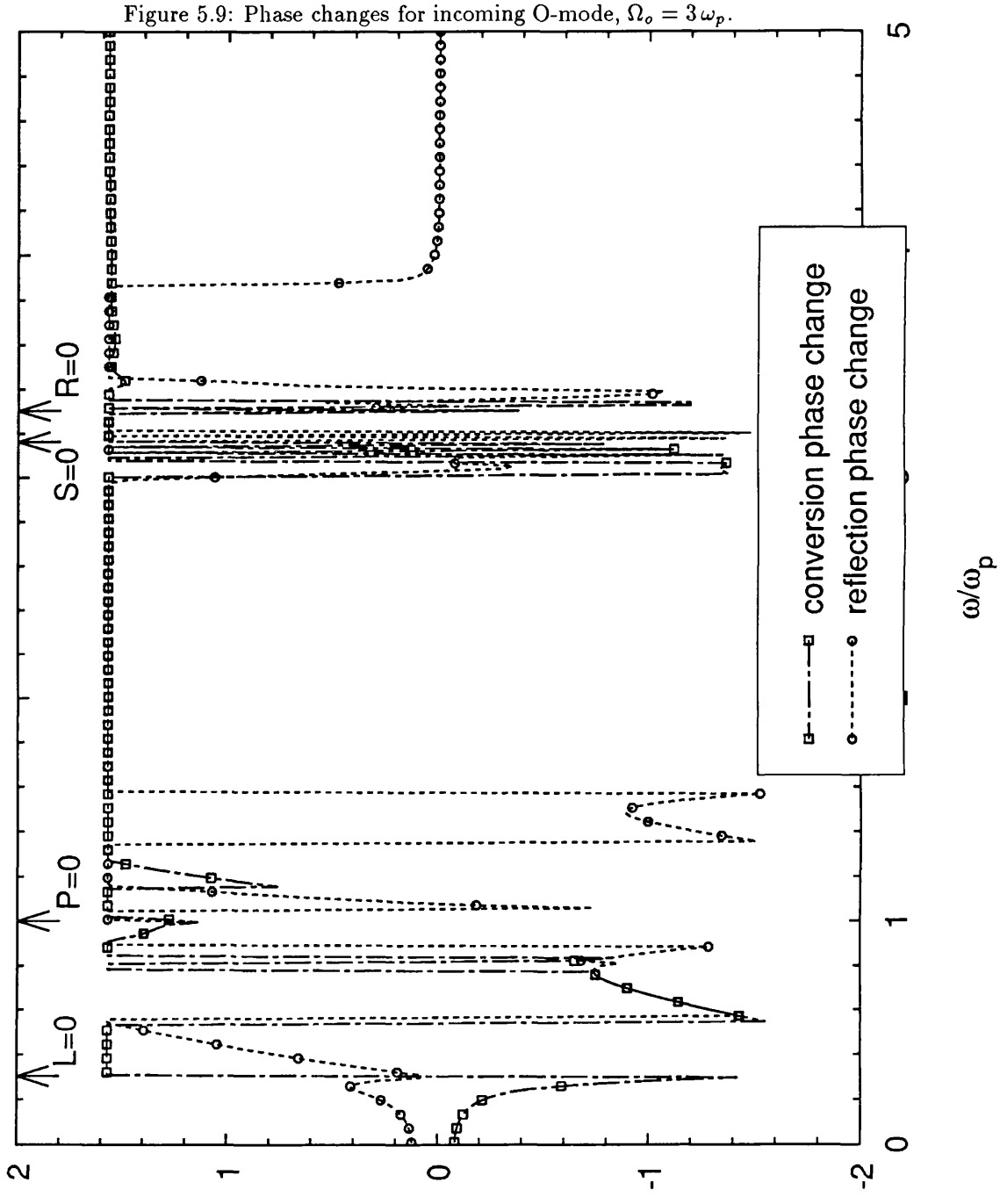

Figure 5.10: Amplitudes for incoming O-mode, $\Omega_o = 3\omega_p$.

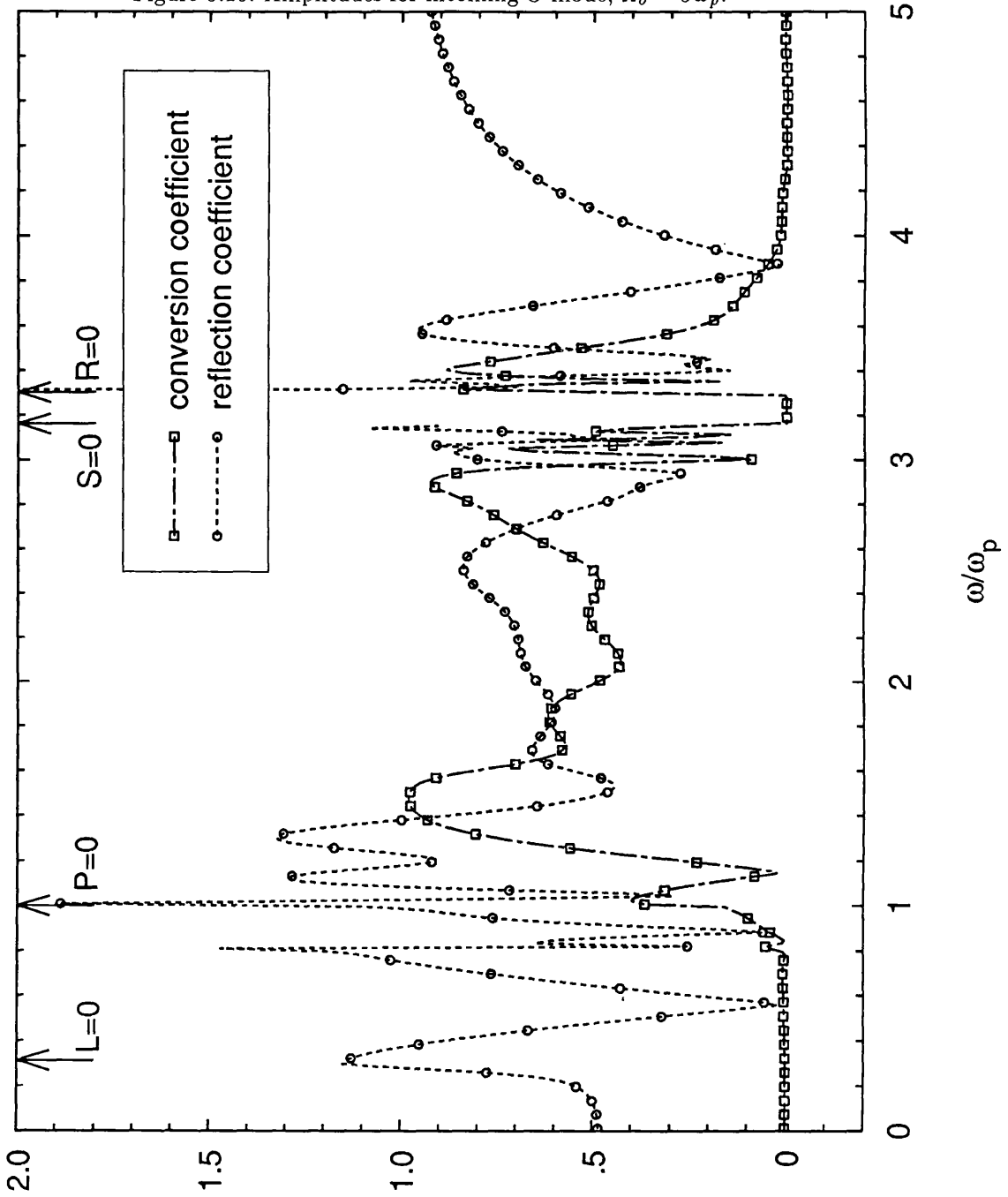

Figure 5.11: Phase changes for incoming X-mode, $\Omega_o = 0.1\,\omega_p$.

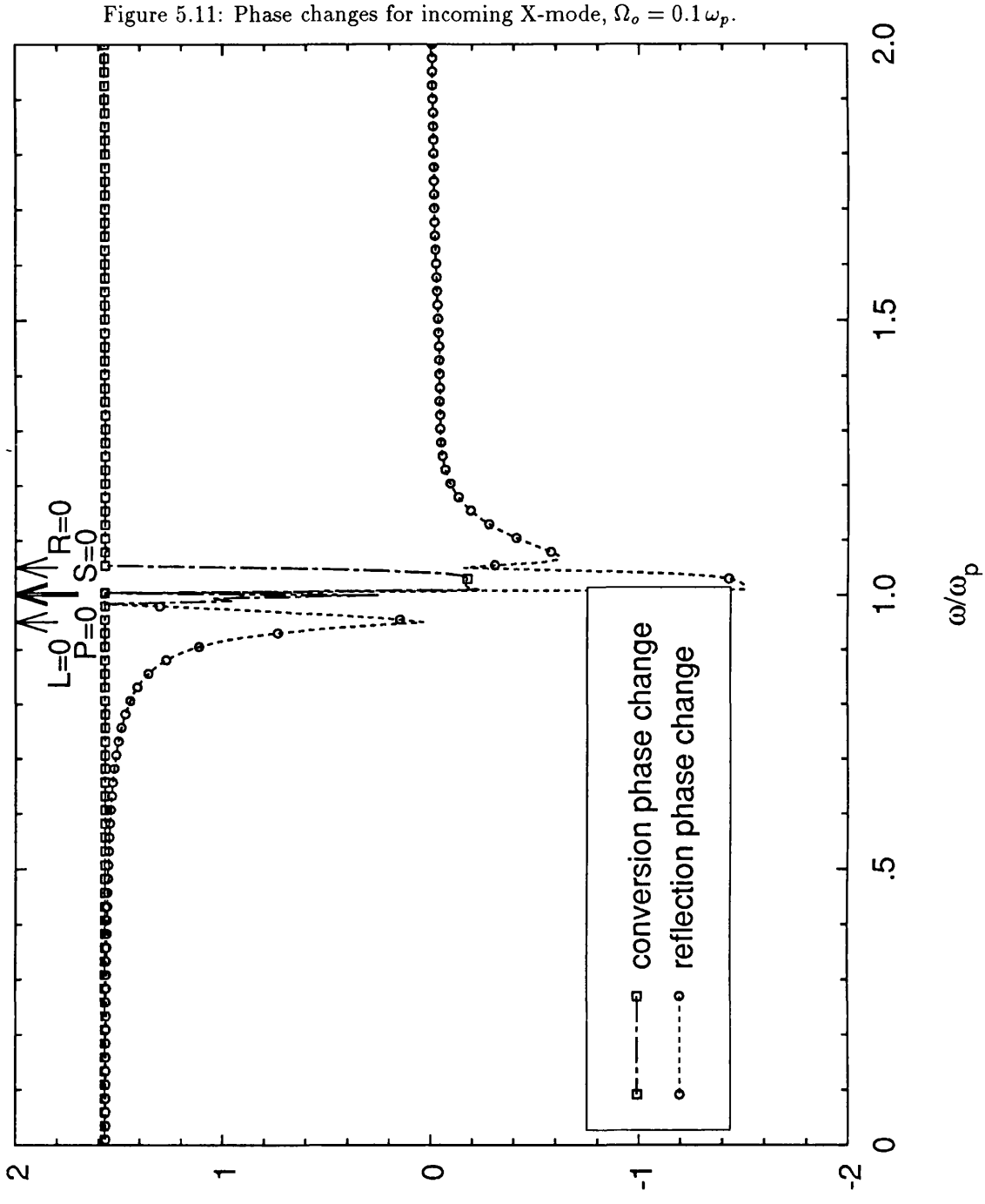

Figure 5.12: Amplitudes for incoming X-mode, $\Omega_o = 0.1\,\omega_p$.

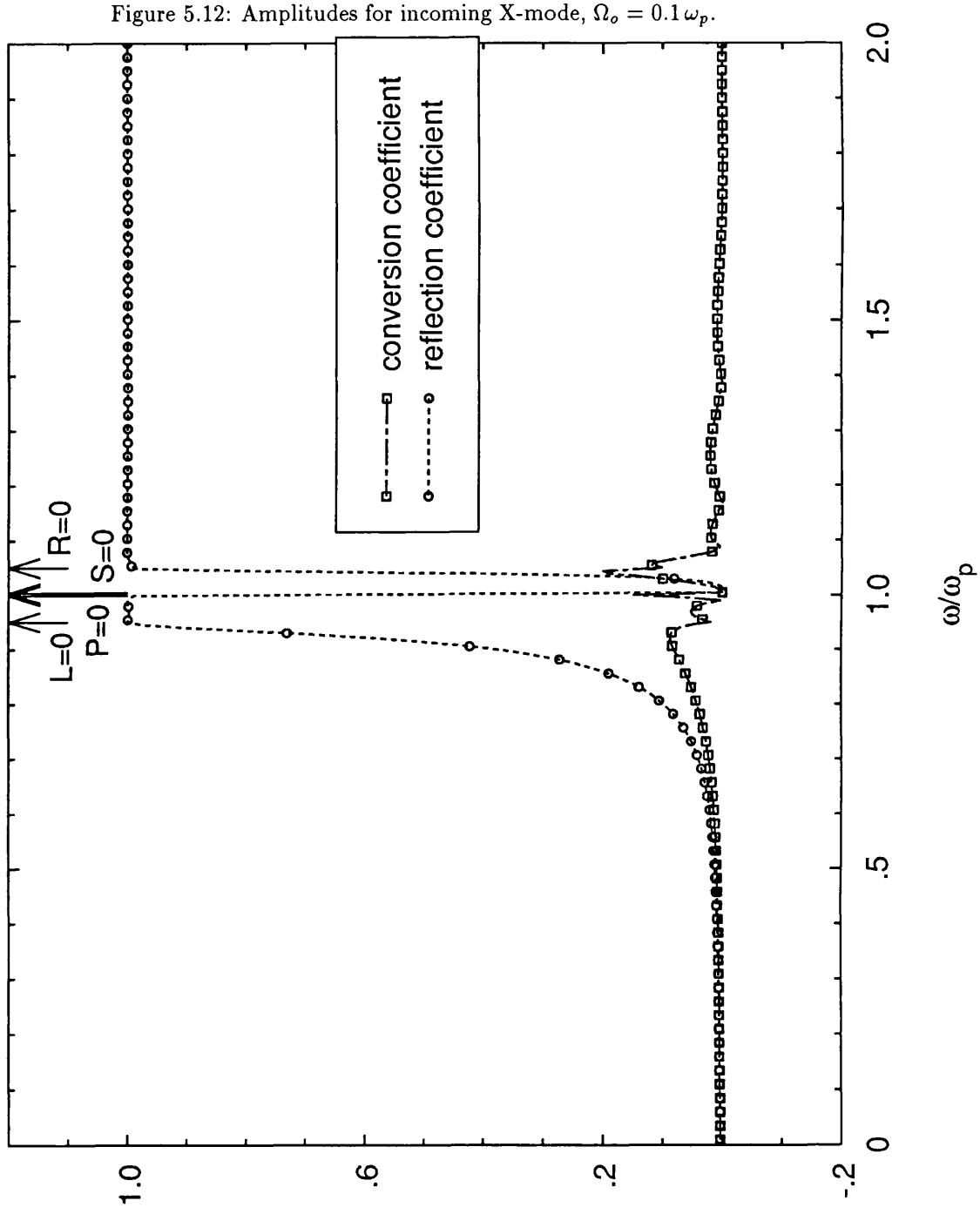

Figure 5.13: Phase changes for incoming X-mode, $\Omega_o = 0.5\,\omega_p$.

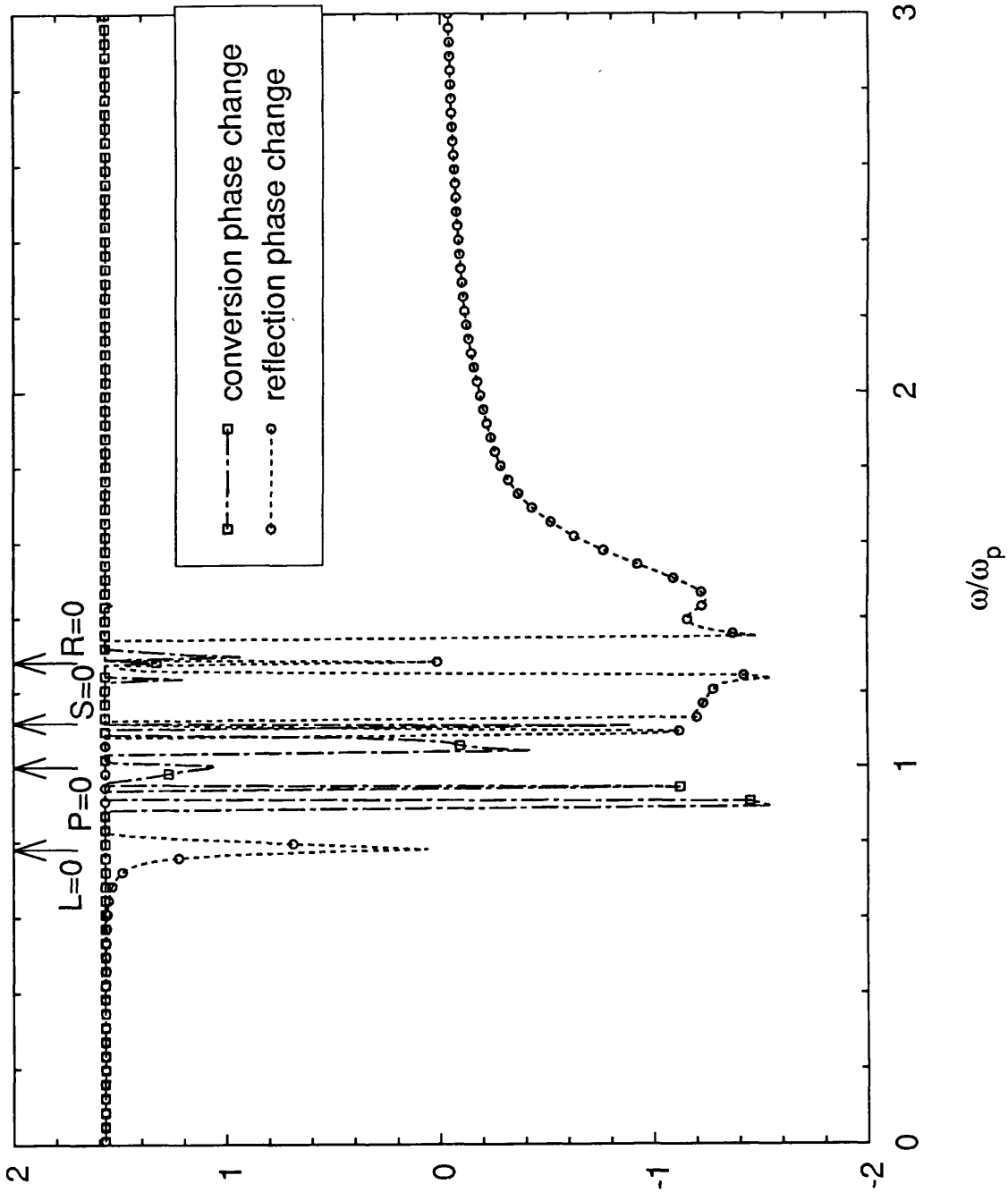

Figure 5.14: Amplitudes for incoming X-mode, $\Omega_o = 0.5\,\omega_p$.

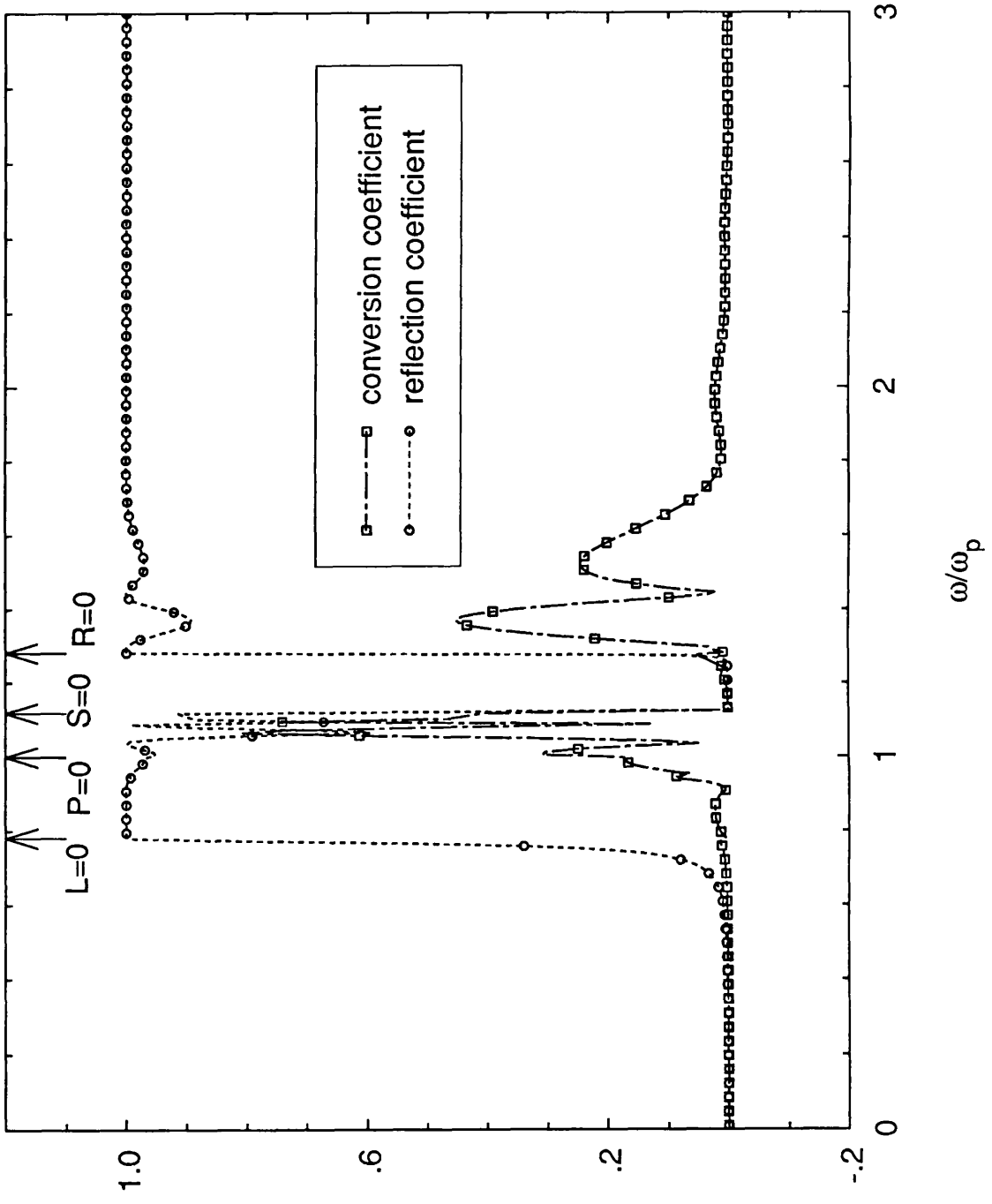

Figure 5.15: Phase changes for incoming X-mode, $\Omega_o = \omega_p$.

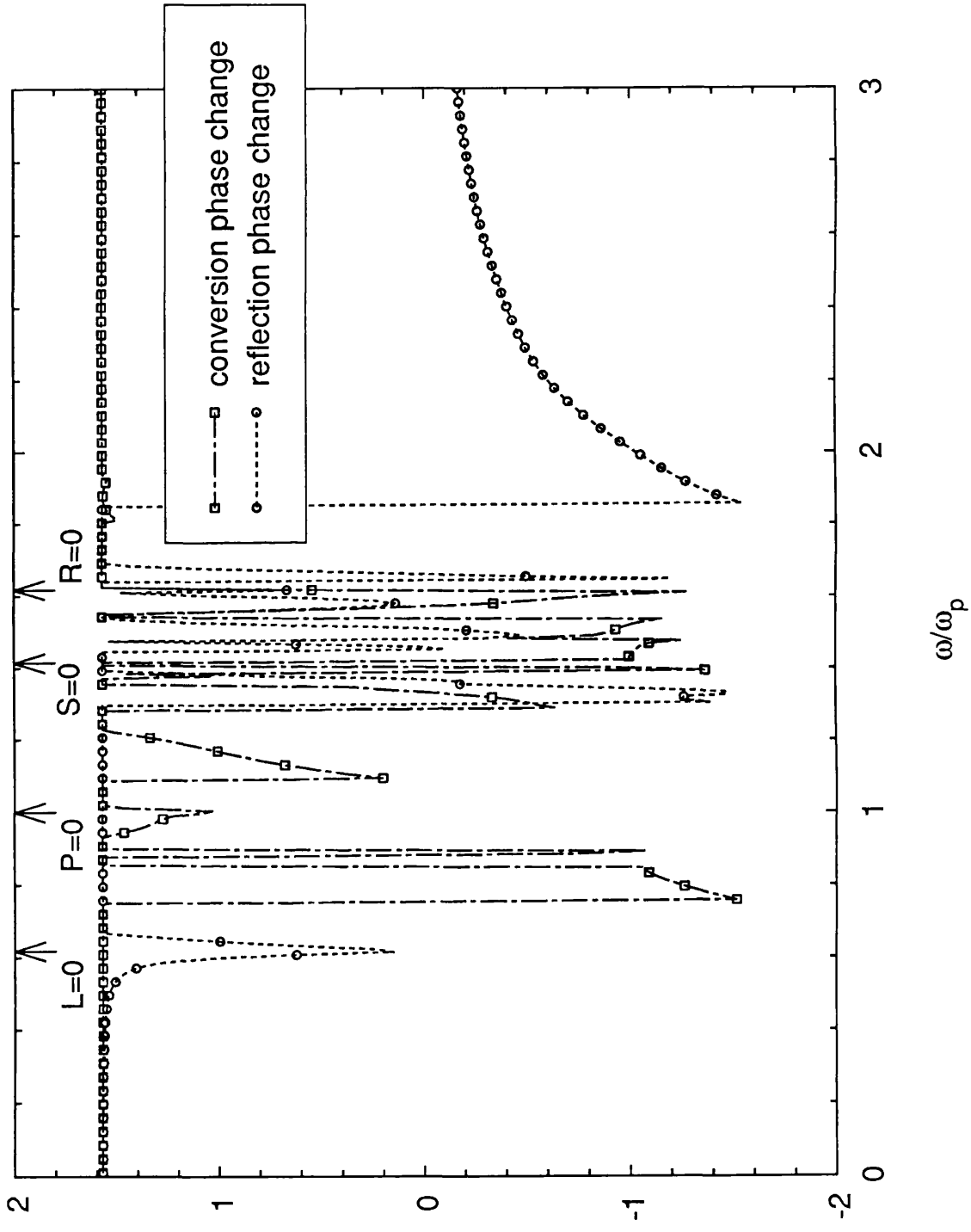

Figure 5.16: Amplitudes for incoming X-mode, $\Omega_o = \omega_p$.

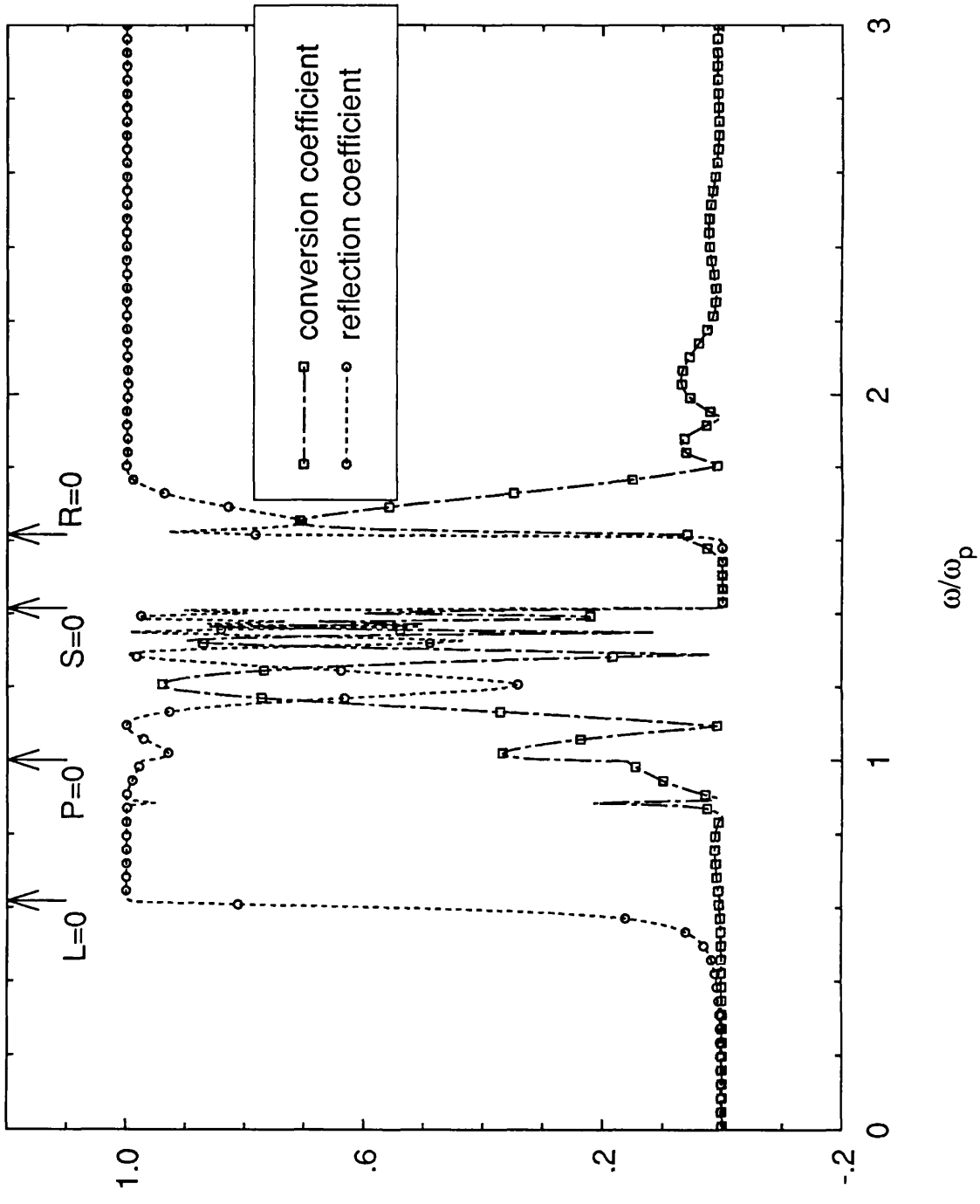

Figure 5.17: Phase changes for incoming X-mode, $\Omega_o = 3\,\omega_p$.

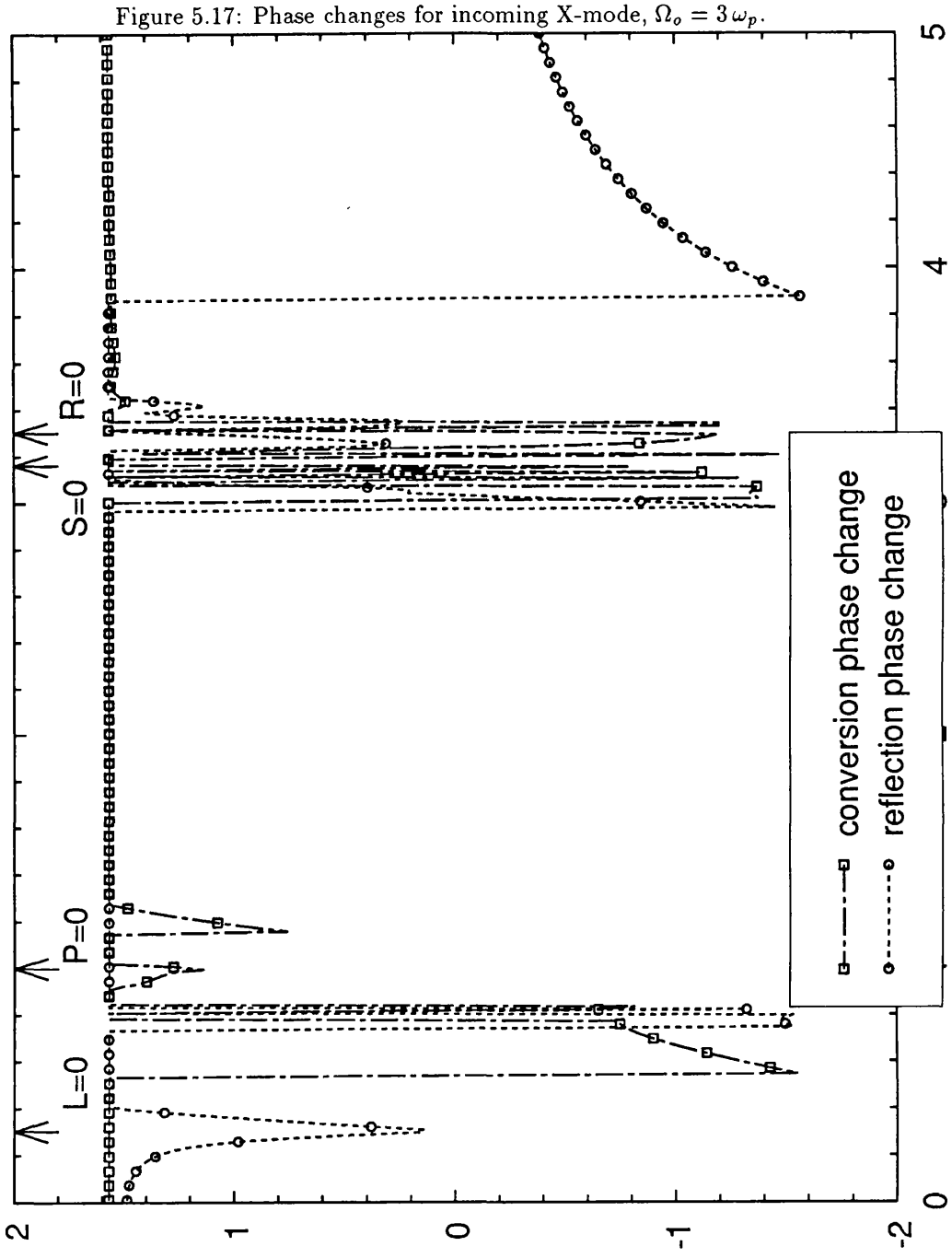

Figure 5.18: Amplitudes for incoming X-mode, $\Omega_o = 3\omega_p$.

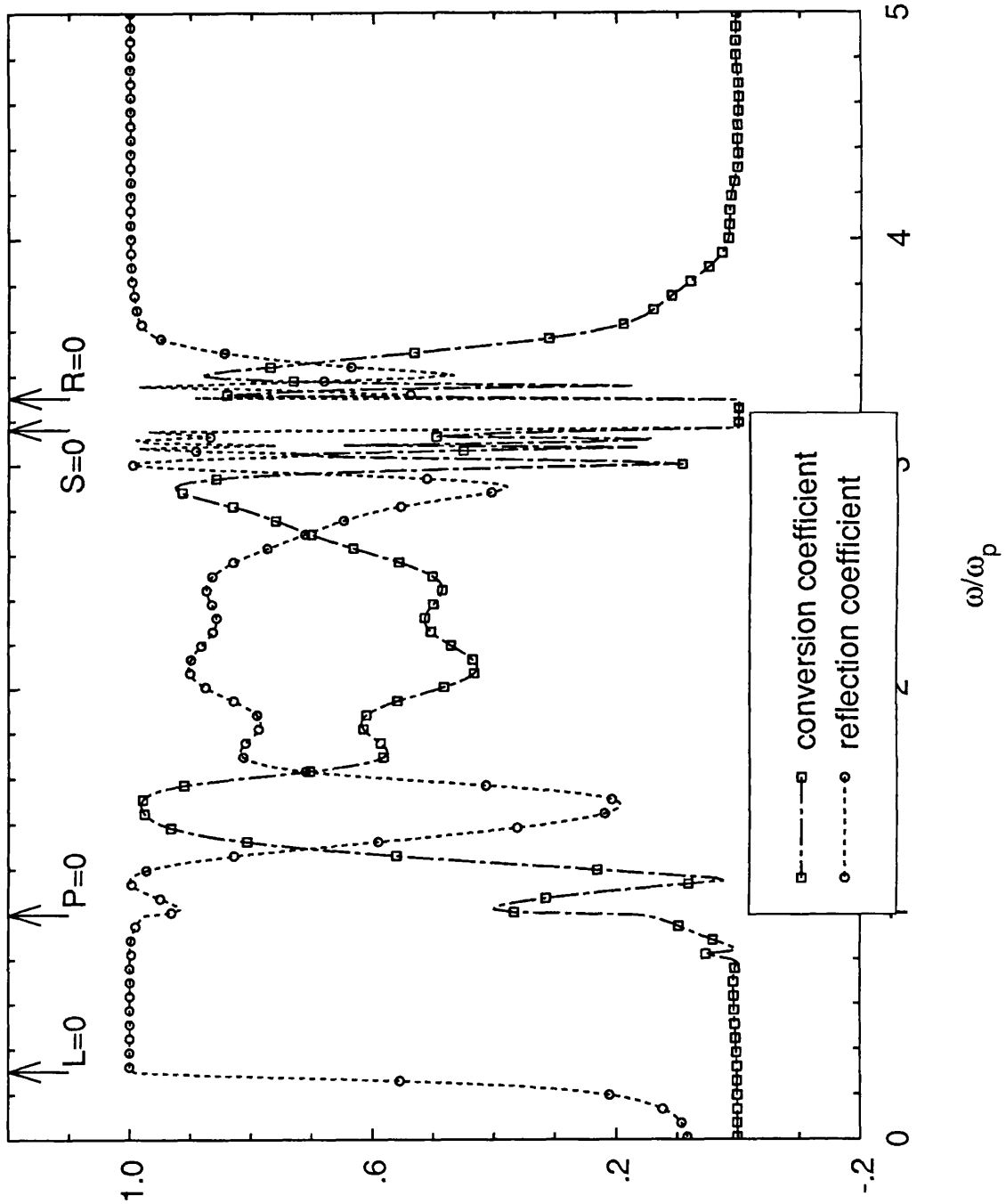

was produced using 400 points, though, for clarity, only every fifth point has been plotted. The range of frequencies plotted was chosen to show the structured region to advantage in each case. Initially, most cases were examined with a greater range of frequency, but no structure was found apart from that illustrated.

The graphs clearly have a complex structure, so that, even with our comparatively simple model of wave propagation, a wide range of possible outcomes may be identified. In most cases, there is some form of correlation between the curves for reflected and converted waves, although the relationship between the two is not as simple as the sum of the squares of the two amplitudes being one, as we discussed in the last section. The modes have different intrinsic energies due to their differing wavenumbers, so that, for instance, an increase in the amplitude of a mode whose wavenumber is decreasing might result in no increase in the overall energy.

It should be noted that the external solutions may be uniquely identified with harmonic waves, because of the asymptotic form of the Bessel functions. Explicitly, we have

$$\begin{aligned} H_o^{(1)}(q\rho) &\sim \sqrt{\frac{2}{\pi q\rho}} \exp i(q\rho - \frac{\pi}{4}) , \\ H_1^{(1)}(p\rho) &\sim \sqrt{\frac{2}{\pi p\rho}} \exp i(p\rho - \frac{3\pi}{4}) , \\ H_o^{(2)}(q\rho) &\sim \sqrt{\frac{2}{\pi q\rho}} \exp i(-q\rho - \frac{\pi}{4}) , \\ H_1^{(2)}(p\rho) &\sim \sqrt{\frac{2}{\pi p\rho}} \exp i(-p\rho + \frac{\pi}{4}) . \end{aligned} \tag{5.6.1}$$

In all the cases given, for frequencies well above all characteristic frequencies in the plasma, the converted component falls to zero and the reflected tends to one, while the phase change for the reflection tends to zero. This is a reasonable result, since, in this case, the incident wave has too high a frequency to couple to any mode in the internal region, and the only available channel for the wave's energy is to be totally reflected. The zero phase change is what one might expect, given that we have a 'free' end (i.e. electric field not set to zero).

Also marked on the graphs are values of frequency at which significant boundaries in the CMA diagram are crossed, and hence where the types of wave present may be expected to change. These boundaries are, in the Stix notation, $R = 0$, $L = 0$, $P = 0$ and $S = 0$ (the upper hybrid resonance). The latter is a case where the cold plasma model breaks down and further physical content (the effect of temperature, for instance) is needed in order to produce any meaningful predictions at this frequency. The spikes which occur in some graphs at this value (namely

Figure 5.19: The sign of RL/S

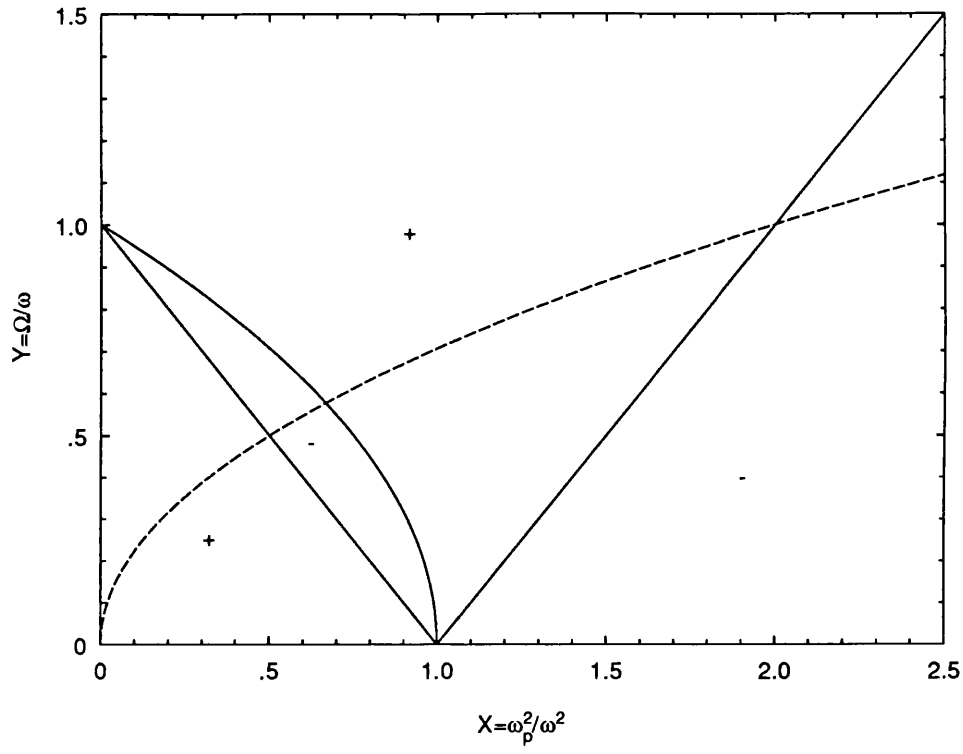

$\omega = \sqrt{\omega_p^2 + \Omega_o^2}$), are caused by this shortcoming.

5.6.1 Relation To Cold Plasma Modes

Some insight into this behaviour can be gained by viewing it in terms of the CMA diagram. Since the uniform field joins smoothly onto the helical field, the uniform cold plasma predictions for uniform magnetic field should be approximately valid near the edge of the structured region. Thus we can predict whether an incoming wave will excite internal oscillations, although this quasi-linear approximation (we have tacitly assumed that the modes are $P(\rho)$, $R(\rho)L(\rho)/S(\rho)$) cannot predict what happens when they propagate inwards. Broadly speaking, it can be predicted whether reflection or conversion will dominate, but we cannot expect to predict exact values.

The choice of Ω_o/ω = constant in these graphs implies that, in the notation of the CMA diagram,

$$Y = \text{constant}\sqrt{X} \; . \tag{5.6.2}$$

Figures 5.19 and 5.20 show how the the signs of RL/S and P change throughout the CMA diagram (shown in Figure 2.1). The dashed curve in each case is an

Figure 5.20: The sign of P

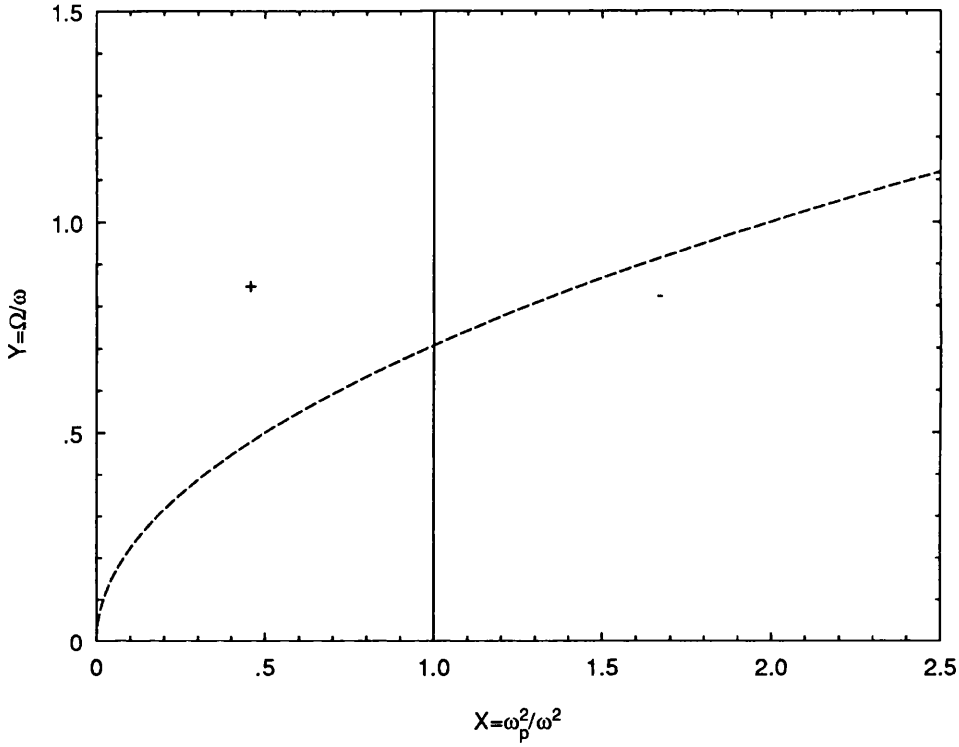

example of the path traced out with one choice of the constant in Eq. 5.6.2. Note that low frequency corresponds to the right, and high frequency to the left of these graphs. Because of the way these parabolae cut boundaries in the CMA diagram we can distinguish five regions, the boundaries between which correspond to a mode changing from propagation to evanescence, or vice versa. The qualitative reasons for the structure of each of these regions are now considered.

Between $\omega = 0$ and the curve $L = 0$

Both modes are evanescent, so one would expect firing in either to give rise to negligible conversion. This is true for the converted wave, but with an incoming O-mode, there is a small, but non-zero reflection coefficient, which scales with the value of cyclotron frequency. $L = 0$, where the X-mode becomes propagating, corresponds to the first peak in the reflection coefficient.

Between the curves $L = 0$ and $P = 0$

The X-mode propagates, but the O-mode is evanescent. We would expect an incoming X-mode to be entirely reflected, and this is seen in the numerical results for this case, but with some deviations: towards $P = 0$ there is some conversion,

and a narrow region occurs where reflection sharply dips and conversion peaks (see Figure 5.8, for instance). Firing in the evanescent O-mode gives a more complex pattern. There is little conversion, but reflection varies considerably, with a number of sharp peaks. One should remember that the coefficients here are normalised to the amplitude of an exponentially damped wave, so that even a large result may mean a small reflection or conversion. O-mode results have a peak in the reflection at the cutoff $P = O$.

Between the curves $P = 0$ and $S = 0$

Both modes propagate. There is no overall constraint on which scattering channel is used, so this argument will predict nothing about this region, which the graphs above show to be very complex.

Between the curves $S = 0$ and $R = 0$

The X-mode is evanescent, and the O-mode propagates. Firing in an X-mode gives negligible reflection or conversion, while an incoming O-mode gives a reflection which is large near the resonance, $S = 0$, and becomes smaller towards $R = 0$, with negligible conversion.

Between $R = 0$ and $\omega = \infty$

Both modes propagate. For high enough ω, the argument outlined in Section 5.6 applies.

5.6.2 Fitting Waves Into The Region

One simple explanation of the peaks observed in the graphs is that they occur at frequencies for which an exact number of wavelengths, or half wavelengths, fit into the inner region.

Suppose we require that an integral number of half wavelengths fit into the range 2π, then, using the uniform modes, and taking E_z as an example, we must satisfy

$$J_o(2\pi q) = 0 \; . \tag{5.6.3}$$

There is an infinite set of solutions to this equation, the lower valued of which are tabulated in Abromowitz & Stegun. Denoting the sth solution by $\mathcal{J}_{o,s}$, we can substitute for q and then solve for ω, to produce

$$\omega_s = \left\{ 1 + \left(\frac{\mathcal{J}_{o,s}}{2\pi} \right)^2 \right\}^{1/2} \; . \tag{5.6.4}$$

The first few of these quantities were calculated, as well as the corresponding quantities derived from fitting E_θ into the same interval. They were found to bear no relation to the peaks or troughs of the graphs. The process was then repeated, assuming that a maximum was at the boundary, so that the condition on the frequencies involved the zeros of the derivatives of Bessel functions, but with no better results.

The principle involved here may well be sound, in fact, but the uniform modes are poor approximations for the actual wave behaviour. Finding the precise way in which the 'wavelengths' fit into the region is a much more complex problem. Section 5.4.1 shows that the internal behaviour is well approximated by harmonic waves with an amplitude of $1/\sqrt{\rho}$, so that the wavenumbers do not vary with radius. However, the coupling of E_θ and E_z means that both must be considered to obtain the result. The dependence of coupling on characteristic frequencies gives the variation of the coefficients shown in the Figures.

The upshot of this section is that the plasma we are modelling has strongly coupled electric field components which behave very differently from uniform approximations.

5.7 Relevance To Plasma Heating

An important parameter for a tokamak or other fusion device is the quantity

$$\beta = \frac{2\mu_o p}{B^2}\,, \tag{5.7.1}$$

which measures the relative sizes of the magnetic pressure and ordinary fluid pressure. Too high a value of β leads to instabilities, but for economic reasons, it is desirable to have β as high as possible (magnetic pressure is more expensive to generate than thermodynamic). Because of this, most fusion experiments have $0.01 \leq \beta \leq 0.1$. Eq. 5.7.1 can be rewritten by substituting for pressure and magnetic field in terms of cyclotron and plasma frequency and noting that $\epsilon_o\mu_o = 1/c^2$:

$$\beta = \frac{2kT}{c^2 m_e}\left(\frac{\omega_p}{\Omega_o}\right)^2 = \frac{4}{3}\left(\frac{\text{kinetic energy}}{\text{rest mass energy}}\right)\left(\frac{\omega_p}{\Omega_o}\right)^2\,. \tag{5.7.2}$$

The ratio of energies is about 0.02 for current JET experiments (the electron temperature reaches 10keV and the electron rest mass is 511 keV), and for projected fusion reactors is still only about 0.2 (assuming electron temperatures of around 100keV). Putting these together with current JET values of $\beta = 0.05$ and taking

$\beta = 0.1$ for future reactors gives

$$\frac{\omega_p}{\Omega_o} = \begin{cases} 1.06 & \text{JET} \\ 1.20 & \text{future reactor} \end{cases} . \tag{5.7.3}$$

Therefore, we can take $\omega_p \sim \Omega_o$ as being typical of fusion plasmas. The relevant graphs are therefore Figures 5.7, 5.8, 5.15, 5.16.

We have concentrated on finding the behaviour external to a structured plasma, while other authors have focussed on purely internal behaviour. However, given a certain admixture of modes at a particular radius then our analysis can be applied to the plasma within this radius, though, of course, the outgoing modes resulting from the scattering will be further coupled at larger radii, rather than propagating with no further change.

In this connection, we might also mention the ray tracing technique, which assumes that the variation of plasma waves with radius results from resolving the electric field along the changing direction of magnetic field, and that substituting in the radial dependence of the plasma parameters into the wavenumbers of the uniform modes. This type of argument has been used extensively to predict paths of plasma waves within a tokamak. However, applying a ray tracing argument to our plasma will give results of little interest, since, within this approximation, the wavenumbers P, and RL/S are constant across the structured region. This is because they can be expressed purely in terms of ω_p^2, and $\Omega^2 \propto \sin^2\rho + \cos^2\rho = 1$, so there can be no cutoffs or resonant surfaces. Note also that our model does not include any of the mechanisms discussed in Section 1.3.1 and so conversion to kinetic modes is not included. Despite this apparent lack of potential for mode conversion, our simulations show that the coefficients of outgoing waves are anything but constant as we move through parameter space. In particular, the region between the $S = 0$ and $P = 0$ curves in Fig. 5.8 shows a number of distinct peaks which reach significantly above 1. At these points, the inner plasma region will act as an effective reflector or combined reflector/convertor for incoming waves, and so we expect penetration of waves at these parameter values to be minimal.

Another noteworthy feature is the rapid variation of the phase change in most of the examples above. This means that if we superpose many different frequencies to produce a wavepacket then they are likely to suffer a wide variety of different phase changes. If these form an approximately random distribution, we anticipate a large degree of cancellation so that the resultant outgoing wave motion in the external region will be very small.

Chapter 6

Comparison With Other Techniques

The most commonly used solution technique for non-uniform propagation problems is the WKB method. It is therefore of interest to consider the numerical solutions obtained from the coupled equations in the light of a consistent eigenvalue and WKB analysis of the same equations, as outlined in Chapter 3. To attack the problem of the last chapter, we need to produce appropriate differential equations for both the internal, helical region and the external uniform region.

We also briefly consider application of the Cairns, Lashmore-Davies technique.

6.1 Eigenvalue Analysis Of Coupled Equations

Tackling the helical region first, we carry out the eigenvalue analysis of Chapter 3, but, rather than starting from a fourth order equation, we use the system 4.2.5, which is already in almost the correct form.

The equations for electric fields in our helical plasma, as derived in Chapter 4, can be written in matrix form as

$$\mathbf{y}' = \begin{bmatrix} 0 & -(a+\frac{b}{2}+\frac{b}{2}\cos 2\rho - \frac{3}{4\rho^2}) & 0 & \frac{b}{2}\sin 2\rho \\ 1 & 0 & 0 & 0 \\ 0 & \frac{b}{2}\sin 2\rho & 0 & -(a+\frac{b}{2}-\frac{b}{2}\cos 2\rho + \frac{1}{4\rho^2}) \\ 0 & 0 & 1 & 0 \end{bmatrix} \mathbf{y} \,, \tag{6.1.1}$$

where

$$y_1 = y_2' \,, \quad y_2 = E_\theta \sqrt{\rho} \,, \quad y_3 = y_4' \,, \quad y_4 = E_z \sqrt{\rho} \,. \tag{6.1.2}$$

In the notation of Chapter 3, the 4×4 matrix above is M, and we define

$$\mathsf{M} = \begin{bmatrix} 0 & k & 0 & m \\ 1 & 0 & 0 & 0 \\ 0 & m & 0 & n \\ 0 & 0 & 1 & 0 \end{bmatrix} , \tag{6.1.3}$$

so that the eigenvalues of M satisfy

$$\begin{vmatrix} -\lambda & k & 0 & m \\ 1 & -\lambda & 0 & 0 \\ 0 & m & -\lambda & n \\ 0 & 0 & 1 & -\lambda \end{vmatrix} = 0 , \tag{6.1.4}$$

which may be reduced to

$$(\lambda^2 - k)(\lambda^2 - n) - m^2 = 0 . \tag{6.1.5}$$

Clearly, if the coupling is ignored entirely, then $m = 0$ and the eigenvalues are $\pm\sqrt{k}$, $\pm\sqrt{n}$. In the general case, the eigenvalues are

$$\lambda = \pm\sqrt{\frac{k+n}{2} \pm \frac{1}{2}\sqrt{(k-n)^2 + 4m^2}} , \tag{6.1.6}$$

with the associated eigenvector being proportional to

$$(-\frac{m\lambda}{k-\lambda^2}, -\frac{m}{k-\lambda^2}, -\lambda, 1) . \tag{6.1.7}$$

The four roots given in Eq. 6.1.6 are given subscripts $1-4$ according to the choice of sign in that equation:

root	1st sign	2nd sign
λ_1	+	+
λ_2	+	−
λ_3	−	+
λ_4	−	−

It can easily be seen that

$$\lambda_1 = -\lambda_3 , \quad \lambda_2 = -\lambda_4 . \tag{6.1.8}$$

Using these relations, and evaluating $\mathsf{A}^{-1}\mathsf{A}'$ using REDUCE we find that the coupling matrix has the structure

$$\begin{bmatrix} \epsilon & \frac{\gamma}{\lambda_1-\lambda_2} & \alpha & \frac{\gamma}{\lambda_1+\lambda_2} \\ -\frac{\delta}{\lambda_1-\lambda_2} & \zeta & \frac{\delta}{\lambda_1+\lambda_2} & \beta \\ \alpha & \frac{\gamma}{\lambda_1+\lambda_2} & \epsilon & \frac{\gamma}{\lambda_1-\lambda_2} \\ \frac{\delta}{\lambda_1+\lambda_2} & \beta & -\frac{\delta}{\lambda_1-\lambda_2} & \zeta \end{bmatrix} , \tag{6.1.9}$$

where

$$\begin{aligned}
\alpha &= -\frac{\lambda_1'}{2\lambda_1}\ ,\ \beta = -\frac{\lambda_2'}{2\lambda_2}\ , \\
\gamma &= \frac{-(k-\lambda_1^2)^3}{2m\lambda_1(k-\lambda_2^2)}\left[\frac{m}{k-\lambda_1^2}\right]'\ ,\ \delta = \frac{-(k-\lambda_2^2)(k-\lambda_1^2)}{2m\lambda_1}\left[\frac{m}{k-\lambda_2^2}\right]'\ , \\
\epsilon &= -\frac{\left\{\left[2m\lambda_1 k' - 2m'\lambda_1(k-\lambda_1^2) - m\lambda_1'(k+3\lambda_1^2)\right](k-\lambda_2^2) + (k-\lambda_1^2)^2 m\lambda_1'\right\}}{2m\lambda_1(k-\lambda_1^2)(\lambda_1^2-\lambda_2^2)}\ , \\
\zeta &= \frac{\left\{\left[2m\lambda_2 k' - 2m'\lambda_2(k-\lambda_2^2) - m\lambda_2'(k+3\lambda_2^2)\right](k-\lambda_1^2) + (k-\lambda_2^2)^2 m\lambda_2'\right\}}{2m\lambda_2(k-\lambda_2^2)(\lambda_1^2-\lambda_2^2)}
\end{aligned} \tag{6.1.10}$$

so that the relative sizes of λ_1 and λ_2 play a key role in the coupling of the dependent variables. Note that the pairs of variables α and β, and ϵ and ζ can be obtained from one another by interchanging λ_1 and λ_2.

6.2 Embedded Systems And WKB

It is possible to attempt a WKB solution of the complete set of equations 6.1.10, but the method is very complex and no less laborious than solution of the complete set by numerical means, as we have done. The main point of this analysis, therefore, is to identify cases where an embedded system of equations occurs which may be soluble by the WKB formalism, with a view to eventually finding connection formulae that correspond to the results in Chapter 5. If a second order system can be consistently isolated, then we can manipulate it as follows.

In Diver (1986) it is shown that if we have the system

$$\begin{aligned}
u_1' - k_1(x)u_1 &= C_{12}u_2\ , \\
u_2' - k_2(x)u_2 &= C_{21}u_1\ ,
\end{aligned} \tag{6.2.1}$$

then one variable can be eliminated to produce

$$\begin{aligned}
u_1'' - (\Phi+\Psi)u_1' &+ (k_1k_2 + k_1\Phi - k_1' - C_{12}C_{21})u_1 = 0\ , \\
\Psi = k_1 + k_2\ &,\ \Phi = \frac{C_{12}'}{C_{12}}\ .
\end{aligned} \tag{6.2.2}$$

Transforming to normal form by setting $v = u_1 \exp\{-\frac{1}{2}\int(\Phi+\Psi)ds\}$ will then produce the equation

$$\begin{aligned}
v'' &- \left[\kappa^2 + \kappa' + C_{12}C_{21}\right]v = 0\ , \\
\kappa &= \frac{1}{2}\left[\frac{C_{12}'}{C_{12}} - k_1 + k_2\right]\ ,
\end{aligned} \tag{6.2.3}$$

which is a suitable candidate for solution by the WKB method. By examining the wave potential, we can now say whether significant mode conversion will occur, and if so, where. Connection formulae can then be derived, either by applying the full-blooded WKB method with consideration of Stokes and anti-Stokes lines, branch points and so on, or more simply, by forcing the equation into the form of a standard equation whose asymptotic behaviour is well-documented. It should be remembered that this will give connection formulae in terms of the u_i and not the y_i, so that, for instance, u_1 being constant means that a linear combination of the y_is is constant, and does not in itself imply constancy of any one of the original variables. The last step in the derivation would be to transform back to the physical variables in the problem.

If the matrix 6.1.10 is examined, then six obvious cases where some of the denominators in Eq. 6.1.10 diverge present themselves: $\lambda_1 + \lambda_2 = 0$, $\lambda_1 - \lambda_2 = 0$, $\lambda_1 \to 0$, $\lambda_2 \to 0$, $k - \lambda_1^2 = 0$ and $k - \lambda_2^2 = 0$. The possibility of $\lambda_1 + \lambda_2 = 0$ can be eliminated because λ_1 and λ_2 must both be positive, by definition. The other cases are considered in turn.

$\lambda_1 = \lambda_2$

Let us pursue the case where $\lambda_1 = \lambda_2$. This means that large couplings between the u_i may be expected, arising from the presence of the difference of these eigenvalues in the denominator of many entries of the matrix 6.1.9. Putting $\lambda_1 - \lambda_2 = \Delta$, and keeping only terms in Δ^{-1}, gives $\alpha = \beta$, $\gamma = \delta$, $\epsilon = \zeta = \gamma/\Delta$ and we obtain the much simpler matrix

$$\frac{\gamma}{\Delta}\begin{bmatrix} 1 & 1 & 0 & 0 \\ -1 & 1 & 0 & 0 \\ 0 & 0 & 1 & 1 \\ 0 & 0 & -1 & 1 \end{bmatrix}, \tag{6.2.4}$$

where the considerable complexity of a fourth order system has been replaced by two coupled second order equations. To reduce these to a form amenable to WKB solution, we need to convert each into an equation of the form 3.5.1. Comparing these two embedded systems with Eq. 6.2.1 gives

equations for	$u_{1,2}$	$u_{3,4}$
k_1	$\frac{\gamma}{\Delta}$	$\frac{\gamma}{\Delta}$
k_2	$\frac{\gamma}{\Delta}$	$\frac{\gamma}{\Delta}$
C_{12}	$-\frac{\gamma}{\Delta}$	$-\frac{\gamma}{\Delta}$
C_{21}	$\frac{\gamma}{\Delta}$	$\frac{\gamma}{\Delta}$

Where, for consistency, $\lambda_{1,2}$ have been ignored compared to objects of $\mathcal{O}(\Delta^{-1})$, giving the same coefficients for both embedded systems. Therefore, if we carry out this procedure for the system involving $u_{1,2}$, we find $\frac{C'_{12}}{C_{12}} = \frac{\gamma'}{\gamma} - \frac{\Delta'}{\Delta}$ from which it is easy to see that,

$$\kappa = \frac{1}{2}\left[\frac{\gamma'}{\gamma} - \frac{\Delta'}{\Delta}\right] \approx \frac{\Delta'}{2\Delta} . \tag{6.2.5}$$

Therefore,

$$\kappa^2 + \kappa' + C_{12}C_{21} = \frac{1}{\Delta^2}\left[\frac{3}{4}\Delta'^2 - \frac{1}{2}\Delta\Delta'' - \gamma^2\right] , \tag{6.2.6}$$

while the change of variables from u_1 to v gives

$$v = u_1 \exp\left\{-\frac{1}{2}\int \frac{2\gamma - \Delta'}{\Delta} ds\right\} = u_1\sqrt{\Delta}\exp\left\{-\int \frac{\gamma}{\Delta} ds\right\} . \tag{6.2.7}$$

To be consistent with the original assumption ($\lambda_1 \approx \lambda_2$), Eq. 6.1.6 shows that we must have

$$(k-n)^2 + 4m^2 \approx 0 ,$$

This implies that we must set $k \approx n$ and $m \approx 0$ for consistency. Pursuing the second condition, we see that either $b = 0$ or $\sin 2\rho = 0$, so that either the system is completely uncoupled, which we have already considered, or the equation we have derived is only valid near zeros of $\sin 2\rho$, so we do not have a single form valid for the whole interval $0 \leq \rho \leq 2\pi$. To further illustrate this point, if we pursue the argument for the moment, then, using 6.2.6, expanding in $k-n$ and m and keeping only the largest terms produces the equation

$$v'' + \frac{n'^2}{16(k-n)^2} v = 0 . \tag{6.2.8}$$

Clearly, the wave potential is always ≥ 0, so that 'cutoffs' occur at the zeros of n', but there is no region of evanescence, and hence little mode conversion can be expected. The wave potential is given by

$$\Theta = \frac{1}{16}\left[\frac{b\rho^3 \sin 2\rho - \frac{1}{2}}{\rho - b\rho^3 \cos 2\rho}\right]^2 . \tag{6.2.9}$$

Obviously, we must have $\sin 2\rho = 0$, but, depending on which zero of sin we are close to, either $\cos 2\rho = 1$ or $\cos 2\rho = -1$ may occur. This point may seem trivial, but it means that two different forms for the wave equations alternate in the internal plasma region, not to mention the fact that, in between zeros of sin, 6.2.9 may not apply at all, and it is not even certain that such a second order system of equations can be found.

$\lambda_1 \to 0$

This gives $\xi \approx 0$, $\beta \approx 0$, and $\epsilon \approx -\alpha$ so that

$$\mathsf{A}^{-1}\mathsf{A}' \approx \begin{bmatrix} -\alpha & -\frac{\gamma}{\lambda_2} & \alpha & \frac{\gamma}{\lambda_2} \\ \frac{\delta}{\lambda_2} & 0 & \frac{\delta}{\lambda_2} & 0 \\ \alpha & \frac{\gamma}{\lambda_2} & -\alpha & -\frac{\gamma}{\lambda_2} \\ \frac{\delta}{\lambda_2} & 0 & \frac{\delta}{\lambda_2} & 0 \end{bmatrix} , \tag{6.2.10}$$

where,

$$\gamma = -\frac{(\frac{m}{k})' k^3}{2m\lambda_1(k-\lambda_2^2)} , \quad \delta = -\frac{(\frac{m}{k-\lambda_2^2})' k(k-\lambda_2^2)}{2m\lambda_1} , \tag{6.2.11}$$

so that this is still coupled in too complex a manner to be of any use.

$\lambda_2 \to 0$

This leads to $\alpha \approx 0$, $\gamma \approx 0$, $\epsilon \approx 0$, $\delta \approx 0$, and $\zeta \approx -\beta$. Therefore

$$\mathsf{A}^{-1}\mathsf{A}' \approx \begin{bmatrix} 0 & 0 & 0 & 0 \\ 0 & -\beta & 0 & \beta \\ 0 & 0 & 0 & 0 \\ 0 & \beta & 0 & -\beta \end{bmatrix} , \tag{6.2.12}$$

where

$$\beta = -\frac{\lambda_2'}{2\lambda_2} , \tag{6.2.13}$$

so that $u_{2,4}$ couple to each other, while the other two amplitudes are uncoupled. This set of equations can be tackled by WKB. Following the procedure outlined in Section 6.2, we produce the equation in normal form,

$$v'' = \left(\frac{\lambda_2'}{\lambda_2}\right)^2 v , \tag{6.2.14}$$

where only the terms of largest order in $1/\lambda_2$ have been retained, and

$$v = u_2 \left(-2\frac{\lambda_2^2}{\lambda_2'}\right)^{1/2} . \tag{6.2.15}$$

Once again, we have $\Theta \geq 0$, and little mode conversion is anticipated. The wave potential here is complex, and there seems little prospect of forcing it into the canonical form of the hypergeometric equation. We do not pursue this argument further.

$k - \lambda_1^2 = 0$

From the form of λ_1, λ_2, this can only happen if $n - \lambda_2^2 = 0$, so that this is just the uniform field case, which will produce Bessel functions as solutions (Section 5.3.2).

$k - \lambda_2^2 = 0$

This gives $\alpha \approx 0$, $\beta \approx 0$, $\epsilon \approx 0$ and

$$\mathsf{A}^{-1}\mathsf{A}' \approx \begin{bmatrix} 0 & \frac{\gamma}{\Delta} & 0 & \frac{\gamma}{\lambda_1+\lambda_2} \\ \frac{\delta}{\Delta} & \zeta & \frac{\delta}{\lambda_1+\lambda_2} & 0 \\ 0 & \frac{\gamma}{\lambda_1+\lambda_2} & 0 & \frac{\gamma}{\Delta} \\ \frac{\delta}{\lambda_1+\lambda_2} & 0 & -\frac{\delta}{\Delta} & \zeta \end{bmatrix}, \tag{6.2.16}$$

which, once again is too complex to fit into the form 6.2.1.

6.3 Assessment

Most examples in the literature consider only equations with polynomial coefficients and have a simply defined wave potential: our example is less tractable. In order to reduce the order of the governing equation, we make assumptions about the eigenvalues which impose conditions on the radius values at which the reduced equation holds. In general, this means that our analysis is only valid near certain points (which may depend on the plasma parameters), so, strictly we cannot use the equation for the whole range of radii $0 \leq \rho \leq 2\pi$. Even if we gloss over this difficulty, there remains the question of the ode for the external region. Although this is simple to find, and we expect the resulting wave potential to join continuously on to that in the internal region, the first and second derivative of the wave potential may not be continuous, so that the error terms in Eq. 3.5.2 are not well defined. This does not mean we need to abandon the method completely, but we are clearly straying into deeper waters. The presence of the condition also means that the result of this rather complex procedure is valid for a certain range of plasma parameters, and would, at best, corroborate only a small part of the results in Chapter 5.

6.4 Cairns, Lashmore-Davies

This technique, revieved in Section 3.3.2, is another method which we might compare with the present analysis. The basic premise here is that propagation of modes is independent, apart from a confined region where coupling occurs. In other words, we want the graphs of local wavenumber to approach each other closely, then diverge. Plotting the eigenvalues of the coupled system of equations using Eq. 6.1.6 will give the same information. This was done for a variety of values of the parameters a and b. A typical plot is shown in Figure 6.1. Although there is a relatively

Figure 6.1: Square of eigenvalues against radius

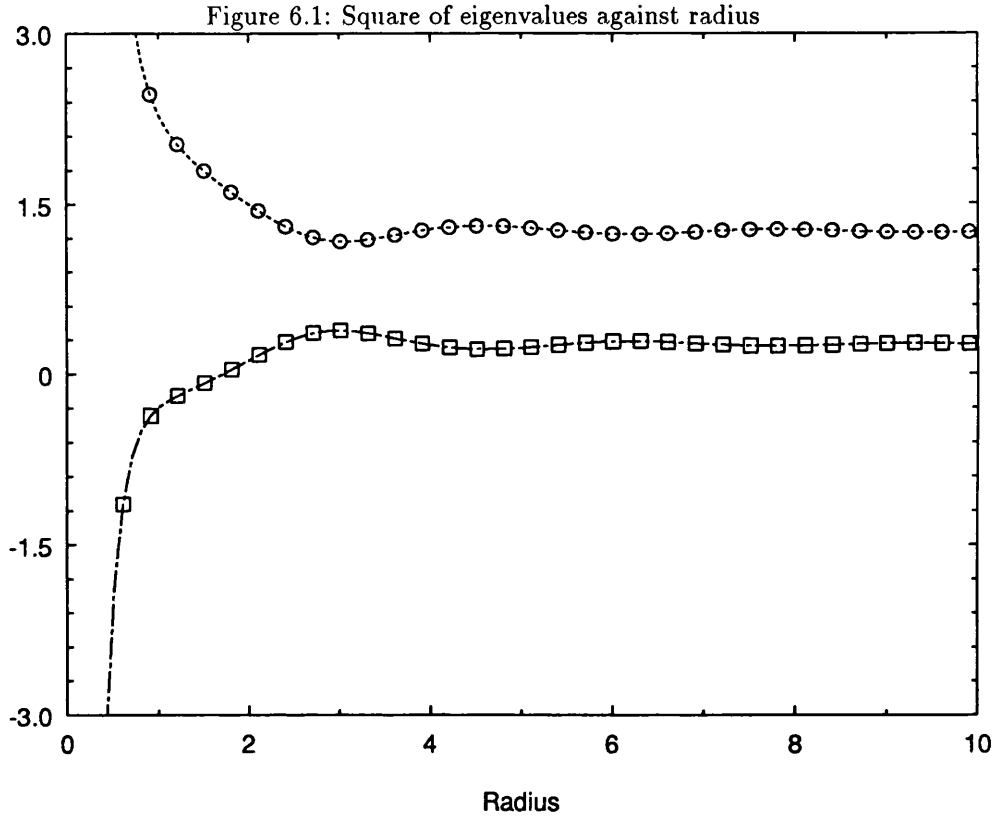

well-defined point of closest approach, the eigenvalues remain almost as close, for a large distance. In fact, λ_1 and λ_2 tend to constants as ρ becomes large, so the distance between the eigenvalues tends to a constant also. Therefore, if the two modes couple, they do so, to some extent, at a wide range of points and not a localised region. We conclude that the Cairns, Lashmore-Davies approach is not applicable here.

Chapter 7

Conclusions And Future Work

We have found the normal modes of a helically structured plasma by means of direct numerical solution of a set of odes derived from the cold plasma model which we expect to be very accurate for fusion plasmas. This contrasts with the sometimes ad hoc assumptions of other approaches to mode conversion. Asymptotic solutions have also been derived and found to be surprisingly good approximations to the numerical solutions. The situation where the structured region is joined onto a uniform magnetic field has been studied and the coefficients of plasma modes in the external region consistently derived using the assumption of continuity of the electric field and its derivative at the boundary.

The results found show a rich structure as we move through parameter space and indicate that complex mode conversion events may occur without the resonant layer inside the plasma which is given prominence in some other theories of mode conversion.

This method of analysis is straightforward, given modern computing facilities, yet utilises a more sophisticated model of non-uniform wave propagation than many other theories. The WKB method, when applied here, poses analytic problems of great complexity. The fitting of the helical onto the uniform field is only one of a number of similar problems which could be solved in a broadly similar way.

We now examine some ways in which this work may be extended.

7.1 Equilibrium Flows

This is probably the most desirable generalisation that can be made of the present work, given that the driving force behind this thesis was to study consistently the wave motion of a non-uniform plasma. Although we have shown that, for many cases of interest, the effect of the equilibrium flows is negligible, it is still intriguing as a point of principle to see what happens when the full effect of plasma inhomogeneity is considered. With a little help from REDUCE and Eqs. 4.4.1 and 4.4.2, one can show that the odes for the electric field values have the form

$$\begin{aligned} a_1 E_\theta'' + a_2 E_\theta' + a_3 E_\theta + a_4 E_z'' + a_5 E_z' + a_6 E_z &= 0\,, \\ b_1 E_\theta'' + b_2 E_\theta' + b_3 E_\theta + b_4 E_z'' + b_5 E_z' + b_6 E_z &= 0\,, \end{aligned} \qquad (7.1.1)$$

where $a_1, \cdots, a_6$ and $b_1, \cdots, b_6$ are functions of the quantities $\mathbf{x}_1$, $\mathbf{x}_2$, $\mathbf{x}_3$, λ, μ, defined in Eq. 4.4.2. In our previous work, the first equation could be considered as being for E_θ, with a driving term which coupled to E_z, and the second as for E_z with a driving term proportional to E_θ, but this viewpoint can no longer be sustained, and there is now no clear distinction between E_θ and E_z.

Although in principle no different to the system of equations solved earlier, the extra terms and more complex coefficients mean that tackling these equations is a serious undertaking. The possibility of error in transcribing and manipulating the complex expressions for the coefficients means that the solution would be best attempted by using a computer algebra package to generate the equations and then producing output suitable for inclusion in a numerical simulation directly from this. The computer time taken to produce the results would rise dramatically in this case, perhaps by a factor of ten. Although one numerical integration would be quite feasible, the 400 or so needed to produce the figures in Chapter 5, would be a large undertaking (when solving the present equations, each of the graphs in Chapter 5 took about 15 minutes to generate on a 486-PC), but one which is quite possible with today's computers. One possible compromise would be to study equilibria where the flows are small. The equilibrium quantities in the final equations do not all occur to the same order and including only the lowest order terms present would provide a useful stepping stone on the road to a consistent solution.

7.2 Arbitrary Wave Number

Setting the perturbed quantities in section 4.2 to be proportional to $exp(-i\omega t + kz + m\theta)$, where k and m are now non-zero, and retaining the other assumptions

of that section, will give rise to a set of equations which are of the same order as those already considered, but contain extra terms which couple the electric field components together more intimately. The final odes are of the same form as Eq. 7.1.1, though with coefficients which are now functions of k and m also.

7.3 Other Equilibrium Fields

We have used the form 4.1.13 for the equilibrium magnetic field, for practical reasons. It avoids singularities arising from a position dependent cyclotron frequency, and expressions for sin and cos are readily available. It is worth remembering that it is only one choice, however, and by excluding the singular fields, we may be neglecting cases of great physical interest. If we use Eqs. 4.2.3, then the existence of the upper hybrid resonance is the most obvious issue to tackle. This is done by retaining only terms which are resonant, to produce a new differential equation, valid very close to the resonant layer in the plasma (if we retain the other assumptions about variation with ρ alone, this is a cylindrical shell). To carry this out for Eqs. 4.2.3, without assuming any particular form for the equilibrium, put

$$\frac{\omega_{uh}}{\omega} = 1 + \eta\,, \quad \rho = \rho_o + \frac{\omega_{uh}(\rho_o)}{\omega'_{uh}(\rho_o)}\eta \stackrel{\partial}{=} \rho_o + A\eta\,. \tag{7.3.1}$$

To zeroth order in η, both equations give

$$gE_\theta - fE_z = 0\,, \tag{7.3.2}$$

which is equivalent to $E_r = 0$. However this does not determine E_θ and E_z, and to do this we must proceed to first order in η. On using the condition obtained for zeroth order to eliminate E_z, we obtain

$$\begin{aligned} E''_\theta + \frac{A}{\rho}E'_\theta + A^2\left[\frac{\kappa^2 a}{L^2} - \frac{1}{\rho_o}\right]E_\theta &= 0\,, \\ E''_\theta + \left[\frac{A}{\rho_o} + \frac{2f}{g}\left(\frac{g}{f}\right)'\right]E'_\theta + \left[\frac{Af}{\rho_o g}\left(\frac{g}{f}\right)' + \left(\frac{g}{f}\right)''\frac{f}{g} + \frac{\kappa^2 A^2 a}{L^2}\right]E_\theta &= 0\,, \end{aligned} \tag{7.3.3}$$

where $'$ now denotes a derivative with respect to η. The terms in E''_θ can be eliminated in Eqs. 7.3.3 to give

$$\frac{2f}{g}\left(\frac{g}{f}\right)'E'_\theta + \left[\frac{Af}{\rho_o g}\left(\frac{g}{f}\right)' + \frac{f}{g}\left(\frac{g}{f}\right)'' + \frac{A^2}{\rho_o}\right]E_\theta = 0\,. \tag{7.3.4}$$

We also have to expand f and g to first order in η to obtain a final answer. This means that the second derivative of g/f in Eq. 7.3.4 is zero, the first derivatives

give constants, and so we can write

$$\frac{E_\theta'}{E_\theta} = \frac{A}{2\rho_o} \frac{\left[\frac{f}{g}\left(\frac{g}{f}\right)' + A\right]}{\frac{f}{g}\left(\frac{g}{f}\right)'} \stackrel{\partial}{=} \frac{c_1\eta + c_2}{c_3\eta + c_4}\,, \tag{7.3.5}$$

giving the solution

$$E_\theta \propto \exp(\frac{c_1}{c_3}\eta)\,[c_3\eta + c_4]^{(c_2 - \frac{c_1 c_4}{c_3})}\,. \tag{7.3.6}$$

The solutions to this equation would be joined onto numerical approximations just before and just after the resonant radius to produce a complete solution. The exponential factor raises a number of interesting possibilities. For suitable choices of c_1 and c_3 the E_θ solutions may grow very rapidly or very slowly in this layer near the resonance, giving rise to enormously different values on either side of the singular surface. The Bessel function field, Eq. 4.1.15 is probably the most obvious choice for use as an equilibrium field, as it has served in the past as a model for the field in a reversed field pinch, and so an obvious application already exists.

Appendix A

Fortran Codes

A.1 Finding Independent Internal Modes

```
c                          ...odeadam.for...
c Solution of our odes using NAG routine d02cbf (variable order,
c variable step, Adams method. This version produces boundary values
c for a range of plasma parameters, as input for concoeff.for

      real tol, x, xend, a, b, ezo, etod, h,
     & om, wc, PI, startf, endf
      integer ifail, j, n, ir, i, npts, modeno, nvals, count
      parameter (n=4, ir=0, npts=40, tol= 1.0d-14, nvals= 400)
      real w(23+21*n), y(n)
      external fcn, out
      common /stuff/ xend, h, i
      common /params/ a,b
      character*8 ofile

      call dclock@( start )

      count = 0
      ofile = 'd0_5_0_5'
      PI = acos(-1.0)
      wc = 2.5
      xend = 2.0*PI
```

```
      startf = 0.01
      endf = 5.0
c Open the file for output
      open( 14, file='boundary\'//ofile, form='unformatted')

      do 40 j=0,nvals
c Repeat calculation for a range of frequencies, from startf to endf
c in nvals steps. Frequency is in units of wp.

         om = startf + real(j)*(endf-startf)/real(nvals)
         a = om**2 - 1.0
         b = -(wc**2)/(om**2 - wc**2 - 1.0)

         write (14) xend, om, wc

c Initial values of the fields set according to the mode required
         do 30 modeno=1,2
            if( modeno.eq.1) then
               ezo = 1.0
               etod = 0.0
            end if
            if( modeno.eq.2) then
               ezo = 0.0
               etod = 1.0
            end if

            x = 1.0d-2
c Set starting values at x(non-zero) to avoid
c singularity at the origin
            y(1) = etod*(x - a*x**3/8.0 + (1.0/24.0)*(b/3.0 +
     &      (a/8.0)*(a-b) )*x**5 ) + (ezo-etod)*b*( x**3/8.0 -
     &      (1.0/192.0)*(3.0*a + b + 16.0/3.0)*x**5 )

            y(2) = etod*(1.0 - a*x**2/4.0 + a**2*x**4/64.0) +
     &      (ezo-etod)*(1.0 - a*x**2/4.0 + (a**2/4.0 - b)*x**4/16.0)
```

```
            y(3) = etod*(1.0 - 3.0*a*x**2/8.0 + (5.0/24.0)*(b/3.0 +
     &      (a/8.0)*(a-b))*x**4 ) + (ezo-etod)*b*( 3.0*x**2/8.0 -
     &      (5.0/192.0)*( 3.0*a + b + 16.0/3.0)*x**4 )

            y(4) = etod*( -a*x/2.0 + a**2*x**3/16.0 + (1.0/6.0)*(
     &      a*b/8.0 - b/3.0 - a**3/64.0 )*x**5 ) + (ezo-etod)*(
     &      -a*x/2.0 + 0.25*(a**2/4.0 - b)*x**3 + (1.0/48.0)*(b**2 +
     &      8.0*b/3.0 + 5.0*a*b/2.0 - a**3/8.0)*x**5 )

            h = (xend - x)/npts
            i = npts - 1
            ifail = 0

c This is the actual integrating routine
            call d02cbf(x, xend, n, y, tol, ir, fcn, out, w, ifail )
            if (tol.lt.0) write (6, 994)
            if (ifail.ne.0) write (6, 996)
            count = count + 1
c Unformatted output
            write (14) y
            if ( mod( count, 10).eq.0 ) then
               write( 6, *) 'Performing', nvals,'integrations,',
     &         count, 'complete'
            end if
30       continue
40    continue

c Close the output file
      close( 14 )
      call dclock@( finish )
      write(6, *)'time taken=', nint((finish-start)/60.0),
     & ' minutes', mod( int(finish-start), 60), ' seconds'
      stop

999   format (64h  x       y(1)=Et       y(2)= Ez      y(3)=Et'
     &y(4)=Ez'  )
```

```
996   format (8h ifail= , I1)
994   format (24h Range too short for tol)
      end

      subroutine fcn(t, y, f)
      real t, f(4), y(4), a, b
      real cos, sin
      common /params/ a, b
      f(1) = y(3)
      f(2) = y(4)
      f(3) = -y(3)/t - (a + b*cos(t)**2 - 1.0/t**2 )*y(1) +
     & (b/2.0)*sin(2.0*t)*y(2)
      f(4) = -y(4)/t - (a+b*sin(t)**2)*y(2) +
     & (b/2.0)*sin(2.0*t)*y(1)
      return
      end

      subroutine out(x, y )
      real x, y(4), h, xend
      integer  i
      common /stuff/ xend, h, i
      x = xend - real(i)*h
      i = i - 1
      return
      end
```

A.2 Finding Conversion And Reflection Coefficients

A.2.1 Incoming O-Mode

```
c                          ...concoefo.for...
c Code to take field values at the interface and produce conversion
c /reflection coefficients.
```

```
      real R, u1, u2, u1d, u2d, v1, v2, v1d, v2d, j, y, k, i, om,
     & wc, wee, big, phiref, phicon, rref, rcon, test, mode1(4),
     & mode2(4), pfactor, qfactor, kp, kq
      character*8 infile
      complex a1, a2, b1, b2, c1, c2, d1, d2, j0, j1, y0, y1, j0d,
     &  j1d, y0d, y1d, p, q, den, refcoeff, concoeff
      integer n, nvals, nin
      parameter (nvals=400, nin=14)

      PI = acos(-1.0)
c wee is to stop arguments of Bessel functions being exactly zero
      wee = 1.0d-150
      big = 1.0d150
c Set infile to the appropriate filename
      infile ='d6_01_5'

c Take boundary values from directory, well, boundary.
      open ( nin, file='boundary\'//infile, form='unformatted')
      do 10 n=0, nvals
c Enter field values at rho = R
         read ( nin ) R, om, wc
         read ( nin ) mode1
         read ( nin ) mode2
         u1 = mode1(1)
         v1 = mode1(2)
         u1d = mode1(3)
         v1d = mode1(4)
         u2 = mode2(1)
         v2 = mode2(2)
         u2d = mode2(3)
         v2d = mode2(4)
c Assign p and q to their complex values
         test = 1.0 + ( 1.0-om**2 )/(om**2*( om**2-wc**2-1.0 ))

         if ( test.ge.0.0 ) then
            p = cmplx( om*sqrt(test), 0.0 )
```

```
      else
         p = cmplx( 0.0, om*sqrt(-1.0*test) )
      endif
      if ( (1.0-1.0/om**2).ge.0.0 ) then
         q = cmplx( om*sqrt( 1.0 - 1.0/om**2  ), 0.0 )
      else
         q = cmplx( 0.0, om*sqrt(1.0/om**2 -1.0) )
      endif

c Different action depending on p being pure real or pure imaginary
c Decide whether Bessel functions or modified BFs are required.
      if ( abs( aimag(p) ).lt.wee ) then
         j1 = cmplx( j(1, real(p)*R), 0.0 )
         y1 = cmplx( y(1, real(p)*R+wee), 0.0 )
         j1d = cmplx( j(0, real(p)*R) - j(1, real(p)*R)/
     &      (real(p)*R),0.0 )
         y1d = cmplx( y(0, real(p)*R+wee) -
     &      y(1, real(p)*R+wee)/(real(p)*R + wee), 0.0 )
         pfactor = p
      else
         j1 = cmplx( 0.0, i(1, aimag(p)*R) )
         y1 = -cmplx( i(1, aimag(p)*R), (2.0/PI)*k(1,
     &      aimag(p)*R+wee) )
         j1d = cmplx( 0.0, i(0, aimag(p)*R ) - i(1, aimag(p)*R)
     &      /(aimag(p)*R) )
         y1d = -cmplx( i(0, aimag(p)*R) - i(1, aimag(p)*R)/
     &      (aimag(p)*R), (-2.0/PI)*( k(0, aimag(p)*R+wee) +
     &      k(1, aimag(p)*R+wee)/(aimag(p)*R+wee) ) )
         pfactor = aimag(p)
      endif

c Coefficients of exterior modes which u1, v1 , u2, v2 match onto
c If p is pure imaginary, use imag. part

      a1=cmplx(PI*R/2.0)*( cmplx(pfactor*u1)*y1d-cmplx(u1d)*y1 )
      a2=cmplx(PI*R/2.0)*( cmplx(pfactor*u2)*y1d-cmplx(u2d)*y1 )
```

```
         b1=cmplx(PI*R/2.0)*( cmplx(u1d)*j1-cmplx(pfactor*u1)*j1d )
         b2=cmplx(PI*R/2.0)*( cmplx(u2d)*j1-cmplx(pfactor*u2)*j1d )
c Different action depending on q being pure real or pure imaginary
c Decide whether Bessel functions or modified BFs are required.
         if( abs( aimag(q) ).lt.wee) then
            j0 = j(0, real(q)*R)
            y0 = y(0, real(q)*R+wee)
            j0d = -j(1, real(q)*R)
            y0d = -y(1, real(q)*R+wee)
            qfactor = q
         else
            j0 = cmplx( i( 0, aimag(q)*R), 0.0 )
            y0 = cmplx( -(2.0/PI)*k( 0, aimag(q)*R + wee),
     &      i( 0, aimag(q)*R) )
            j0d = cmplx( i( 1, aimag(q)*R), 0.0 )
            y0d = cmplx( (2.0/PI)*k( 1, aimag(q)*R + wee),
     &      i( 1, aimag(q)*R) )
            qfactor = aimag(q)
         endif

         c1=cmplx(PI*R/2.0)*( cmplx(qfactor*v1)*y0d-cmplx(v1d)*y0 )
         c2=cmplx(PI*R/2.0)*( cmplx(qfactor*v2)*y0d-cmplx(v2d)*y0 )
         d1=cmplx(PI*R/2.0)*( cmplx(v1d)*j0-cmplx(qfactor*v1)*j0d )
         d2=cmplx(PI*R/2.0)*( cmplx(v2d)*j0-cmplx(qfactor*v2)*j0d )

c      This evaluates the reflection/conversion coeffs
         if( abs(a1).gt.big.or.abs(a2).gt.big.or.abs(b1).gt.big.or.
     &   abs(b2).gt.big.or.abs(c1).gt.big.or.abs(c2).gt.big.or.
     &   abs(d1).gt.big.or.abs(d2).gt.big ) goto 10

         den = -a1*c2+a2*c1+b1*d2-b2*d1 + (0.0,1.0)*
     &    ( a1*d2-a2*d1+b1*c2-b2*c1 )

         refcoeff =  ( a2*c1-a1*c2+b2*d1-b1*d2 + (0.0,1.0)*
     &   ( b1*c2-b2*c1-a1*d2-a2*d1 ))/den
         concoeff = (0.0,2.0)*(b1*a2-b2*a1)/den
```

```
         if( real(refcoeff).lt.wee ) then
            phiref = PI/2.0
         else
            phiref = atan( aimag(refcoeff)/real(refcoeff) )
         endif

         if( real(concoeff).lt.wee ) then
            phicon = PI/2.0
         else
            phicon = atan( aimag(concoeff)/real(concoeff) )
         endif

         rref = sqrt( real(refcoeff)**2 + aimag(refcoeff)**2 )
         rcon = sqrt( real(concoeff)**2 + aimag(concoeff)**2 )

         write( 5, 999) om, rref, phiref, rcon, phicon
c        if (aimag(q).gt.wee.or.aimag(p).gt.wee) goto 10

c These give the refractive index squared (useful check)
c        write(5 , *) om, real(p*p)/(om**2), real(q*q)/(om**2)
   10 continue
c Close input file
      close ( nin )

998   format(17h Results with om=,e10.3,4h wc=,e10.3)
999   format( 5e13.5 )
      end

c Functions to evaluate Bessel functions of order 0,1,
c any real argument
      real function j( ord, arg)
      real arg, oldj, olderj
      external s17aef, s17aff
      integer ord, n
c Deal with negative orders
```

```
      n = abs(ord)
c Find values of J0 and J1
      olderj = s17aef( arg, 0)
      oldj = s17aff( arg, 0)
      if ( n.eq.0 ) j = olderj
      if ( n.eq.1 ) j = oldj
      if ( ord.lt.0 ) j = j*(-1.0)**n
      end

      real function y( ord, arg)
      real arg, oldy, oldery
      external s17acf, s17adf
      integer ord, i, n
c Deal with negative orders
      n = abs(ord)
c Find Y0, Y1
      oldery = s17acf( arg, 0)
      oldy = s17adf( arg, 0)
      if ( n.eq.0 ) y = oldery
      if ( n.eq.1 ) y = oldy
      do 20, i= 2, n
         y = 2*(real(i)/arg)*oldy - oldery
         oldery = oldy
   20    oldy = y
      if ( ord.lt.0 ) y = y*(-1.0)**n
      end

c Find modified Bessel functions of order 0 and 1
      real function i( ord, arg)
      real arg, s18aef, s18aff
      integer ord
      if ( ord.eq.0 ) i = s18aef( arg, 0)
      if ( ord.eq.1 ) i = s18aff( arg, 0)
      end

      real function k( ord, arg)
```

```
real arg, s18acf, s18adf
integer ord
if ( ord.eq.0 ) k = s18acf( arg, 0)
if ( ord.eq.1 ) k = s18adf( arg, 0)
end
```

A.2.2 Incoming X-Mode

The program concoefx.for is used, which is the same as the last program, but with the definitions of `refcoeff, concoeff` replaced by

```
      refcoeff =  -1.0 + 2.0*( a2*c1-a1*c2 + (0.0, 1.0)*
     &   ( a1*d2-a2*d1 ) )/den
      concoeff = (0.0,2.0)*(d2*c1-d1*c2)/den
```

Appendix B

Bibliography

ABROMOWITZ, M., STEGUN, I.A., *Handbook Of Mathematical Functions*, Dover, New York, 1965

ALFVÉN, H.O.G., *Cosmology In The Plasma Universe: An Introductory Exposition*, IEEE Transactions On Plasma Science, **18**, 5, 1990

AUERBACH, S.P., *Energy Of Waves In A Plasma*, Phys. Fluids, **22**, 9, 1979

BOOK, D.L., *NRL Plasma Formulary* (aka *The wee plasma book*) , The Office Of Naval Research, Washington, D.C., 1978

BRAY, R.J., CRAM, L.E., DURRANT, C.J., LOUGHHEAD, R.E., *Plasma Loops In The Solar Corona*, Cambridge University Press, 1991

BROWNELL, J.H., *Wave Number Space Analysis Of Propagation In Nonuniform Media* , Amer. J. Physics, **41**, 207, 1973

BROWNELL, J.H., *Wavenumber Space Analysis Of Oscillations In Weakly Non-Uniform Magnetoplasmas*, J. Plasma Physics, **9**, 275, 1973

CAIRNS, R.A., *Radiofrequency Heating Of Plasmas*, Adam Hilger, 1991

CAIRNS, R.A., LASHMORE-DAVIES, C.N., *A Unified Theory Of A Class Of Mode Conversion Problems*, Physics Fluids, **26**, 1268, 1983

CAIRNS, R.A., LASHMORE-DAVIES, C.N., DENDY, R.O., HARVEY, B.M.,

HASTIE, R.J., *Wave Propagation Near A Cyclotron Resonance In A Non-Uniform Equilibrium Magnetic Field*, Physics Fluids B, **3**, 11, 2953-9, 1991

CHOUDHURY, S.R., *Lower Hybrid Wave Propagation And Absorbtion In Inhomogeneous Plasmas*, Physics Fluids B, **31**, 8, 2206-2213, 1988

CLEMMOW, P.C., DOUGHERTY, J.P., *The Electrodynamics Of Particles And Plasmas*, Addison-Wesley, Reading (USA), 1969

DIVER, D.A., *Wave Propagation In Non-Uniform Plasmas*, Ph.D. Thesis, University Of Glasgow, 1986

DIVER, D.A., LAING, E.W., *On Conservation Laws In Fourth-Order Potential Barriers*, J.Phys. A: Math. Gen., **23**, 1699-1704, 1990

DIVER, D.A., LAING, E.W., SELLAR, C.C., *Waves In A Cold Plasma With Spatially Periodic Sheared Fields*, J. Plasma Physics, **42**, 153, 1989

FUCHS, V., KO, K., BERS, A., *Theory Of Mode-Conversion In Weakly Inhomogeneous Plasma*, Physics Fluids, **24**, 1251, 1981

HEADING, J., *An Introduction To Phase-Integral Methods*, Methuen, London, 1962

HEARN, A.C., *REDUCE User's Manual Version 3.4*, RAND, Santa Monica, 1991

HU, J.L., SWANSON, D.G., *Mode Conversion At Electron Cyclotron Harmonics With Finite* $k_{\|}$, Physics Fluids B, **5**, 11, 4207-20, 1993

HU, J.L., SWANSON, D.G., *Synchrotron Radiation And Absorbtion At* $3\Omega_{ce}$ *With X-Mode-O-Mode Coupling*, Physics Fluids B, **5**, 11, 4221-36, 1993

INCE, E.L., *Ordinary Differential Equations*, Longmans, Green & Co., 1926

JET TEAM, *The JET Preliminary Tritium Experiment*, Plasma Physics And Controlled Fusion (special issue), **34**, 13, 1749-1758, 1992

LANDAU, L.D., LIFSHITZ, E.M., PITAEVSKIĬ, *Electrodynamics Of Continuous Media*, Pergamon Press, 1984

LANGMUIR, I., TONKS, L., *Oscillations In Ionized Gases*, Physical Review, **33**, 195, 1929

LAWSON, J.D., *Some Criteria For A Power Producing Thermonuclear Reactor*, Proc. Phys. Soc. B, **70**, 6, 1957

McDONALD, D.C., CAIRNS, R.A., LASHMORE-DAVIES, C.N., *Electron Cyclotron Resonant Heating: A Simpler Method For Deriving The Linear Wave Equations In A Non-Uniform Magnetic Field*, Physics Plasmas, **1**, 4, 843-849, 1994

MARMET, P., *Non-Doppler Redshift Of Some Galactic Objects*, IEEE Transactions On Plasma Science, **18**, 56, 1990

NUMERICAL ALGORITHMS GROUP, THE, *NAG Fortran Library Introductory Guide, Mark 13*, NAG, Oxford, 1988

PERATT, A.J., , IEEE Transactions On Plasma Science, **14**, 639, 1986

REBER, G.,*Intergalactic Plasma*, IEEE Transactions On Plasma Science, **14**, 678, 1986

STIX, T.H., *The Theory Of Plasma Waves*, McGraw-Hill, New York, 1962

STIX, T.H., *Radiation And Absorption Via Mode Conversion In An Inhomogeneous Collision-Free Plasma*, Physical Review Letters, **15**, 878, 1965

STIX, T.H., *Waves In Plasmas*, American Institute Of Physics, New York, 1992

TAYLOR, J.B., *Relaxation Of Toroidal Plasma And Generation Of Reverse Magnetic Fields*, Phys. Rev. Letters, **33**, 1139, 1974

WATSON, G.N., *Bessel Functions*, Cambridge, 1944